HEAT-STERILIZABLE, REMOTELY ACTIVATED BATTERY DEVELOPMENT PROGRAM

Final Report

by
Jack N. Brill

Contract No. 952214
NAS7-100

March 11, 1970

JET PROPULSION LABORATORY
California Institute of Technology
4800 Oak Grove Drive
Pasadena, California 91103

EAGLE-PICHER INDUSTRIES, INC.
Electronics Division
Couples Department
Joplin, Missouri 64801

HEAT-STERILIZABLE, REMOTELY ACTIVATED BATTERY DEVELOPMENT PROGRAM

Final Report

by
Jack N. Brill

Contract No. 952214
NAS7-100

March 11, 1970

"This work was performed for the Jet Propulsion Laboratory, California Institute of Technology, as sponsored by the National Aeronautics and Space Administration under Contract NAS7-100."

EAGLE-PICHER INDUSTRIES, INC.
Electronics Division
Couples Department
Joplin, Missouri 64801

"This report contains information prepared by Eagle-Picher Industries, Inc., under JPL Sub-Contract. Its content is not necessarily endorsed by the Jet Propulsion Laboratory, California Institute of Technology, or the National Aeronautics and Space Administration."

ABSTRACT, CONCLUSIONS AND RECOMMENDATIONS

This report describes the development of a heat sterilizable remotely activated battery under Contract JPL No. 952214 with Eagle-Picher Industries. In the first of two phases a study was made of the effects of heat sterilization on all cell and battery components. In the second phase, three engineering model batteries were built from the components selected in the first phase. These batteries were sterilized and tested to demonstrate the validity of the design.

In phase one it was shown that as a result of heat sterilization, the silver oxide electrode lost 38% of its actual capacity. This loss was the result of thermal reduction of AgO to Ag_2O. In addition, electrode dimensions increased by 8% in width, 4% in height and 0-10% in thickness because of particle size increase during sterilization. Microscope studies of the electrodes revealed that particle size tended to become more uniform from plate to plate but less uniform in a given plate. Excessive pressure build-up caused by oxygen from the silver oxide reduction (400 cc/electrode) and dimensional stability problems were minimized by presterilization of the electrodes and trimming to final size before assembly into the cells.

The zinc electrodes suffered an 18% capacity loss during sterilization. Microscope scanning studies and surface area measurements showed no change as the result of heat sterilization. Surface area values of 3.6 - 6.1 m^2/gm before sterilization and of 4.8 - 5.8 m^2/gm after sterilization were found. X-ray measurements indicated that only a trace of zinc oxide was formed during sterilization.

Several separator materials were tested for use in the heat sterilizable battery. Based on their ability to survive sterilization and to absorb and wick electrolyte solution, cotton and asbestos were found best suited while nylon, polypropylene and hemp were inferior. Cotton required 19-33 seconds to wick 31% KOH electrolyte solution 1/2" in the vertical direction and absorbed 16.5 gm of 31% KOH solution/gm material. Asbestos required 83-300 seconds to wick 1/2" under similar conditions and absorbed typically 7 gm of solution/gm material. The cotton separator was selected for use in the prototype batteries.

In studying the effect of electrolyte concentration on cell performance, it was found that the cell plateau voltage was reduced by a factor of 0.03 times the specific gravity of the solution. Neither the specific gravity, within the range of 1.30 to 1.45, nor sterilization of the electrolyte was found to affect cell capacity.

A conventional electrolyte reservoir made from copper tubing was found to be unaffected by heat sterilization. The reservoir used in the 3 batteries was sealed at either end by 0.004 inch thick diaphragms and held 800 cc's of 31% KOH electrolyte solution.

Polysulfone was selected as the best case material because of its transparency and its ability to be solvent bonded. Nevertheless, it was necessary to cure all solvent joints in vacuum at 85°C for 72 hours to prevent bubbling and weakening of the joints during sterilization. Lap joints and butt joints prepared in this manner failed between 1660 and 5330 psi. Sterilization did not change these values. Cell cases were found to burst at a pressure of 160 psi before sterilization and at 90 psi after sterilization.

Several types of squibs and propellants were tested for use in the gas generator. A squib manufactured by Network Electronics Corp., was found to be unaffected by sterilization. This unit uses lead styphnate as the initiator. A polyester-styrene-ammonium perchlorate propellant, made by Aerojet General Corp., was least affected by sterilization. The gas output, peak pressure and time to reach peak pressure were determined for this and other propellants before and after sterilization.

In phase two three batteries were assembled from the components described above. They were designed to have a capacity of ten ampere hours. The dimensions were 7.14 x 6.65 x 6.04 inches and the volume was 287 in^3. The weight was 17 pounds yielding an energy density of 15.3 watt hours per pound. The batteries were heat sterilized for 128 hours at 135°C, activated and discharged. The performance was normal in one out of three developmental batteries. The remaining two units worked poorly because of unforeseen assembly problems. All batteries were vented at the end of discharge to prevent possible rupture. No component failures were encountered.

Based on the work performed here, the following conclusions can be drawn: Remotely activated silver oxide-zinc batteries can be made to be heat sterilizable if a 40% loss in energy density is acceptable. The energy density for these batteries is about 15 watt hours per pound. Because of gassing during and after discharge, batteries fabricated based on these model batteries would have to be equipped with a vent; venting could perturb the motion or orientation of a descending planetary capsule. Additional work in this area would have to focus on the pressure problems and means to eliminate them.

TABLE OF CONTENTS

SECTION		PAGE
ABSTRACT, CONCLUSIONS AND RECOMMENDATIONS		iii
LIST OF FIGURES		viii
LIST OF TABLES		ix
1.0	INTRODUCTION	1
2.0	TECHNICAL DISCUSSION	2
2.1	Phase I	2
2.1.1	Silver Plate	2
2.1.1.1	Dimensional and Weight Changes	2
2.1.1.2	Gassing of Silver Electrode	5
2.1.1.3	Structural Changes	9
2.1.1.4	Electrical Characteristics	13
2.1.2	Zinc Plate	14
2.1.2.1	Dimensional and Weight Changes	14
2.1.2.2	Structural Changes	14
2.1.3	Separator	16
2.1.3.1	Dimensional and Weight Changes	18
2.1.3.2	Wetting Characteristics	18
2.1.3.3	Electrical Resistivity	22
2.1.4	Electrolyte Solution	22
2.1.5	Cell Case and Cell Case Sealing	27
2.1.5.1	Sealing	27
2.1.5.2	Physical Properties	30
2.1.5.2.1	Mechanical Tests	30
2.1.5.2.2	Chemical Resistance	32
2.1.6	Battery Container	33
2.1.7	Electrolyte Solution Reservoir	33
2.1.8	Pyrotechnics	37
2.1.8.1	Ignitors	37
2.1.8.2	Propellants	38
2.1.9	Cell Tests	40
2.2	Phase II	46
2.2.1	Battery Design	46
2.2.1.1	Positive Plate	46
2.2.1.2	Negative Plate	46
2.2.1.3	Separator	48
2.2.1.4	Cell Case	48
2.2.1.5	Electrolyte Reservoir	51
2.2.1.6	Electrolyte Solution	51
2.2.1.7	Gas Generator	55
2.2.1.8	Container	55

TABLE OF CONTENTS (Continued)

SECTION		PAGE
2.2.2	Prototype Tests	55
2.2.2.1	Prototype Number 1	57
2.2.2.2	Prototype Number 2	59
2.2.2.3	Prototype Number 3	63
3.0	CONCLUSIONS	65
4.0	RECOMMENDATIONS	66
5.0	NEW TECHNOLOGY	67
APPENDIX I	MICROSCOPIC STUDY OF SILVER OXIDE ELECTRODES	68
APPENDIX II	MICROSCOPIC STUDY OF ZINC ELECTRODES	98

LIST OF FIGURES

FIGURE		PAGE
I	Gassing Characteristics of Silver Oxide Plates during Heat Sterilization	7
II	Gassing Characteristics of Silver Oxide Plates	8
III	Gassing of Silver Oxide Plates at 135°C	10
IV	Fixture for Separator Resistance Measurement	25
V	BA 472/U Electrolyte Reservoir	34
VI	GAP 4230 Electrolyte Reservoir	35
VII	Water Displacement Test Fixture	39
VIII	Discharge Characteristics after Heat Sterilization (Wet Stand - 10 Minutes)	43
IX	Discharge Characteristics after Heat Sterilization (Wet Stand - 30 Minutes)	44
X	Discharge Characteristics after Heat Sterilization (Wet Stand - 1 Hour)	45
XI	Plate Size	47
XII	Cell Block	49
XIII	Manifold	50
XIV	Manifold Cover	52
XV	Electrolyte Reservoir	53
XVI	Connection of Electrolyte Reservoir to Manifold	54
XVII	Gas Generator	56
XVIII	Battery Assembly	58
XIX	Discharge Characteristics of GAP 4374 Battery S/N 1	60
XX	Discharge Characteristics of GAP 4374 Battery S/N 2	61
XXI	Discharge Characteristics of GAP 4374 Battery S/N 3	64

LIST OF TABLES

TABLE		PAGE
I	Effect of Sterilization on Plate Dimensions	3
II	Effect of Sterilization Cycles on Silver Oxide Electrodes	4
III	Effects of Two Sterilization Cycles on Silver Oxide Plates	6
IV	Effects of Sterilization on Electroformed Zinc Plates	15
V	Effects of 135°C Sterilization on the Surface Area of Zinc Plates	17
VI	Effect of Heat Sterilization on Separator Materials	19
VII	Absorption Characteristics of Separating Materials	20
VIII	Wicking Characteristics of Separation Material	23
IX	Effects of Heat Sterilization on the Resistance of Separator Materials	26
X	Effects of Sterilization on Cell Voltage and Capacity	28
XI	Mechanical Strengths of Sterilized and Unsterilized Polysulfone Joints	31
XII	Sterilization of Electrolyte Reservoirs	36
XIII	Performance of Gas Generator GG 208 After Sterilization	41
XIV	Effects of Sterilization on X30-50A-2 and AN583AF Propellants	42

1.0 INTRODUCTION

This report describes the development of a heat sterilizable remotely activated silver zinc battery under contract number 952214 between the Jet Propulsion Laboratory and Eagle-Picher Industries, Inc. The work was divided into two phases. The first phase consisted of a study of the effects of heat sterilization on the components for a remotely activated battery. In the second phase three prototype batteries were made from the best components. The batteries were sterilized for 128 hours at 135°C, activated and discharged. The requirements for this battery were as follows:

Capacity - 200 watt hours

Output Voltage - 26 to 30 volts D.C.

Currents - 1200 watts for 10 minutes or 500 watts for 24 minutes

Battery Seal - Hermetic

Shelf Storage - One year minimum at temperatures between -10°C and +25°C and a relative humidity less than 50%

- Nine month storage dry charged at temperatures between -10°C and +60°C

Activation - At 20°C to 45°C the battery must reach operating voltage within two minutes after application of current to gas generator.

Wet Life - The battery must be capable of performance after 30 minutes activated stand under no load.

Sterilization - The battery must be capable of performance after two cycles at 135°C for 64 hours per cycle and ethylene oxide decontamination.

1.0 INTRODUCTION (Continued)

Operating Conditions - The battery must be capable of activation under conditions of 10^{-4} mm Hg between 20°C and 45°C and zero gravity.

2.0 TECHNICAL DISCUSSION

2.1 Phase I

2.1.1 Silver Plate

Tests were conducted to determine the effects of heat sterilization on the silver plate. The tests were performed using a plate size of 2.00 inches high by 1.625 inches wide. The weights and thicknesses were varied so as to provide a range of weights and densities. In each test the final parameters measured were the discharge characteristics of the plates. This information was obtained by testing the plates in cells comprised of one positive and two negative (zinc) electrodes separated by a single layer of 2409 cotton as manufactured by Kendall Mills.

2.1.1.1 Dimensional and Weight Changes

Two characteristics of the silver oxide electrode are the increase in size and loss in weight during exposure to elevated temperatures. Studies were conducted to determine the extent of each after 128 hours of sterilization at 135°C. Plates were selected to represent a wide range of weights and densities. They were then stored in a tin container and sterilized at 135°C for 128 hours. The results may be seen in Table I.

A second set of plates was subjected to two 128 hour cycles at 135°C. Measurements were made as before. The results (see Table II) show only minor changes after those experienced during the first cycle. This indicates that

TABLE I

Effect of Sterilization on Plate Dimensions

Plate Number	Thickness (in.)		% Change	Width (in.)		% Change	Height (in.)		% Change
	Before	After		Before	After		Before	After	
1	.011	.012	+ 9.1	1.625	1.676	+3.13	1.751	1.762	+0.63
2	.011	.012	+ 9.1	1.623	1.673	+3.08	1.751	1.761	+0.57
3	.011	.0115	+ 4.5	1.625	1.679	+3.32	1.750	1.761	+0.63
4	.010	.011	+10.0	1.624	1.671	+2.89	1.750	1.755	+0.29
5	.011	.0115	+ 4.5	1.625	1.670	+2.77	1.751	1.758	+0.40
6	.011	.012	+ 9.1	1.624	1.669	+2.77	1.750	1.757	+0.40
7	.011	.012	+ 9.1	1.625	1.675	+3.07	1.751	1.757	+0.34
8	.011	.012	+ 9.1	1.625	1.674	+3.01	1.750	1.756	+0.34
9	.011	.012	+ 9.1	1.625	1.672	+2.89	1.750	1.758	+0.46
10	.010	.0115	+15.0	1.625	1.672	+2.89	1.750	1.758	+0.46
11	.010	.012	+20.0	1.625	1.680	+3.38	1.750	1.759	+0.51
12	.010	.0115	+15.0	1.625	1.680	+3.38	1.750	1.760	+0.57
13	.010	.0115	+15.0	1.625	1.674	+3.01	1.751	1.755	+0.23
14	.010	.0115	+15.0	1.625	1.668	+2.64	1.750	1.751	+0.06
15	.011	.012	+ 9.1	1.625	1.669	+2.77	1.750	1.758	+0.46

TABLE II

Effect of Sterilization Cycles
on
Silver Oxide Electrodes

Plate Number	% Loss in Weight			% Increase in Thickness			% Increase in Height			% Increase in Width		
	1st Cycle	2nd Cycle	1 & 2 Cycle	1st Cycle	2nd Cycle	1 & 2 Cycle	1st Cycle	2nd Cycle	1 & 2 Cycle	1st Cycle	2nd Cycle	1 & 2 Cycle
38	3.953	0.427	4.364	8.461	-0.709	7.692	3.999	0.048	4.049	8.430	0.283	8.739
57	4.209	0.064	4.271	10.416	0.000	10.416	4.349	0.095	4.449	8.061	-0.056	7.999
326	4.705	0.831	5.498	0.645	0.961	1.612	3.999	-0.048	3.950	9.046	-0.112	8.923
177	4.325	0.704	4.999	6.875	0.877	7.812	4.849	-0.333	4.499	8.799	0.113	8.923
296	5.025	0.522	5.521	10.370	0.671	11.111	3.950	0.048	3.999	9.661	-0.112	9.538
241	4.428	0.379	4.791	8.214	-0.990	7.142	4.749	-0.238	4.499	7.692	0.000	7.692
255	4.493	0.386	4.862	10.714	0.000	10.714	4.749	0.095	4.849	7.323	0.057	7.384

2.1.1.1 Dimensional and Weight Changes (Continued)

the plates are relatively stable after the initial sterilization cycle. The plates were discharged in cells as described previously. Plates similar to those sterilized were discharged in order to determine the total capacity loss due to sterilization. The results are discussed in section 2.1.1.4 of this report.

The average loss in capacity was 42%. Based on the data in Table II pertaining to weight loss, approximately 4% of the 42% capacity loss may be attributed to the second 128 hour, 135°C sterilization cycle. The voltages of the sterilized cells (see Table III) were characteristic of monovalent silver oxide plates.

2.1.1.2 Gassing of Silver Electrode

Since previous testing gave indications that a point of stability occurred at some time interval during sterilization at 135°C, the rate of gassing of a group of eight silver oxide electrodes was measured in an attempt to demonstrate physical dormancy. This was accomplished by sealing the plates in a tin container, placing the container inside an oven stabilized at 135°C, and measuring the gas emitted at room temperature. Readings were taken at various time intervals to establish a rate. The test consisted of two 128 hour cycles at 135°C.

A plot of gas collected with respect to time for the two cycles is shown in Figures I and II. From Figure I it can be seen that 90% of the gas measured during the first cycle was collected during the initial 24 hours of test. After 60 hours at 135°C, the plates appear to reach a point of stability. The total gas collected during the two cycles was 3430 cc's.

TABLE III

Effects of Two Sterilization Cycles
on
Silver Oxide Plates

Plate Number	Original Weight (gms)	Original Thickness (in.)	Original Density (gms/in^3)	Plateau Voltage (volts)	Open Circuit Voltage (volts)	Capacity (amp-min)	Remarks
38	7.79	.026	92.19	1.23	1.57	84	Sterilized
57	8.10	.024	103.85	1.30	1.60	84	Sterilized
326	8.33	.031	82.68	1.29	1.58	78	Sterilized
177	8.90	.032	85.58	1.24	1.58	84	Sterilized
296	7.68	.027	89.57	1.23	1.62	72	Sterilized
241	9.10	.028	100.00	1.27	1.59	88	Sterilized
255	9.48	.028	104.18	1.30	1.62	94	Sterilized
48	7.79	.026	92.19	1.33	1.85	140	Unsterilized
297	7.85	.027	89.46	1.34	1.85	140	Unsterilized
60	8.10	.025	99.69	1.36	1.85	148	Unsterilized
316	8.33	.030	85.44	1.34	1.77	162	Unsterilized
188	8.90	.032	85.58	1.28	1.85	128	Unsterilized
248	9.10	.029	96.55	1.30	1.87	144	Unsterilized
251	9.48	.028	104.18	1.33	1.90	148	Unsterilized

FIGURE I

Gassing of Silver Oxide Plates
during
Heat Sterilization
(8 Plates)
First Cycle @ 135°C

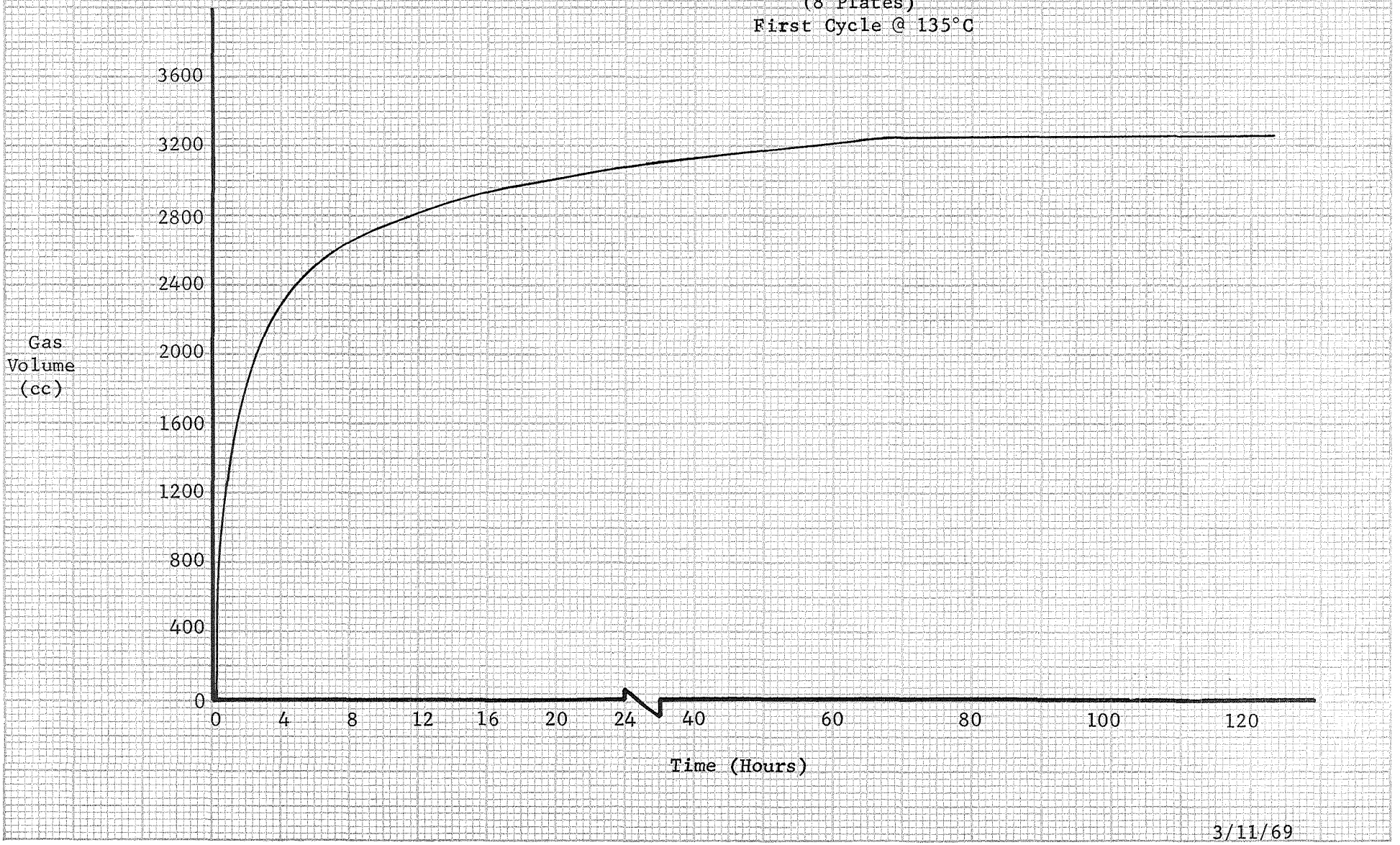

3/11/69

FIGURE II

Gassing of Silver Oxide Plates
(8 Plates)
Second Cycle @ 135°C

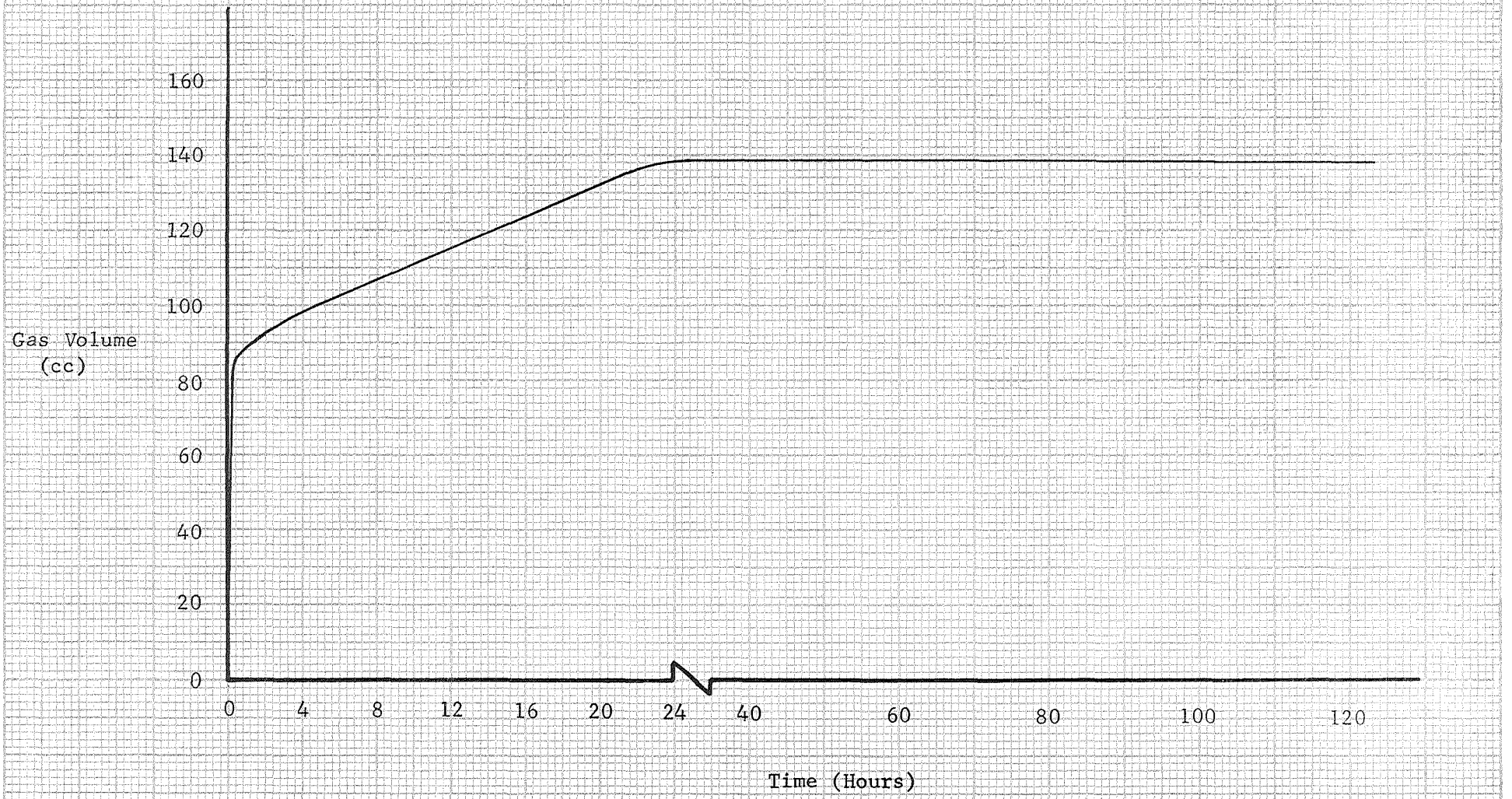

2.1.1.2 Gassing of Silver Electrode (Continued)

In order to estimate the potential gas evolution of the plates over extended storage times at 135°C, the quantity of gas collected was plotted as a reciprocal of time. This is shown in Figure III - a and b. Figure III-a indicates that a maximum gas emission of 3400 cc's would result from the plates tested. A pronounced stability is indicated by the curve depicted in Figure III-b.

2.1.1.3 Structural Changes

In view of the dimensional changes occurring in the silver oxide plaques during sterilization, the effects of sterilization on the physical structure of the plates was studied. The methods used were microscope scanning and X-ray diffraction. These studies were conducted by the University of Missouri at Rolla. In each instance the analysis was made on plates before and after sterilization.

The microscope examination was made of nine plates grouped into four weight classes. Each plate was pressed to a different thickness to establish a range of densities. Observations were made of the flat surface and transverse sections of the plates. Magnifications of 300X and 1000X were used. Photographs may be seen in Appendix I.

The transverse shots revealed variations in density through the thickness of the electrodes. This was due to the pressing operation and pressure variations through the thickness caused by both depth and the presence of the silver grid. In general, however, the electrode structure was fairly uniform.

One noteworthy feature was the very angular nature and large overall size of the AgO at lower weights and density. The porosity or void area was also extensive for these electrodes. Both the structure and void area changed

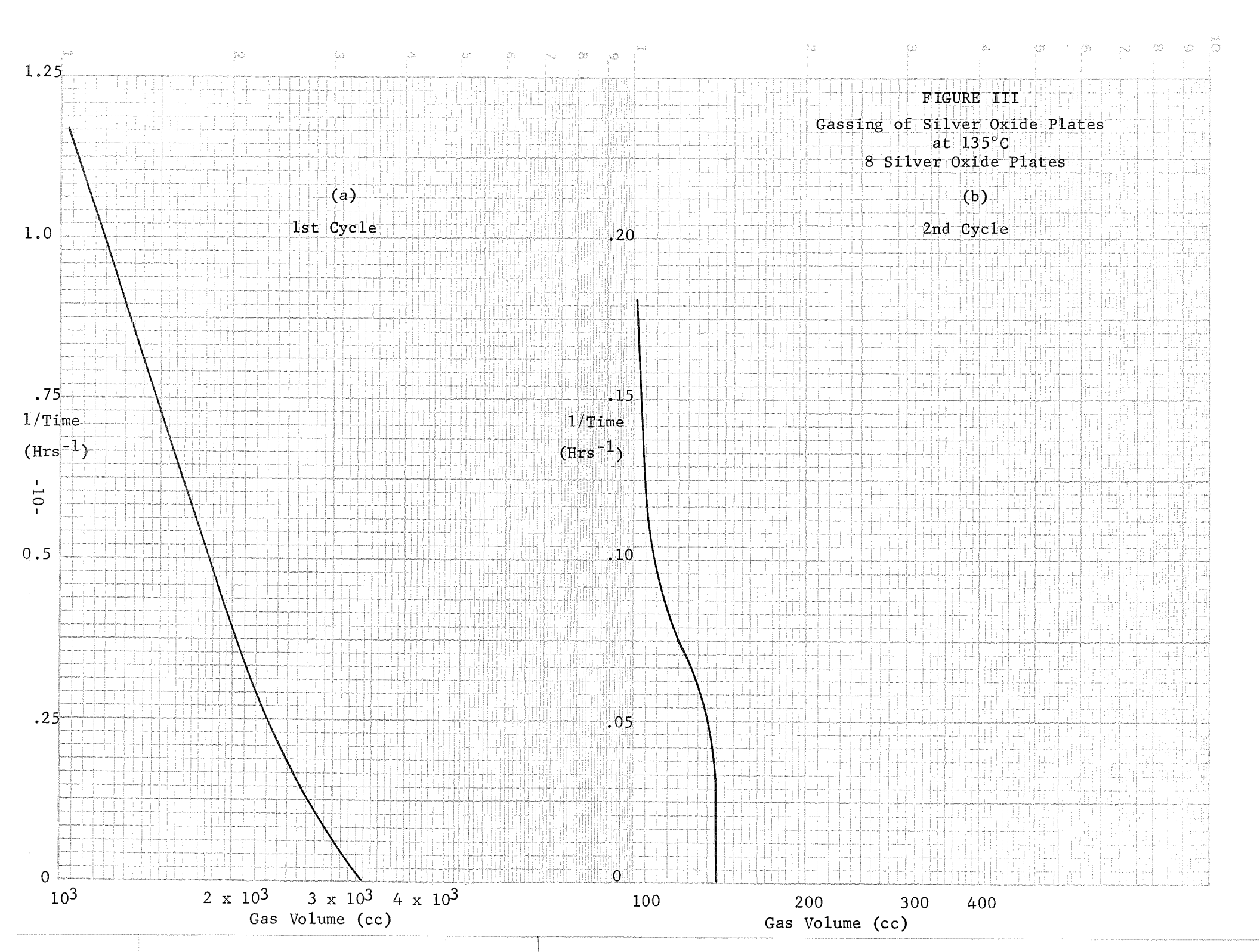
FIGURE III
Gassing of Silver Oxide Plates
at 135°C
8 Silver Oxide Plates
(a)
1st Cycle
(b)
2nd Cycle
1/Time
(Hrs-1)
1.25
1.0
.75
0.5
.25
0
.20
.15
.10
.05
0
10³
2 x 10³
3 x 10³
4 x 10³
100
200
300
400
Gas Volume (cc)
Gas Volume (cc)

2.1.1.3 Structural Changes (Continued)

considerably with increased weight and density. The angularity was not evident and the particles tended to form a more continuous mass, made up of smaller, more rounded agglomerated particles.

The angular particles ranged from a maximum in the range of 10 microns for one particle down to one micron or less. The smaller particles appeared to be more agglomerated, whereas the larger ones retained their identity and remained more separated from the mass. No two specimens were necessarily alike, but arrangement into a scale from very angular and open to agglomerated and dense would be possible.

In some cases it was difficult to obtain a clean, even break on the transverse sections, so it is possible that a few of the pictures could have been misleading.

The sterilized samples were very brittle and susceptible to crumbling. Because of the difficulty in getting a good sample, only surface shots were made.

The structures of all the samples appeared to become much more similar after sterilization. An overall agglomeration occurred with less apparent void space. There were no longer any of the individual angular particles that were present initially. All the particles appeared to be made up of a large number of small particles of about micron size.

The particles appeared to result from some growth mechanism outward from the starting particle. All the electrodes after heating approached the structure that the denser, heavier plates possessed before heating, namely the agglomerated small particle-type structure. There was also a needle type growth in a few areas on some of the electrodes (see Appendix I).

2.1.1.3 Structural Changes (Continued)

In general, there was much less uniformity over the entire surface area of a sterilized electrode than in the initial unsterilized plates, even though all the samples approached the same type. In other words, the majority of the electrodes will have similar areas, but the color, phases, and structure are more prone to vary within any one given electrode.

X-rays were made primarily on one set of electrodes with common weights but varying densities. Patterns were made on the whole surface as well as of powders made by grinding up pieces taken from the electrodes.

Initially, the only phase present was AgO. After sterilization at 135°C for 128 hours, the samples appeared to be of a uniform dark to black color. Upon cooling a more mottled look appeared. The colors ranged from a light tan to intermediate shades of grey-brown to almost black. In examining surface X-rays of sterilized plates, the samples were different in many respects. However, the powdered samples of these materials were very similar. This would indicate that either only the surface has any variations, or that the method of preparing the powdered specimens causes preferred phases to be collected. For example, a brittle phase (oxide, carbonate) would remain fine grained and powdery, while a ductile phase (silver) would agglomerate and flatten out being less likely to remain on the glass slide used to hold the powder for X-ray.

The surface samples appeared to be predominantly Ag and Ag_2O, with possibly a small amount of $AgCO_3$. When powdered, a considerable amount of $AgCO_3$ was found to be present. This may not be representative of the amount in the plate, but it does show that this phase is present in all three. The carbonate may have been introduced during the formation cycle of the plates.

2.1.1.4 Electrical Characteristics

The silver oxide electrodes described in paragraph 2.1.1.1 were used to build cells which were discharged at a constant 4 ampere rate. Plates subjected to a single sterilization cycle experienced a nominal 38% loss in capacity. After two sterilization cycles the loss was found to average 42%. In each case the loss was determined by unsterilized control cells. The results may be seen in Table III. The cell voltages after sterilization were characteristic of monovalent silver oxide.

During the course of Phase I of the contract it was decided that a regression of data gathered might provide some insight into the influence of the various physical parameters on the electrical characteristics of the sterilized plates. With 90.7% of the capacity accounted for and a standard error of estimate of 5.76 the prediction equation would be:

$$\text{Capacity} = 84.07 + 92.54A - 42.81B - 3.06C - 37.47\,A^3 - 12.63\left[\frac{D_2 - D_1}{D_1}\right](100)$$

where: A = Original plate weight (gms)

B = Final plate weight (gms)

C = Original plate density (gms/in^3)

D_1 = Original plate width (in)

D_2 = Final plate width (in)

The effects of heat sterilization are indicated by the significance of the final plate weight and dimensional change in the equation.

Since the dimensional changes resulted in significant effects on the capacity of the silver oxide electrode, another regression was performed to determine which controllable parameters cause the changes. This analysis

2.1.1.4 Electrical Characteristics (Continued)

showed greater values of the density and thickness to be concomitant with decreased plate expansion. Since density is a function of the reciprocal of the thickness, a value of density could be obtained to minimize the dimensional variations and capacity losses.

2.1.2 Zinc Plate

Tests similar to those performed with silver oxide plates were made using zinc electrodes. These included studies of dimensional stability. A 2.00 inch high by 1.625 inch wide plate size was used. Electrical characteristics of the material were measured in cells using a single zinc plate separated between two silver plates by 2409 webril.

2.1.2.1 Dimensional and Weight Changes

Zinc electrodes were found to experience no significant dimensional changes after sterilization. However, an average gain in weight of .07 gram per plate was measured. Assuming the gain in weight is oxygen, the theoretical capacity loss would be 14 ampere minutes. Discharges of these plates reflected the weight gain in that when compared to unsterilized plates of comparable weights an average capacity loss of 15.6 ampere minutes was calculated. This represents a loss of approximately 18% of the original capacity. Data from these discharges may be seen in Table IV.

2.1.2.2 Structural Changes

Since previous studies of the zinc plates showed a small weight increase accompanied by a loss in capacity, it was suspected that the increase in weight was oxygen. In order to verify the oxidation during heat sterilization, studies were made at the University of Missouri at Rolla to determine

TABLE IV

Effects of Sterilization
on
Electroformed Zinc Plates

Plate Number	Unsterilized Weight (gms)	Sterilized Weight (gms)	Weight Gain (gms)	Plateau Voltage (volts)	Open Circuit Voltage (volts)	Capacity (amp-min)	Remarks
208	4.11	4.21	.10	1.38	1.83	76	Sterilized
205	4.14	4.25	.11	1.40	1.83	76	Sterilized
376	4.15	4.20	.05	1.36	1.85	76	Sterilized
242	4.21	4.29	.08	1.38	1.85	69	Sterilized
203	4.22	4.31	.09	1.41	1.86	88	Sterilized
134	4.40	4.45	.05	1.39	1.85	84	Sterilized
19	4.40	4.46	.06	1.38	1.85	88	Sterilized
145	4.40	4.45	.05	1.42	1.85	96	Sterilized
251	4.40	4.48	.08	1.37	1.84	92	Sterilized
202	4.40	4.45	.05	1.38	1.86	76	Sterilized
44	4.66	4.73	.06	1.38	1.85	88	Sterilized
143	4.66	4.73	.07	1.39	1.85	80	Sterilized
313	4.66	4.73	.07	1.38	1.84	79	Sterilized
233	4.67	4.73	.06	1.37	1.84	96	Sterilized
264	4.99	5.04	.05	1.36	1.84	88	Sterilized
175	5.00	5.03	.03	1.41	1.85	96	Sterilized
59	5.04	5.11	.07	1.39	1.85	96	Sterilized
191	5.34	5.37	.03	1.39	1.85	96	Sterilized
77	4.89			1.42	1.85	114	Unsterilized
102	4.73			1.39	1.84	94	Unsterilized
115	4.40			1.42	1.84	100	Unsterilized
132	4.89			1.40	1.84	108	Unsterilized
192	4.73			1.41	1.85	112	Unsterilized
254	4.23			1.42	1.85	92	Unsterilized
285	4.40			1.42	1.85	107	Unsterilized
306	4.23			1.42	1.85	108	Unsterilized

2.1.2.2 Structural Changes (Continued)

the effects of heat sterilization on the crystalline structure, porosity, and surface area of the zinc plate. Phase study determinations (X-ray) as well as microscope scanning shots (Appendix II) were made of several plates. There did not appear to be an appreciable oxidation of the zinc electrodes. The X-rays taken before and after sterilization were essentially identical, with only a zinc phase appearing. No evidence of an extensive amount of a ZnO phase was found. As can be seen from the microscope scanning shots in Appendix II, no appreciable structural changes occurred during heat sterilization. Also, by visual inspection the porosity of the plates appeared to remain the same.

A two plate study was conducted at the American Instruments Company to verify the lack of physical change of the zinc electrode. B.E.T. measurements were made before and after sterilization. The tests indicated very little change, if any, in the surface area of the test samples. The results are shown in Table V. The variances between the unsterilized and sterilized readings are within the error of the technique.

2.1.3 Separator

Since the requirements of the contract involve a remotely activated battery with a relatively short wet life, only absorbent materials were selected for study. The properties deemed most desirable in this instance are: physical stability during dry sterilization, good electrolyte absorption, wicking and retention properties, and low electrical resistivity in a 1.30 specific gravity solution of potassium hydroxide.

TABLE V

Effects of 135°C Sterilization
on the
Surface Area of Zinc Plates

Plate Number	Condition	B.E.T. Measurement (square meters/gram)
43	Unsterilized	6.1
	Sterilized	5.8
312	Unsterilized	3.6
	Sterilized	4.8

2.1.3.1 Dimensional and Weight Changes

Separator materials were screened via dry sterilization. The procedure involved measurements of sample length, width and weight before and after sterilization. Length and width were measured to the nearest 1/64th of an inch and weight to the nearest milligram. All test specimens were cut to 2.0 inches by 5.0 inches. Each was measured and then suspended in an oven maintained at 135°C for a period of 120 hours. The results are shown in Table VI in the form of percent change. In general, those least affected were pure nylon (items 11 and 12), cellulosics (items 23-25), and asbestos (items 1-10). Polypropylene material (items 20-22) were severely affected.

2.1.3.2 Wetting Characteristics

The ability of the materials, observed to have successfully passed 135°C heat sterilization, to absorb and retain electrolyte was studied. Absorption was determined by immersing the samples into a 1.30 specific gravity solution of potassium hydroxide, removing any droplets formed while suspending the sample and comparing weights prior to and after immersion. Since the value of absorption by weight may be misleading, the calculated value of the amount of electrolyte retained was also tabulated. Results of the study are shown in Table VII. Asbestos samples exhibited little change. Nylon material had better absorption subsequent to sterilization. As would be expected the cotton material (items 39-42) had the highest absorption by weight and amount of electrolyte.

Another characteristic of the materials determined was the ability to absorb electrolyte above the liquid level. This was accomplished by marking the separator in one-half inch graduations. It was then immersed into a 1.30 specific gravity solution of electrolyte to the level of the

TABLE VI

Effect of Heat Sterilization on Separator Materials

Item Number	Material Type	Description	Supplier	Average (±.5%) Dimensional Change (%)		Average (±.01%) Weight Change (%)	Appearance
				Width	Length		
1	Asbestos	.010 Sintered	Johns-Manville	- .01	+ .12	+ .58	No Change
2	Asbestos	.020 Sintered	Johns-Manville	- .32	- .02	+ .42	No Change
3	Asbestos	.010 As Required	Johns-Manville	+ .15	- .04	+ .39	No Change
4	Asbestos	.020 As Required	Johns-Manville	+ .25	- .12	+ .10	No Change
5	Asbestos	7410 40% Glass	Raybestos	- .18	+ .18	-1.69	No Change
6	Asbestos	7410/5 40% Glass	Raybestos	- .05	+ .29	-1.33	No Change
7	Asbestos	7401 5% Binder	Raybestos	- .12	+ .33	-1.80	No Change
8	Asbestos	7401/5 5% Binder	Raybestos	- .35	+ .06	-2.66	No Change
9	Asbestos	7301 Sintered	Raybestos	- .12	- .07	-1.04	No Change
10	Asbestos	7301/5 Sintered	Raybestos	- .12	- .08	- .08	No Change
11	Nylon (100%)	Non-Woven KS-900	Kimberly-Stevens	+ .12	+ .75	-1.56	Slight Yellowing
12	Nylon (100%)	Woven 9031	Stern & Stern	- .41	- .51	+ .02	Slight Yellowing
13	Nylon/Dynel	75/25 M1406	Kendall Mills	-1.72	-1.61	-2.10	Brown
14	Nylon/B	2504K	Pellon Corp.	-1.87	-4.12	-6.10	Dark Brown
15	Nylon/B	2505	Pellon Corp.	-3.18	-1.39	-2.90	Yellow
16	Nylon/B	2505K	Pellon Corp.	-1.25	-2.49	-2.98	Yellow, Distorted
17	Nylon/B	2505ML	Pellon Corp.	-5.57	-2.32	-8.77	Dark Yellow, Distorted, Separated
18	Nylon/B	2506K	Pellon Corp.	-3.99	-2.94	-9.63	Yellow, Brittle
19	Nylon/B	2506ML	Pellon Corp.	-1.50	-3.77	-7.05	Yellow, Distorted
20	Nylon/PP	SM124.3	Kendall Mills	-28.48	-14.78	-9.00	Yellow, Distorted, Swelled
21	Polypropylene	EM476	Kendall Mills	---	---	---	Disintegrated
22	Polypropylene	2530	Pellon Corp.	---	---	---	Disintegrated
23	Rayon	R75D	Chicopee Mills	-2.24	-1.09	+1.81	Light Yellow, Distorted
24	Cotton	2409	Kendall Mills	+ .05	- .64	-2.64	Slight Discoloration
25	Hemp	Filpaco 4366T	Dexter	- .44	- .60	-1.37	Slight Discoloration

TABLE VII

Absorption Characteristics of Separating Materials

Item Number	Material Type	Description	Supplier	A Dry Wt. (gms)	B Wet Wt. (gms)	Absorption of KOH by Wt. $\frac{B-A}{A}$	Absorption of KOH Amount (cc)	Sterilized
1	Asbestos	.010 as Required	Johns-Manville	1.20	3.55	1.96	1.81	Yes
2				1.20	3.97	2.13	2.13	No
3	Asbestos	.020 as Required	Johns-Manville	2.75	10.20	3.71	5.72	Yes
4				2.67	9.82	3.68	5.50	No
5	Asbestos	7410 40% Glass	Raybestos	.55	3.77	5.85	2.48	Yes
6				.60	3.66	5.10	2.35	No
7	Asbestos	7410/5 40% Glass	Raybestos	.40	2.85	6.13	1.88	Yes
8				.41	2.76	5.73	1.80	No
9	Asbestos	7401 5% Binder	Raybestos	.25	2.00	7.00	1.34	Yes
10				.25	2.46	8.82	1.70	No
11	Asbestos	7401/5 5% Binder	Raybestos	.36	3.25	8.02	2.22	Yes
12				.39	3.60	8.23	2.47	No
13	Asbestos	7301 Sintered	Raybestos	.30	1.87	5.23	1.21	Yes
14				.27	1.57	4.81	1.00	No
15	Asbestos	7301/5 Sintered	Raybestos	.32	1.50	3.69	0.91	Yes
16				.29	1.30	3.48	0.78	No
17	Nylon (100%)	Non-Woven KS-900	Kimberly-Stevens	.40	2.66	5.64	1.74	Yes
18				.48	2.10	3.38	1.24	No
19	Nylon (100%)	Woven 9031	Stern & Stern	.30	.94	2.13	0.49	Yes
20				.31	.93	2.00	0.48	No
21	Nylon/Dynel	75/25 M1406	Kendall Mills	.19	1.70	7.95	1.16	Yes
22				.23	1.19	4.18	0.74	No
23	Nylon/B	2504K	Pellon Corp.	.20	1.40	6.00	0.92	Yes
24				.23	.98	3.26	0.58	No
25	Nylon/B	2505	Pellon Corp.	.40	3.23	7.08	2.18	Yes
26				.40	2.50	5.25	1.62	No

TABLE VII (Continued)

Absorption Characteristics of Separating Materials

Item Number	Material Type	Description	Supplier	A Dry Wt. (gms)	B Wet Wt. (gms)	Absorption of KOH by Wt. $\frac{B-A}{A}$	Absorption of KOH Amount (cc)	Sterilized
27	Nylon/B	2505K	Pellon Corp.					Yes*
28				.39	1.54	2.95	0.89	No
29	Nylon/B	2505ML	Pellon Corp.	.38	12.52	31.90	9.32	Yes
30				.47	4.54	8.67	3.13	No
31	Nylon/B	2506K	Pellon Corp.	.36	1.36	2.77	0.77	Yes
32				.37	1.03	1.78	0.51	No
33	Nylon/B	2506ML	Pellon Corp.	.31	2.87	6.75	1.92	Yes
34				.37	2.87	6.75	1.92	No
35	Nylon/PP	SM124/3	Kendall Mills	.37	1.00	1.70	0.48	Yes
36				.43	1.85	3.30	1.09	No
37	Polypropylene	EM476	Kendall Mills					Yes*
38				.12	.28	1.33	0.12	No
39	Polypropylene	2530	Pellon Corp.					Yes*
40				.77	2.73	2.55	1.51	No
41	Rayon	R75D	Chicopee Mills	.38	3.50	8.20	2.40	Yes
42				.41	3.87	8.45	2.66	No
43	Cotton	2409 -	Kendall Mills	.80	14.00	16.50	10.15	Yes
44				.92	15.03	16.40	10.83	No
45	Cotton	2409	Kendall Mills	.79	13.99	16.70	10.15	Yes
46				.95	15.06	14.80	10.83	No
47	Hemp	Filpaco 4366T	Dexter	.17	1.59	8.35	1.09	Yes
48				.17	1.79	9.54	1.24	No
49	Hemp	Filpaco 4366T	Dexter	.19	1.42	6.47	0.94	Yes
50				.19	1.69	7.90	1.15	No

*Sample destroyed during the heat sterilization cycle

2.1.3.2 Wetting Characteristics (Continued)

first graduation. The time required for the material to absorb electrolyte to each graduation was measured. The data are tabulated in Table VIII. The cotton separator (items 23-25) exhibited the highest level of capillarity and absorbed the solution most rapidly.

2.1.3.3 Electrical Resistivity

The values for the resistance of various open type separators were measured. This was done by installing the material in the fixture shown in Figure IV and applying a 0.5 ampere current across the electrodes with a 1000 Hz A.C. voltage. The voltage drop before and after installation of the separator was measured.

Unsterilized and sterilized samples were measured. Two layers of material were used in order to obtain a voltage differential sufficient to calculate accurate values for the resistance. Since the materials used were essentially open separators, the value of resistance with respect to the number of layers should be relatively linear.

The results of the study are shown in Table IX. Sterilization apparently causes a more constant and usually a lower resistivity. In almost every instance the values after sterilization were either equal to or slightly greater than the value recorded after a 24 hour soak in a 1.30 specific gravity solution of potassium hydroxide.

2.1.4 Electrolyte Solution

A study was made to determine the effects of heat sterilization and concentration of electrolyte on the electrical characteristics of silver oxide zinc cells. The tests involved combinations of unsterilized cells with

TABLE VIII

Wicking Characteristics of Separation Material

Item Number	Material Type	Description	Supplier	Wicking Time (sec) 1/2"	1"	1 1/2"	2"	Sterilized	Remarks
1	Asbestos	.010 As Required	Johns-Manville					Yes No	After 5 min. 1/8" rise Held @ 1/4"
2	Asbestos	.020 As Required	Johns-Manville	300				Yes No	After 5 min. 7/16"rise
3	Asbestos	7410 40% Glass	Raybestos	120 83	300			Yes No	Held @ 1 1/4"
4	Asbestos	7410/5 40% Glass	Raybestos	298 255				Yes No	
5	Asbestos	7401/5 5% Binder	Raybestos	105 83				Yes No	
6	Asbestos	7301/5 Sintered	Raybestos					Yes No	Held @ 7/16" Held @ 7/16"
7	Nylon (100%)	Non-Woven KS-900	Kimberly-Stevens	240				Yes No	No wicking
8	Nylon (100%)	Woven 9031	Stern & Stern					Yes No	No wicking No absorption
9	Nylon/Dynel	75/25 M1406	Kendall Mills					Yes No	No absorption No wicking
10	Nylon/B	2504K	Pellon Corp.	70				Yes No	No wicking
11	Nylon/B	2505	Pellon Corp.					Yes No	No wicking No wicking
12	Nylon/B	2505K	Pellon Corp.	300 138				Yes No	Held @ 7/16"
13	Nylon/B	2505ML	Pellon Corp.	45	168			Yes No	No wicking

TABLE VIII (Continued)

Wicking Characteristics of Separation Material

Item Number	Material Type	Description	Supplier	Wicking Time (sec) 1/2"	1"	1 1/2"	2"	Sterilized	Remarks
14	Nylon/B	2506K	Pellon Corp.	42				Yes No	Held @ 1/8"
15	Nylon/B	2506ML	Pellon Corp.	223				Yes No	No wicking
16	Rayon	R75D	Chicopee Mills	19 7	70 23	47	85	Yes No	
17	Cotton	2409	Kendall Mills	33	54	165		Yes	
18	Cotton	2409	Kendall Mills	23	45	170		Yes	
19	Cotton	2409	Kendall Mills	19	32	70		Yes	
20	Hemp	Filpaco 4366T	Dexter					Yes	No wicking

FIGURE IV

Fixture for Separator Resistance Measurement

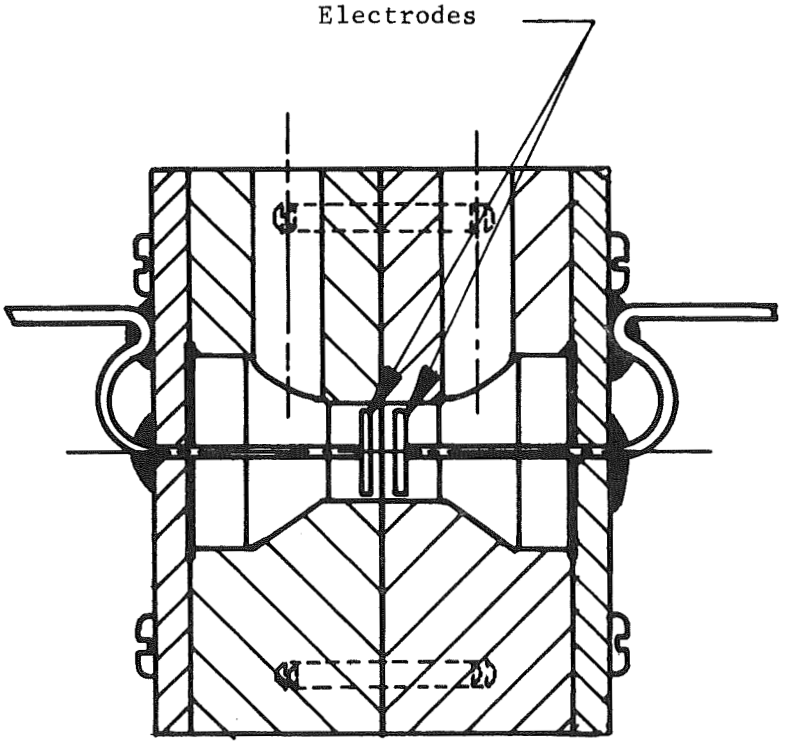

TABLE IX

Effects of Heat Sterilization
on the
Resistance of Separator Materials

Sample Number	Material Type	Description	Supplier	E*	Layers Tested	Resistance/Layer (ohms) 0.5 min.	5 min.	24 hrs.	Status
1	Asbestos	7410 40% Glass	Raybestos	.13	2	0.0235	0.0235	0.0039	Unsterilized
2				.15	2	0.037	0.029	0.029	Sterilized
3	Asbestos	7410/5 40% Glass	Raybestos	.03	2	0.0058	0.0058	0.002	Unsterilized
4				.03	2	0.0058	0.0058	0.0039	Sterilized
5	Asbestos	7401/5 5% Binder	Raybestos	.03	2	0.0058	0.0058	0.002	Unsterilized
6				.02	2	0.0058	0.0039	0.0039	Sterilized
7	Asbestos	7401 5% Binder	Raybestos	.02	2	0.0039	0.0039	0.002	Unsterilized
8				.01	2	0.002	0.002	0.002	Sterilized
9	Nylon/B	2504K	Pellon Corp.	.03	2	0.0058	0.0058	0.0039	Unsterilized
10				.02	2	0.0058	0.0039	0.0039	Sterilized
11	Nylon/B	2505	Pellon Corp.	.04	2	0.0098	0.0078	0.0058	Unsterilized
12				.03	2	0.0058	0.0058	0.0058	Sterilized
13	Nylon/B	2505K	Pellon Corp.	.04	2	0.0078	0.0078	0.0058	Unsterilized
14				.05	2	0.0118	0.0098	0.0098	Sterilized
15	Nylon/B	2505ML	Pellon Corp.	.04	2	0.0078	0.0078	0.0039	Unsterilized
16				.08	2	0.0156	0.0078	0.0078	Sterilized
17	Nylon/B	2506K	Pellon Corp.	.08	2	0.0156	0.0156	0.0118	Unsterilized
18				.07	2	0.0137	0.0137	0.0137	Sterilized
19	Nylon/B	2506M	Pellon Corp.	.04	2	0.037	0.0078	0.0058	Unsterilized
20				.11	2	0.035	0.0215	0.0196	Sterilized
21	Rayon	R75D	Chicopee Mills	.04	2	0.0078	0.0078	0.0058	Unsterilized
22				.04	2	0.0098	0.0078	0.0078	Sterilized
23	Cotton	2409	Kendall Mills	.03	2	0.0058	0.0058	0.0039	Unsterilized
24				.06	2	0.0118	0.0058	0.0058	Sterilized
25	Hemp	Filpaco 4366T	Dexter	.02	2	0.0039	0.0039	0.002	Unsterilized
26				.01	2	0.002	0.002	0.002	Sterilized

*This is the differential voltage between readings taken without separator and with separator.

2.1.4 Electrolyte Solution (Continued)

unsterilized electrolyte, unsterilized cells with sterilized electrolyte, and sterilized cells with sterilized electrolyte. Four concentrations of electrolyte were used in each group. The cells consisted of one positive and two negative plates cut 2.00 inches high by 1.62 inches wide. A single layer of Kendall Mills' 2409 cotton was used to separate the plates. Each cell was discharged at a 4.0 ampere rate to an end voltage of 1.00 volt. The results are shown in Table X.

By analyzing the data statistically, the capacity of the cells was found to be independent of the concentration or sterilization condition of the electrolyte. With more than 99% of the variance explained, the capacity was found to be dependent on the state of sterilization of the cell and the original weights of the positive and negative plates. The plateau voltage was found to be dependent on the specific gravity of the potassium hydroxide.

2.1.5 Cell Case and Cell Case Sealing

During the contract several types of thermoplastics were investigated. A careful study of manufacturer's performance data for polysulfone, polyphenylene oxide, and polycarbonate materials was conducted followed by a few cursory experiments. As a result, polysulfone was selected for use. This material offered several factors desirable for a fabricated cell case. Among these were the ability to successfully join the material with solvents, reasonable strength and the ability to see through the material.

2.1.5.1 Sealing

It was determined that, in order to successfully join polysulfone, a vacuum cure of 72 hours at 80°C is required after joining. Without this cure,

TABLE X

Effects of Sterilization
on
Cell Voltage and Capacity

Cell		Electrolyte		Plate Wts. (gms)		Voltage		Capacity
Number	Sterilized	Sp.Gr.	Sterilized	Positive	Negative	Plateau	Open Circuit	(amp-min)
1	No	1.30	Yes	8.39	4.45 4.42	1.40	1.68	172
2	No	1.35	Yes	8.20	4.37 4.41	1.38	1.85	160
3	No	1.40	Yes	8.83	4.45 4.42	1.37	1.85	182
4	No	1.45	Yes	8.20	4.38 4.19	1.36	1.84	164
5	No	1.30	Yes	9.00	4.18 4.43	1.39	1.84	184
6	No	1.35	Yes	8.86	4.65 4.24	1.37	1.84	172
7	No	1.40	Yes	8.65	4.14 4.22	1.38	1.84	182
8	No	1.45	Yes	8.65	4.30 4.37	1.36	1.85	176
9	No	1.30	No	8.00	4.85 4.39	1.38	1.86	152
10	No	1.35	No	8.20	4.41 4.32	1.39	1.85	164
11	No	1.40	No	7.82	4.25 4.58	1.37	1.85	154
12	No	1.45	No	8.40	4.63 4.60	1.36	1.85	166

TABLE X (Continued)

Effects of Sterilization
on
Cell Voltage and Capacity

Cell		Electrolyte		Plate Wts. (gms)		Voltage		Capacity
Number	Sterilized	Sp.Gr.	Sterilized	Positive	Negative	Plateau	Open Circuit	(amp-min)
13	No	1.30	No	8.83	4.65 4.80	1.38	1.87	168
14	No	1.35	No	8.10	4.57 4.82	1.38	1.87	148
15	No	1.40	No	9.05	4.58 4.58	1.37	1.85	186
16	No	1.45	No	8.48	4.44 4.27	1.34	1.85	164
17	Yes	1.30	Yes	7.74	4.32 4.32	1.38	1.61	84
18	Yes	1.35	Yes	8.32	4.43 4.41	1.39	1.62	86
19	Yes	1.40	Yes	8.95	4.46 4.51	1.38	1.62	96
20	Yes	1.45	Yes	7.90	4.60 4.59	1.34	1.64	84
21	Yes	1.30	Yes	8.96	4.93 4.31	1.40	1.61	96
22	Yes	1.35	Yes	8.85	4.56 4.26	1.39	1.63	94
23	Yes	1.40	Yes	8.65	4.52 4.34	1.36	1.63	92
24	Yes	1.45	Yes	9.00	4.78 4.35	1.37	1.63	96

2.1.5.1 Sealing (Continued)

the joints outgas during sterilization, causing bubbling and weakening of the joint. The combination of vacuum and temperature permit the gradual removal of the solvent without weakening the bond.

2.1.5.2 Physical Properties

Tests were made to determine certain physical characteristics of the polysulfone material. Among these were the effect of heat sterilization on the physical strength of the material and on areas bonded with solvent. Resistance of the polysulfone to a 1.30 specific gravity solution of potassium hydroxide was also verified through sterilization temperatures as well as by electrical discharge of cells contained in sealed fabricated cell cases.

2.1.5.2.1 Mechanical Tests

Mechanical tests were performed to determine the strength of polysulfone solvent bonds before and after heat sterilization. The parts were joined or sealed with methylene chloride. Residual solvent was removed from the weld area by the vacuum cure described previously. The vacuum was maintained below 300 microns absolute pressure. The results of the tests are shown in Table XI.

Tensile and shear specimens were prepared for testing as follows: The tensile samples were tapered to obtain a joint approximately 0.5 inch in width by 0.125 inch in thickness. Those prepared for shear testing were made with an overlap of approximately 0.6 inch with a width of 1.0 inch. Conventional test equipment and a cross head speed of 0.25 in/min were used to break the samples. The parts were positioned in the jaws according to the type break desired. The shear specimens tested had some bending introduced as a result of

TABLE XI

Mechanical Strengths of Sterilized
and Unsterilized Polysulfone Joints

Sample	Area of Fracture (sq.in.)	Load at Failure (psi)	Stress (psi)	Sterilized	Remarks
1	.128	430	3360	Yes	Lap joint, failed adjacent to joint
2	.127	460	3630	No	Lap joint, failed adjacent to joint
3	.128	320	2500	Yes	Lap joint, failed adjacent to joint
4	.128	550	4300	No	Lap joint, failed adjacent to joint
5	.0631	200	3170	Yes	Butt joint, failed at joint
6	.0562	300	5330	Yes	Butt joint, failed at joint
7	.0602	100	1660	No	Butt joint, failed at joint
8	.0610	200	3280	No	Butt joint, failed at joint
9	2.828 x 1.375	85	*	Yes	Cell case, failed at wall described
10	2.828 x 1.375	90	*	Yes	Cell case, failed at wall described
11	2.828 x 1.375	175	*	No	Cell case, failed at wall described
12	2.828 x 1.375	140	*	No	Cell case, failed at wall described

* Value not determined

2.1.5.2.1 Mechanical Tests (Continued)

the positioning in the jaws. The breaks occurred adjacent to the lap joints. Loads ranging between 320 and 550 pounds were recorded at the time of fracture. Assuming strictly tensile loading, this represents stresses of approximately 2500 to 4300 psi. Samples broken in direct tension failed within a range of 100 to 300 pounds. This represents stresses of 1660 to 5330 psi. In both the shear and tensile tests, the sterilized samples fell in the middle or upper half of the values. Since the strength of a polysulfone joint is affected by the amount of pressure applied during the juncture, it may be assumed that the low values of strength were at least in part due to insufficient pressure.

Tests conducted with molded polysulfone cell cases provide more definitive information concerning the effects of heat sterilization. Four cases molded from 1700 grade polysulfone were sealed with methylene chloride and exposed to a reduced atmosphere of 300 microns and 80°C for 72 hours. Two of the four were sterilized at 135°C for 128 hours. A pressure increase of 0.5 psi/sec was used to break each case in order to permit a visual inspection for crazing. No crazing was seen prior to actual failure of the part. Each part failed at the major surface of 1.37 inches by 2.828 inches with a wall thickness of 0.068 inch. An apparent loss in strength was found after sterilization. Cases which had been sterilized failed at 85 and 90 psig while those unsterilized ruptured at 140 and 175 psig. This represents a reduction in strength of approximately 40%.

2.1.5.2.2 Chemical Resistance

Since the primary function of the cell case material is to contain the cell activated with a solution of potassium hydroxide during electrical discharge, it was important that the capabilities of the material be verified

2.1.5.2.2 Chemical Resistance (Continued)

after heat sterilization. Several cell cases molded from 1700 grade polysulfone were partially filled with a 31% potassium hydroxide solution, sealed with methylene chloride and subjected to 135°C for 128 hours. No degradation or leakage was found after sterilization.

2.1.6 Battery Container

Since the battery had to survive heat sterilization and ETO decontamination, stainless steel was selected as the material best suited for the battery case.

2.1.7 Electrolyte Solution Reservoir

The effects of heat sterilization on two types of reservoirs commonly used in Eagle-Picher remotely activated batteries were determined. The two configurations are shown in Figures V and VI. Both were basically tubular copper reservoirs sealed at each end with two frangible copper diaphragms. The diaphragms were separated by a void of approximately 1.5 cc. Each reservoir was filled with a 31% solution of potassium hydroxide to 93% of capacity. The remaining 7% was air. At one end of the reservoir an adaptor was attached to provide a means of connecting the reservoir to the battery manifold. A brass fitting to accept the gas generator was silver brazed to the remaining end. Measurements of length were taken at the points indicated in Figures V and VI. The weight of each was also recorded. After exposure to 135°C for 128 hours the same measurements were taken while the reservoirs were still warm. The results may be seen in Table XII.

Visual examination of the reservoirs immediately after the sterilization cycle revealed no deterioration. The diaphragms contained the electrolyte and

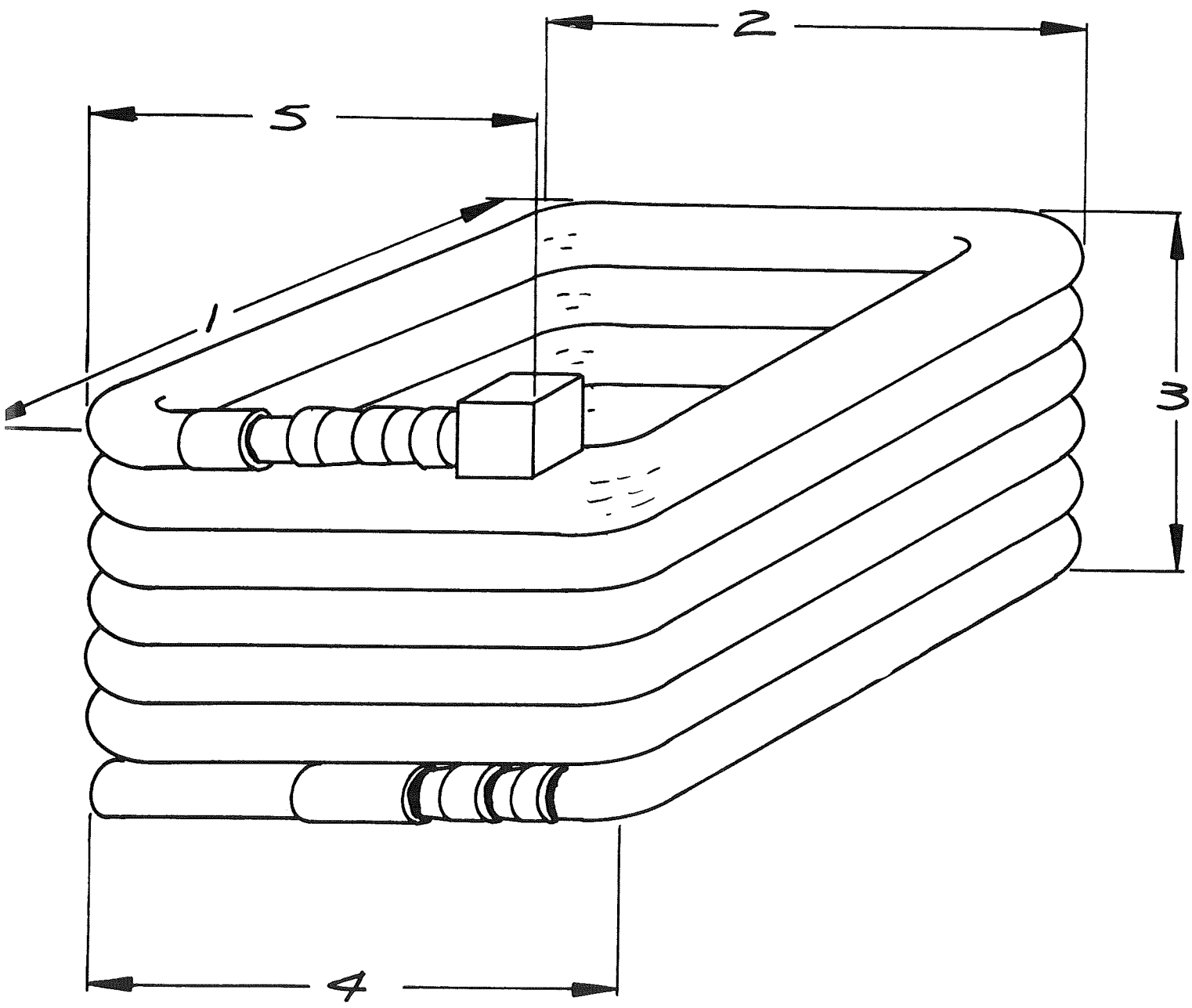

FIGURE V

BA 472/U

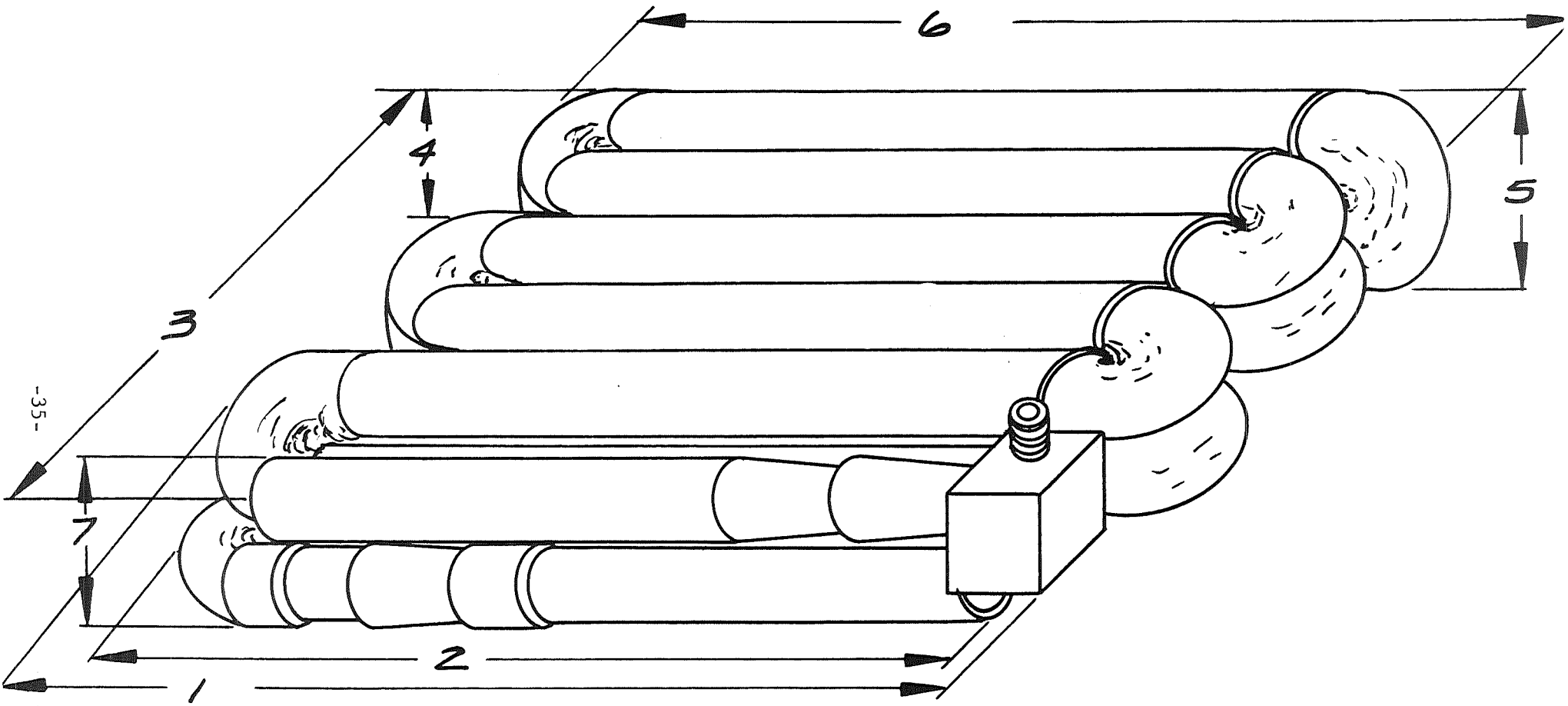

FIGURE VI

GAP 4230

TABLE XII

Sterilization of Electrolyte Reservoirs

Reservoir	Dimension	Before Sterilization	After Sterilization (warm)	% Change	Weight (gms)		% Change
					Before	After	
BA 472/U	1	5.691	5.712	+0.37	967	961	-0.62
	2	5.705	5.724	+0.33			
	3	3.090	3.090	0.0			
	4	5.347	5.340	-0.13			
	5	5.050	5.060	+0.20			
GAP 4230	1	5.595	5.600	+0.09	907	896	-1.21
	2	5.390	5.392	+0.04			
	3	3.888	3.920	+0.82			
	4	1.325	1.355	+2.26			
	5	1.263	1.262	0.00			
	6	5.845	5.845	0.00			
	7	1.293	1.310	+1.21			

2.1.7 Electrolyte Solution Reservoir (Continued)

gas expansion during the elevated temperature without leakage. Two months after the test the reservoirs were taken apart and examined for effects. No leakage or degradation of the material was found.

2.1.8 Pyrotechnics

Several types of propellants and ignitors were studied. The tests included the measurement of gas volumes generated, the rate of pressure rise and the maximum pressure.

2.1.8.1 Ignitors

A survey of available ignitors did not reveal a heat sterilizable unit of the desired size. Testing of two commercially available ignitors IGN 17 (Atlas Chemical Industries) and NEI-3 (Network Electronics) showed that the former was damaged during sterilization while the latter survived unharmed. NEI-3 ignitors were subjected to vibration at levels up to 30 g's, exposed to 135°C for 128 hours, no fired at 0.55 ampere for 16 seconds and then fired at 1.75 amperes without failure.

In order to determine the capabilities of the NEI-3 ignitor after heat sterilization, a Bruceton test was performed on 50 sterilized units. This test establishes the statistical reliability of the ignitor at specific current levels and provides an indication of the safety margin between no-fire and fire levels. The procedure involves the selection of a starting point and an increment of change. The first unit is subjected to the starting current level. If it fires, the next unit is subjected to a current one increment lower. If it doesn't fire, the unit is set aside and the next unit is subjected to a current one increment higher. This procedure continues until each unit has been subjected to test. At this time all units not fired are subjected to a current at which all should fire to verify that there are no duds.

2.1.8.1 Ignitors (Continued)

Prior to actual firing of the ignitors, each unit was subjected to a no fire of 0.55 ampere in an ambient of 100°F. The results of the Bruceton are as follows:

1. Mean value of fires = 1.446 amperes
2. Sigma (σ) value (standard deviation) = 0.0786
3. Mean plus three sigma = 1.682 (0.997 reliability)
4. All units not fired were fired at 1.7 amperes.

The results of the test verify that the NEI-3 ignitor is capable of meeting the requirements after heat sterilization.

2.1.8.2 Propellants

Four materials were selected for study. These propellants were an ammonium perchlorate (X30-50A-2) from Talley Industries, two RTV zirconium potassium perchlorate formulations (LB-PL394-P29 and LB-429D-19) from Atlantic Research, and a polyester styrene ammonium perchlorate (AN583AF) made by Aerojet General. Initial tests were conducted by sterilizing samples of each propellant, machined to a fixed size. The samples were then assembled into gas generators and tested in a water displacement fixture (see Figure VII). This series of tests eliminated the two propellants manufactured by Atlantic Research as they were determined to have too rapid a burning rate as a result of heat sterilization.

Samples of the Talley Industries (X30-50A-2) and Aerojet General (AN583AF) propellants large enough to produce 3300 cc's of gas were assembled into gas generators each with two NEI-3 ignitors. The housing was stainless steel. A glass to metal seal four pin connector was used to seal the generator while the other end was sealed with a .001 inch thick, 0.5 inch diameter

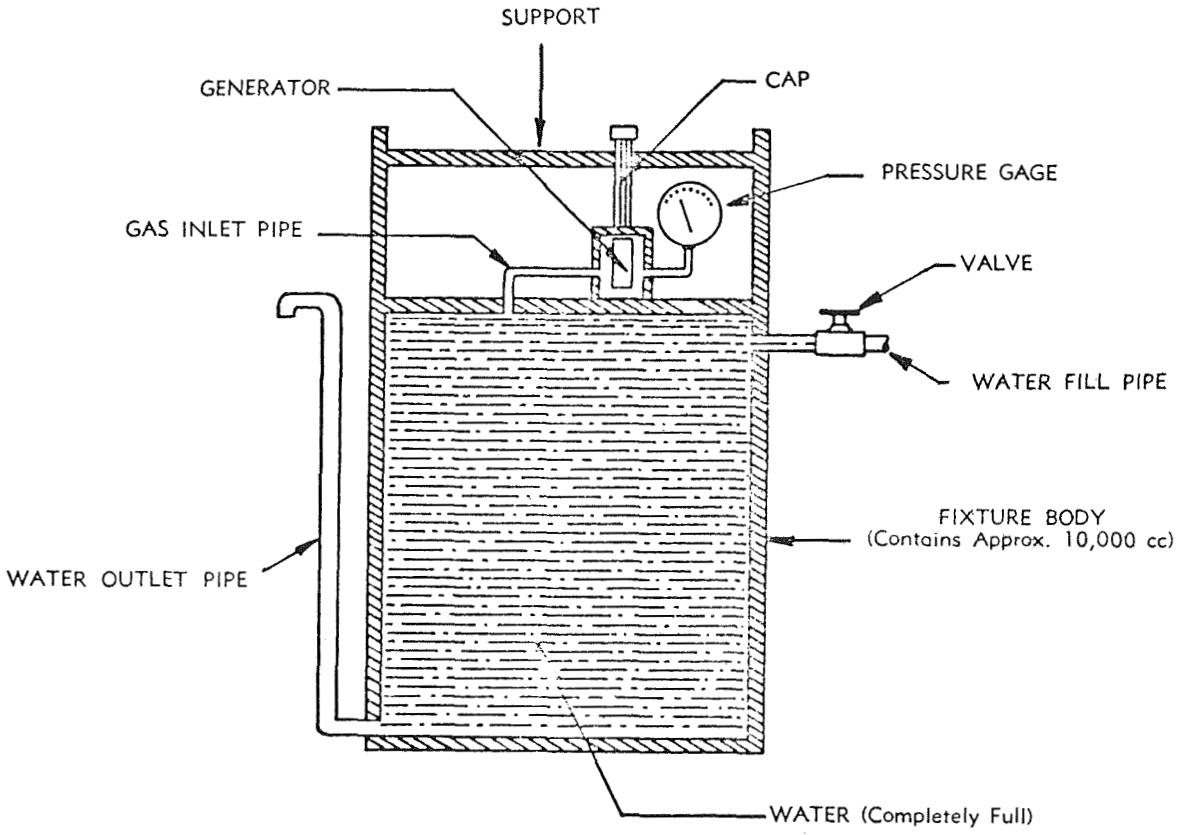

Water Displacement Test Fixture.

FIGURE VII

2.1.8.2 Propellants (Continued)

stainless steel diaphragm. An orificing device was placed between the propellant and diaphragm to restrict the flow of gas and to hold the propellant in place. The assembled generators were sterilized and then tested in the water displacement fixture. During these tests, the X30-50A-2 propellant was found to be unsatisfactory. The stainless steel housings ruptured creating a hazardous situation. All tests using the Aerojet General AN583AF propellant were satisfactory. Data from these and previous tests are tabulated in Tables XIII and XIV.

2.1.9 Cell Tests

In order to determine the best cell design to use in Phase II of the contract a series of cells, sealed in fabricated polysulfone cell cases, were tested. Each of these used four positive and five negative plates separated by either single layers of .010 inch thick asbestos and 4366T hemp or a single layer of 2409 cotton webril. The positive plates had a nominal weight of 2.4 grams per square inch and an average thickness of .028 inch. There were two types of negative plates used. The two outside negatives were nominally 0.66 gram per square inch and .027 inch thickness while the three middle plates were 1.18 grams per square inch and .027 inch thickness. The cells were activated with 1.3 specific gravity potassium hydroxide and discharged after having been sterilized. The discharges were accomplished at rates of 19.2 and 46.2 amperes to meet the contract requirements. Voltage profiles are shown in Figures VIII through X. The results show that the 2409 cotton separator gives a better performance if the wet stand life prior to discharge is 30 minutes or less. Past this point the 4366T hemp and .010 inch asbestos combination offer the best characteristics.

TABLE XIII

Performance of Gas Generator GG 208
After Sterilization

S/N	Type Propellant	Type Ignitor	Volume (cc)	Displacement Time (sec)	Peak Pressure (psig)	Time to Peak (msec)
1	AN583AF	NEI-3	3430	16	26	2270
2	AN583AF	NEI-3	3400	16	26	2260
3	AN583AF	NEI-3	3460	16	30	2300
4	AN583AF	NEI-3	3300	15	21	1920
5	AN583AF	NEI-3	3250	14	21	1830

TABLE XIV

Effects of Sterilization
on
X30-50A-2 and AN583AF
Propellants

Item No.	Propellant	Volume (cc)	Displacement Time (sec)	Peak Pressure (psig)	Time to Peak (msec)	Propellant Weight (gm)
1	X30-50A-2	1300	3	12	180	1.85
2	X30-50A-2	1320	4	15	170	1.85
3	X30-50A-2	1330	4	10	180	1.85
4	X30-50A-2	1390	5	8	50	1.80
5	AN583AF	1430	5	11	70	2.00
6	AN583AF	1440	5	6	120	2.00
7	AN583AF	1460	5	7	50	2.00
8	AN583AF	1600	6	36	170	2.00

NOTES:

1. Items 1, 2, 5 and 7 were unsterilized.
2. Items 3 and 4 had the propellant sterilized separately.
3. Items 6 and 8 were sterilized as assembled units.

FIGURE VIII

Discharge Characteristics
after
Heat Sterilization
Wet Stand - 10 Minutes
A - 4366T Hemp and .010 Asbestos
B - 2409 Webril

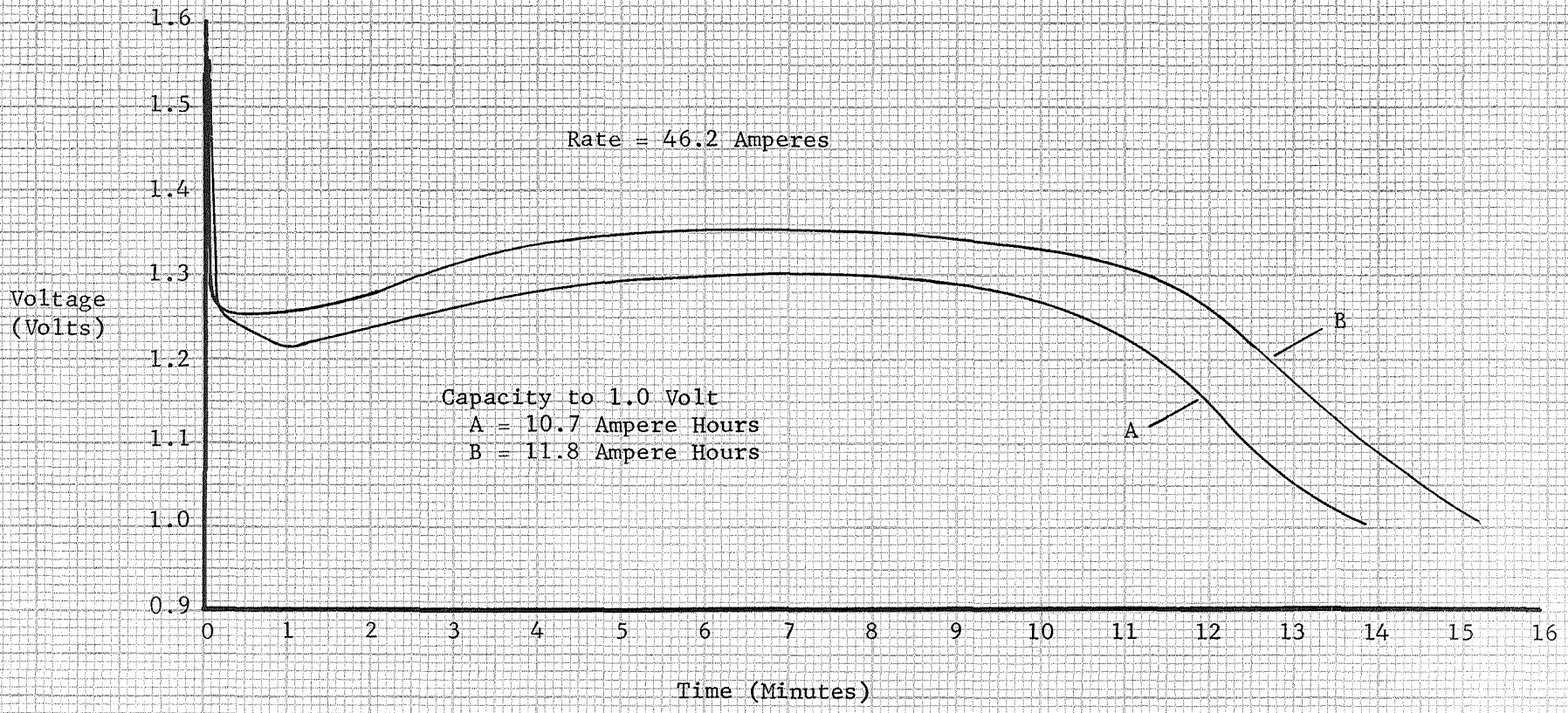

FIGURE IX

Discharge Characteristics
after
Heat Sterilization
Wet Stand - 30 Minutes
A - 4366T Hemp and .010 Asbestos
B - 2409 Webril

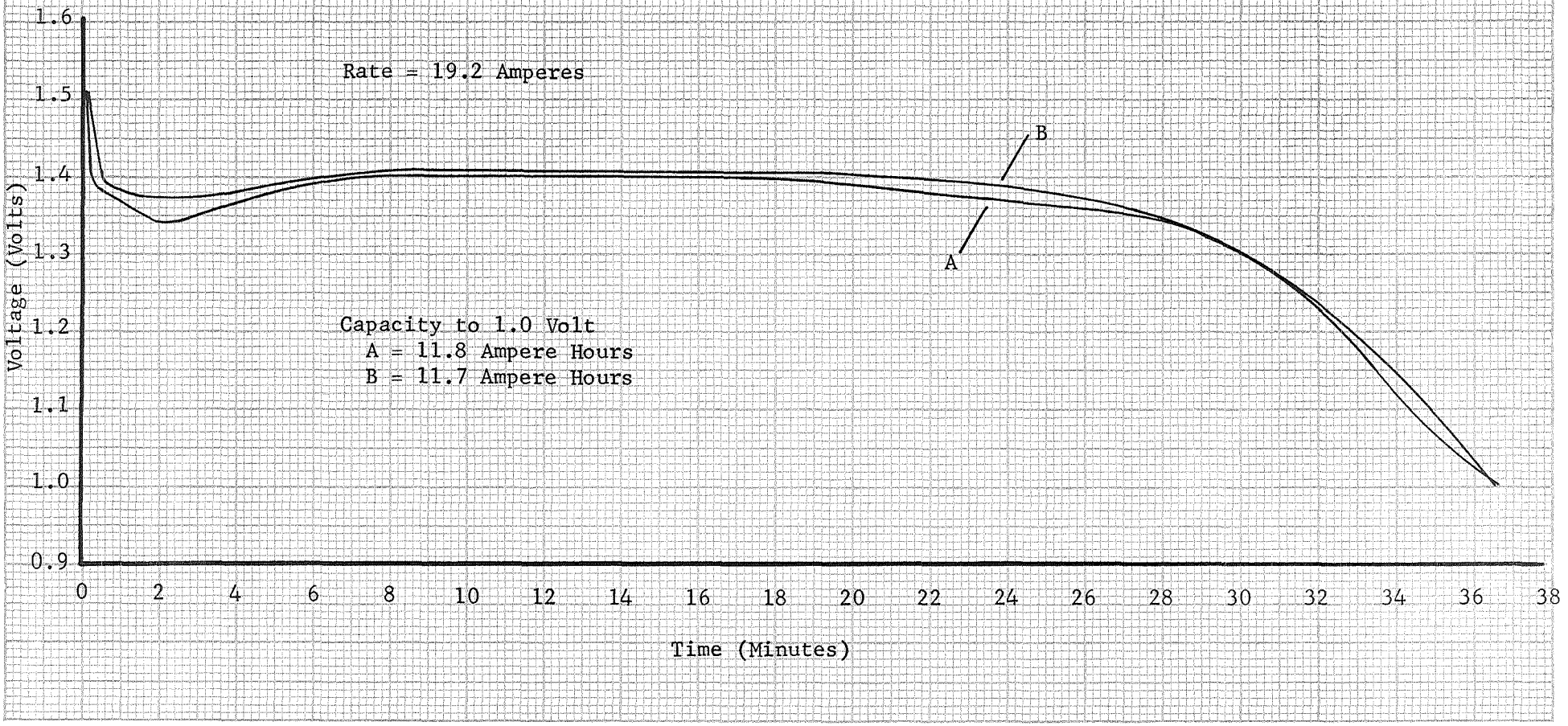

FIGURE X

Discharge Characteristics
after
Heat Sterilization
Wet Stand - 1 Hour

A - 4366T Hemp and .010 Asbestos
B - 2409 Webril

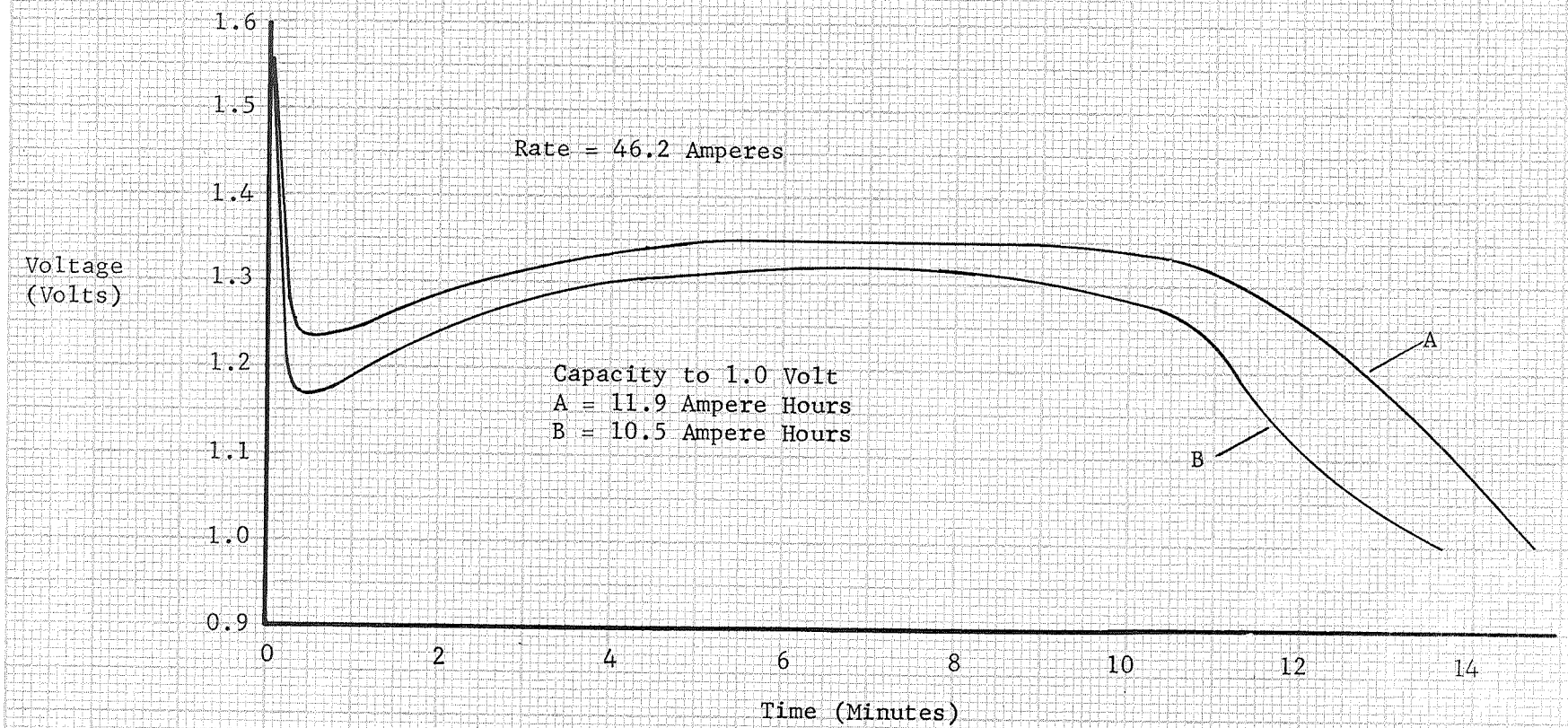

2.2 Phase II

2.2.1 Battery Design

As a result of the tests conducted during Phase I, components were selected for use in a prototype battery design. The initial effort consisted of the cell design to supply the power as required in the contract. The remaining battery components were then designed in accordance with the configuration of the cell. Each of the components are described separately. The basic design used 22 cells separated with 2409 cotton separator. The complete battery was encapsulated and sealed within a fabricated stainless steel housing.

2.2.1.1 Positive Plate

Silver oxide electrodes used in the batteries were electrically formed and pressed to a weight of 2.40 grams per square inch. The average density of these plates was 85 grams per cubic inch. Since the plates were found to grow in size during heat sterilization they were cut to a size slightly under that desired for the cell assembly. Each plate was then exposed for 72 hours to 135°C in order to stabilize the physical size and minimize any gassing after the battery was sealed. Five plates were used per cell. The final size is shown in Figure XI. Assuming characteristic efficiency losses (25% of theoretical) and losses caused by heat sterilization (30% of theoretical), the estimated positive capacity was 9.5 ampere hours.

2.2.1.2 Negative Plate

Six negative plates were used in each cell. Each plate was electroformed to a weight of 1.25 grams per square inch and pressed to a density of 48 grams per cubic inch. Since the zinc plate was found to be physically

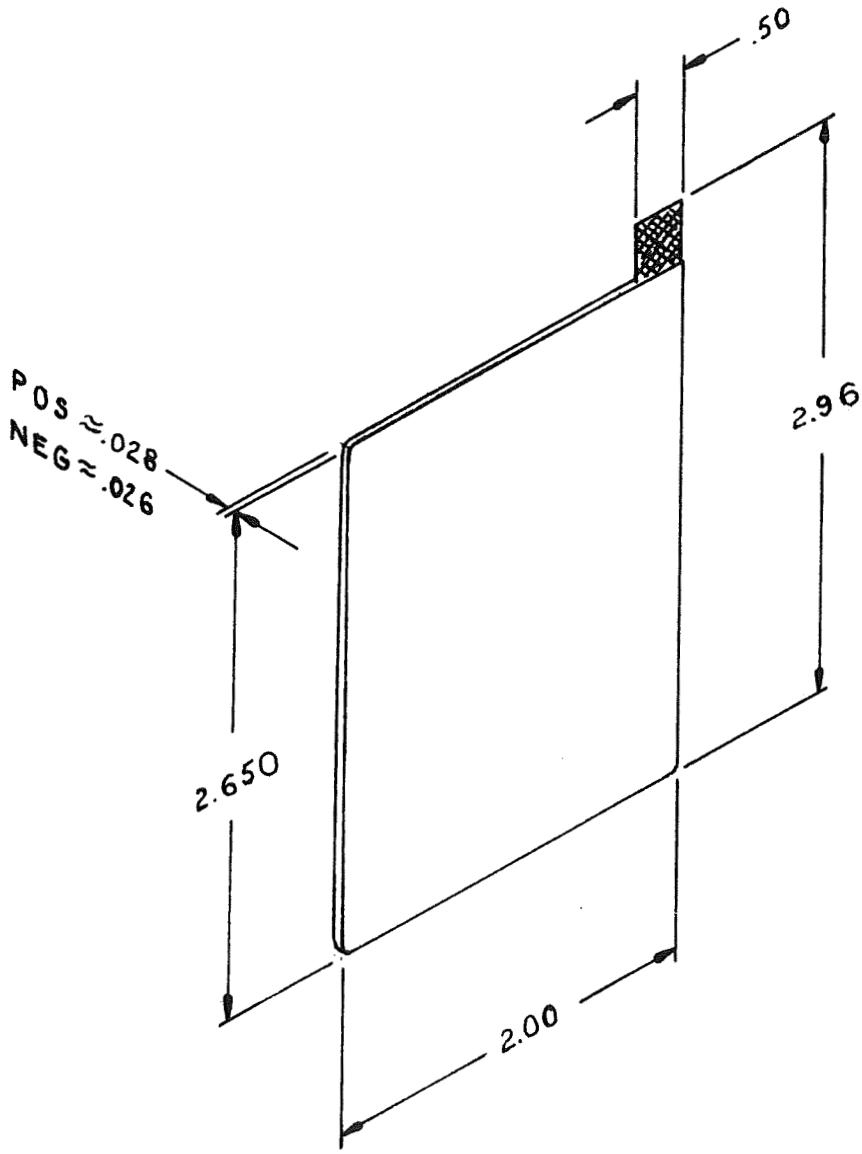

PLATE SIZE
FIGURE XI

2.2.1.2 Negative Plate (Continued)

stable during heat sterilization, no special treatment was required prior to assembly of the cell. With efficiency and heat sterilization losses deducted, the zinc capacity of the cell was estimated to be 13 ampere hours. The plate size is shown in Figure XI.

2.2.1.3 Separator

As a result of the cell tests described in paragraph 2.1.9 of this report and in consideration of the wet life requirements of the Work Statement, 2409 cotton as manufactured by Kendall Mills was selected for use as the separator material. This material offers a total wet life capability of 1.5 hours. The requirement is a maximum wet time, including discharge, of 54 minutes. The cell tests of paragraph 2.1.9 verified the materials' capability under these conditions. A single layer of the separator was folded around the lower edges of the positive plate. No separator material was used around the negative electrode.

2.2.1.4 Cell Case

As a result of tests conducted during Phase I it was decided to use a polysulfone fabricated cell case. As shown in Figure XII the cell case consists of 2 rows of 11 cells with 4 compartments along the side to capture excess electrolyte during the activation of the battery. The cell cases were assembled using ethylene dichloride as a solvent. Each cell case was given a vacuum cure of 72 hours at 85°C.

The battery manifold was machined of polysulfone. The cell entry holes were match drilled to the cell case prior to the manifold being joined to the cell case with ethylene dichloride. The manifold is shown in Figure XIII.

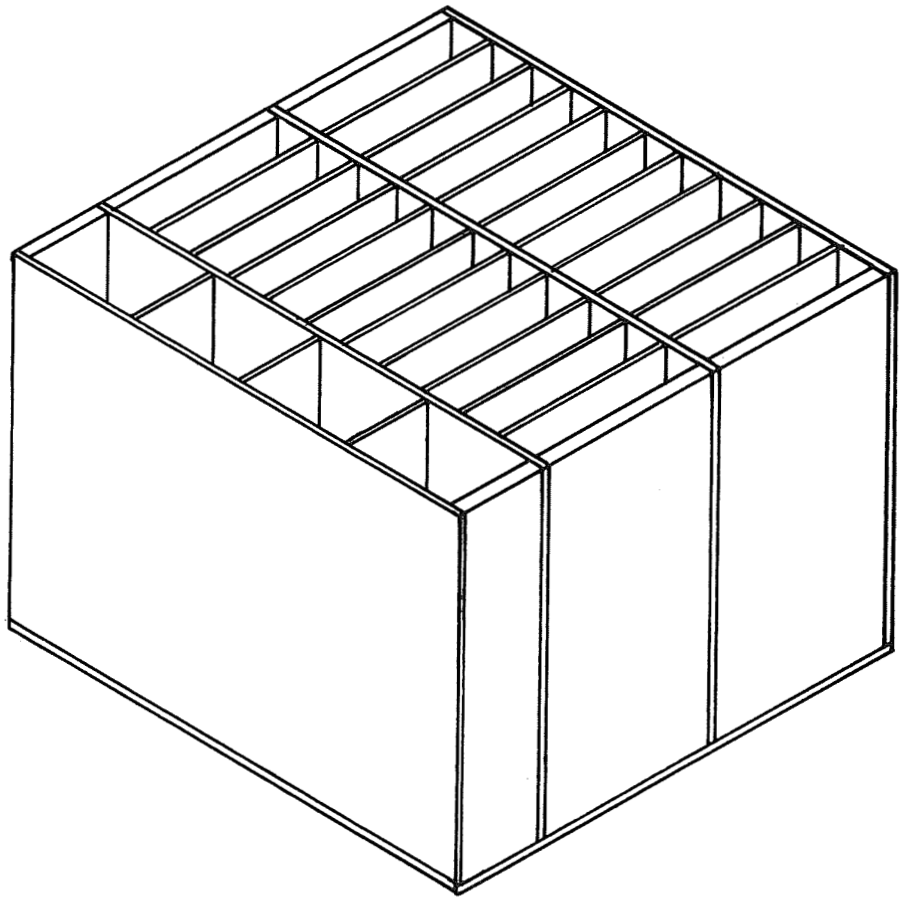

CELL BLOCK
FIGURE XII

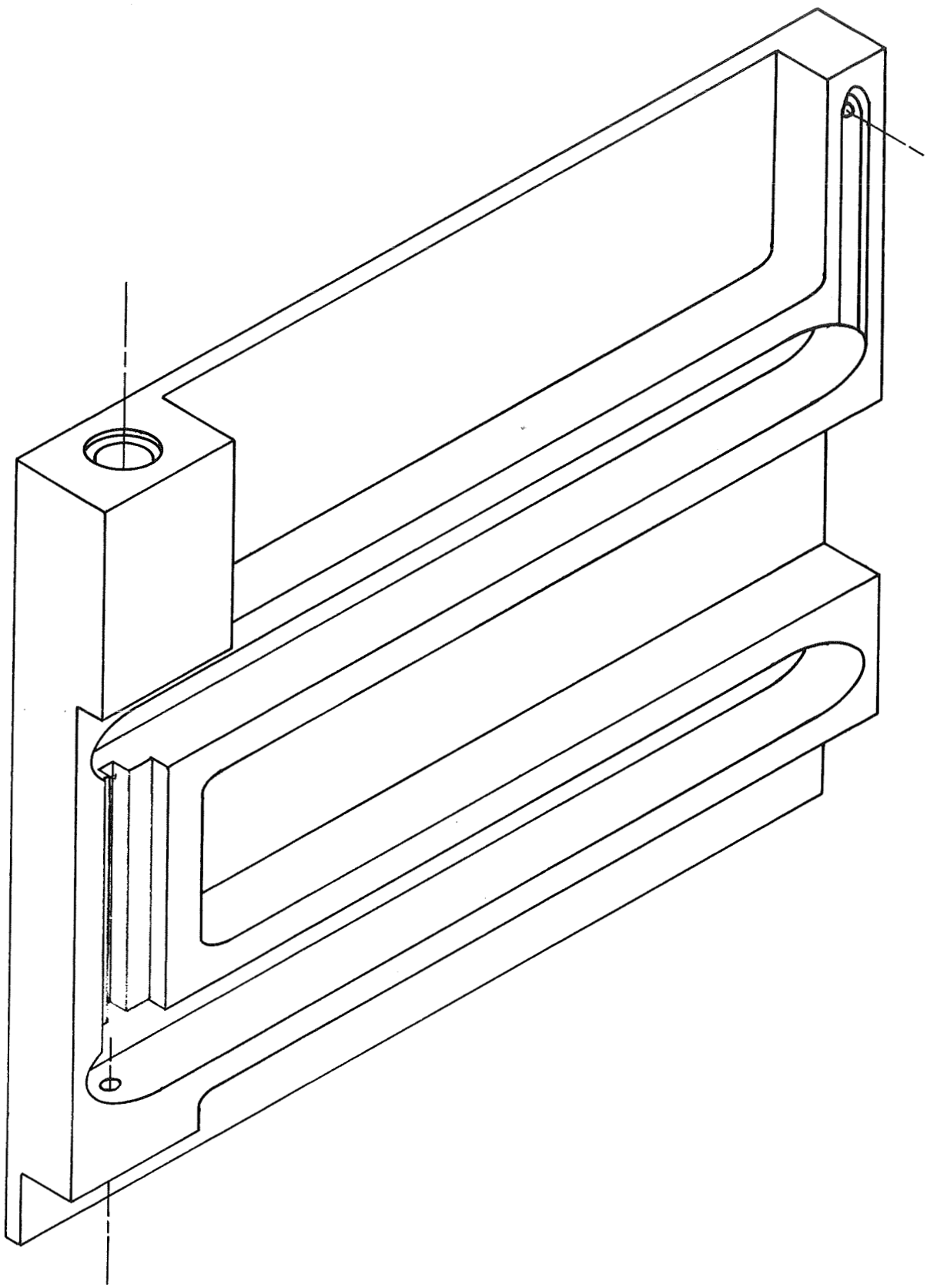

MANIFOLD
FIGURE XIII

2.2.1.4 Cell Case (Continued)

After joining the manifold to the cell case, a manifold cover plate (see Figure XIV) was bonded to the manifold. The entire battery block assembly was then subjected to the thermal vacuum described previously to remove all excess solvent prior to the heat sterilization cycle.

2.2.1.5 Electrolyte Reservoir

A tubular copper reservoir (see Figure XV) holding 690 cc's was assembled to wrap around the battery block assembly. The connection between the reservoir and the battery manifold was made through the use of an O-ring seal and a bolt passing through the reservoir manifold adaptor and the manifold. The O-ring material used in the prototypes was ethylene propylene. After the seal was made, the threaded fastener head was sealed with 63/37 solder to the electrolyte reservoir adaptor (see Figure XVI). A high temperature epoxy, EC 2214, was then applied around the soldered connection and the mating areas of the reservoir and battery manifold. This was done to provide a redundant seal for the system. The electrolyte was contained within the reservoir by two .002 inch thick copper diaphragms at each end. A 5% void was left in the reservoir to allow for expansion during the heat sterilization cycle.

2.2.1.6 Electrolyte Solution

A solution of potassium hydroxide with a specific gravity of 1.30 was selected for use in the battery. Due to the inherent transfer inefficiency of the system, 130% of the volume required to activate the cells was used.

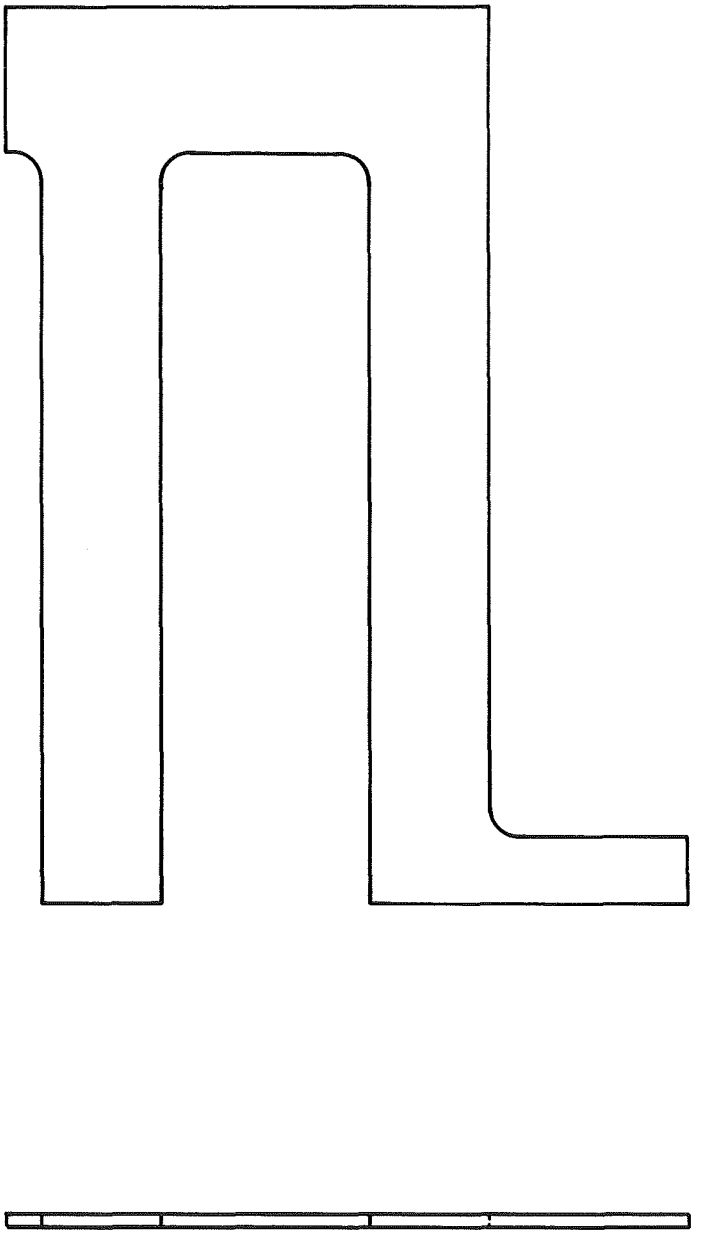

MANIFOLD COVER
FIGURE XIV

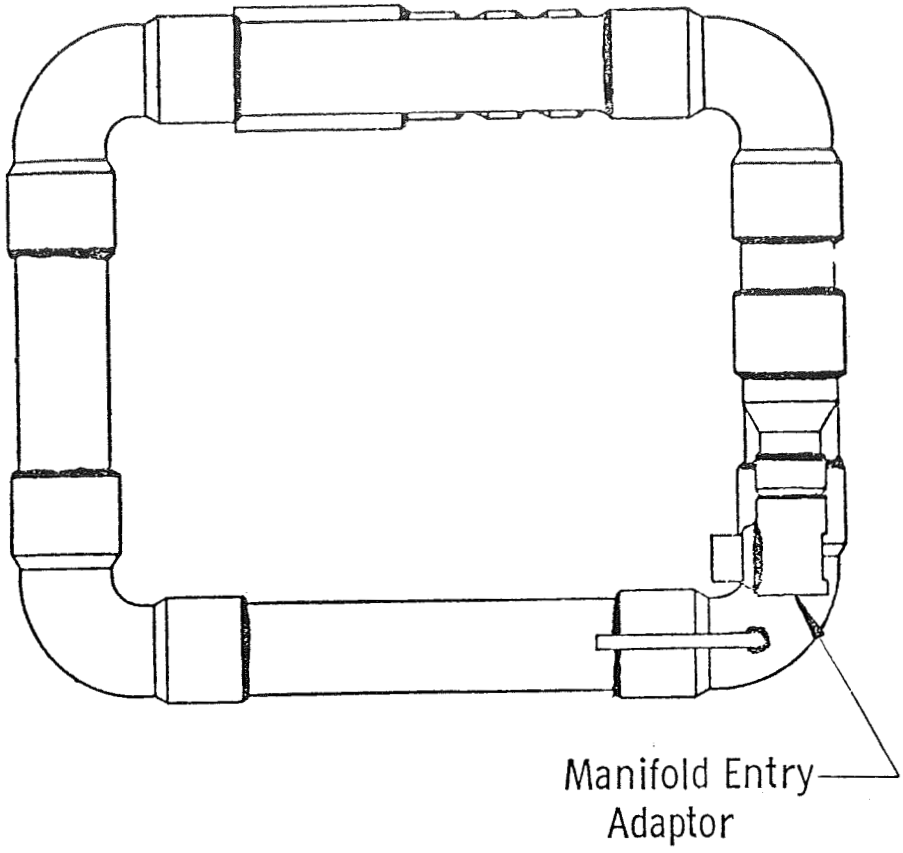

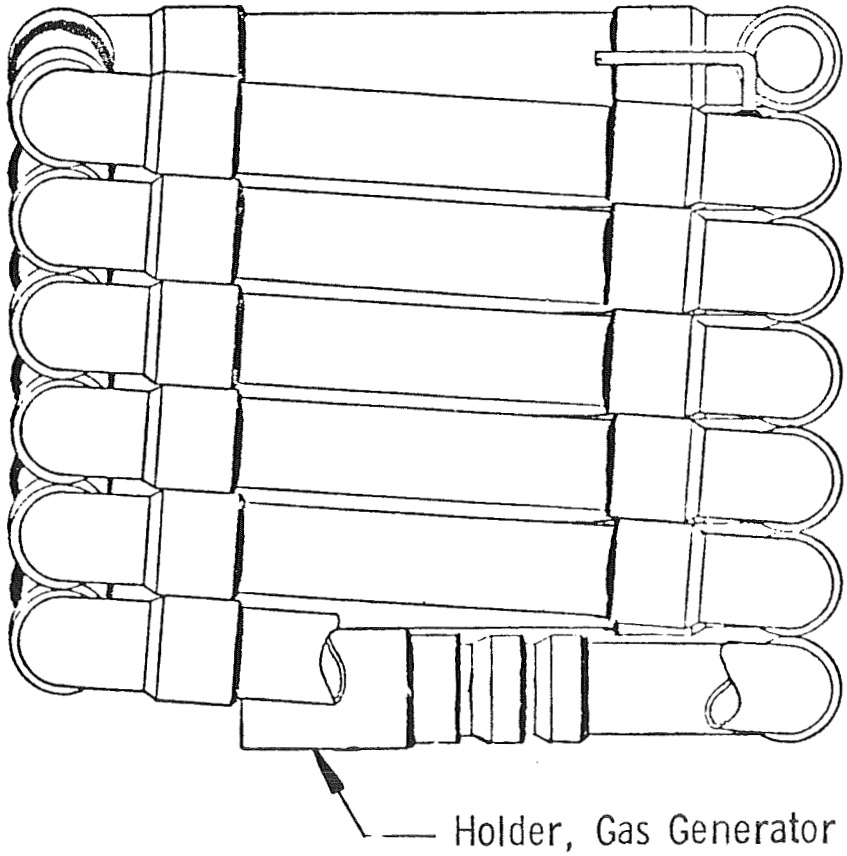

ELECTROLYTE RESERVOIR
FIGURE XV

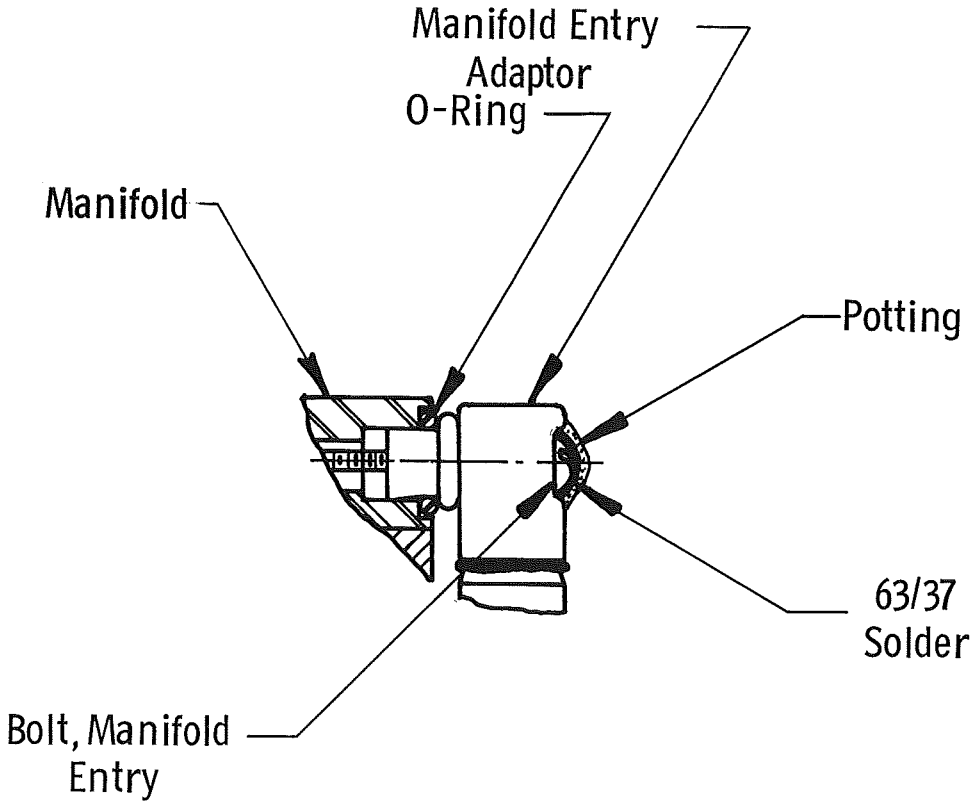

CONNECTION OF ELECTROLYTE
RESERVOIR TO MANIFOLD
FIGURE XVI

2.2.1.7 Gas Generator

The gas generator designed for use in the prototype batteries utilized two NEI-3 ignitors described in paragraph 2.1.8.1 of this report, in conjunction with 4.5 grams of Aerojet General AN583AF propellant. The design, as determined in a water displacement fixture, provided a gas output of 3300 cc's. A stainless steel housing with an orificing device to maintain sufficient pressure on the burning propellant as well as to restrain it from being expelled into the electrolyte was used. The generator was sealed by soldering a .001 inch thick stainless steel diaphragm to the orificed end. Electrical connections were made through the use of a four pin glass to metal seal connector soldered to the stainless steel housing. This unit was attached to the electrolyte reservoir through a threaded connection which was sealed with an ethylene propylene O-ring. A sectional view of the generator may be seen in Figure XVII.

2.2.1.8 Container

The container was made of .025 inch thick 304 stainless steel. The battery assembly was potted within the container with 614T lockfoam manufactured by Nopco Chemical. A cover of the same material as the container was then welded to the container effecting a hermetic seal. A glass to metal seal connector was used to provide the electrical connections required to activate and discharge the battery. This was attached through the container wall with 63/37 solder.

2.2.2 Prototype Tests

Three prototype batteries, as described above, were built and tested. Each battery was assembled and tested individually in order that data

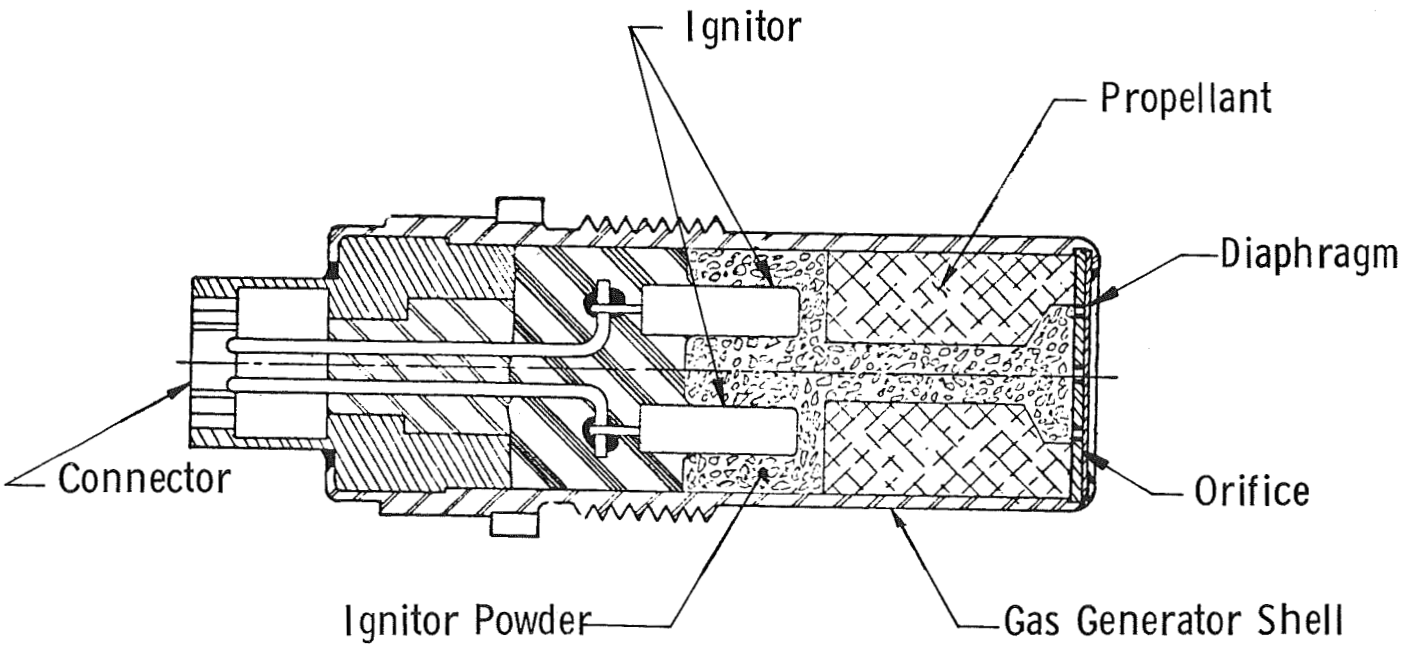

GAS GENERATOR
FIGURE XVII

2.2.2 Prototype Tests (Continued)

gathered from one could be evaluated and used to improve the following unit. The batteries shall be discussed separately in the order of fabrication and testing. The battery assembly may be seen in Figure XVIII.

2.2.2.1 Prototype Number 1

The first prototype was assembled in accordance with the description of paragraph 2.2.1. The assembled battery had a weight of 17 pounds. If the 200 watt hour requirement of the Statement of Work is considered to be the actual energy delivered, the battery would have an energy density of 11.8 watt hours per pound. Prior to heat sterilization the battery was measured and the dimensions recorded. The battery was sterilized and the dimensions were measured once again. Some permanent deflection was noted as a result of sterilization. The results were as follows:

Dimension		
Before	After	% Increase
7.14	7.35	2.9
6.65	6.84	2.8
6.04	6.27	3.8

The dimensions on which the calculations are based were taken at the centers of each side.

The battery was stabilized at room ambient and activated under open circuit conditions. On activation it was found that there was no voltage response. All circuits leading into the battery container were checked to determine if any broken leads or shorted conditions had occurred. It was found that the positive and negative leads of the test cable had been shorted during the assembly of the mating connector. Due to the high current level the battery connector pins had failed, leaving no reliable method of further discharging the battery. The battery container was then removed after which

BATTERY ASSEMBLY
FIGURE XVIII

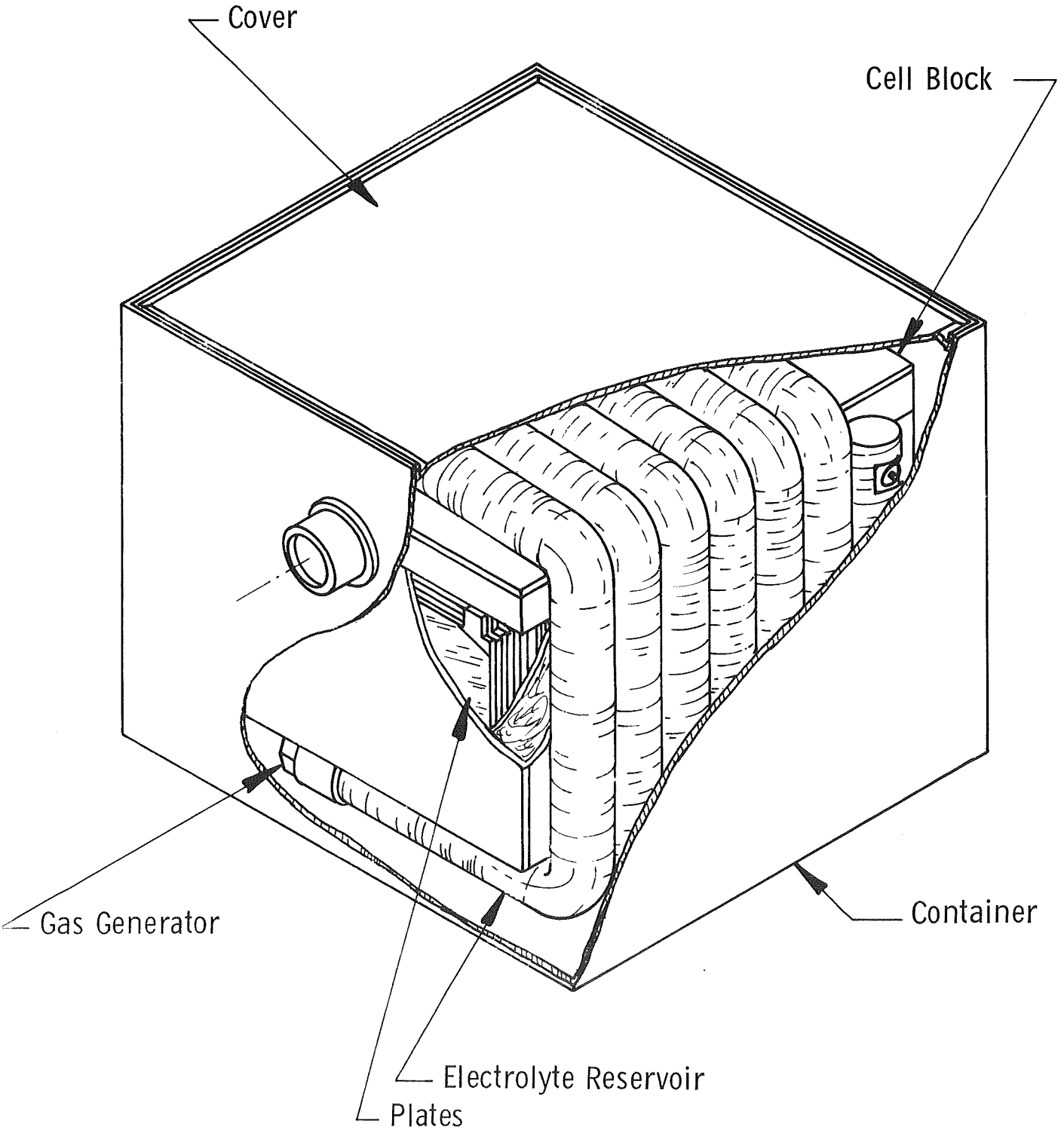

2.2.2.1 Prototype Number 1 (Continued)

the power leads were connected to the load panel and the battery discharged. The discharge profile was as shown in Figure XIX. As can be seen from the curve, the current levels attained were 30 and 82 amperes. By integrating the area under the curve, the total capacity removed from the battery was 5.9 ampere hours to an end voltage of 21 volts. After discharge the battery was completely disassembled to determine the wetting efficiency of the manifolding system during activation. It was found that two cells were not completely activated. The cell entry pattern was modified for use on battery serial number 2 to activate the cells more evenly.

2.2.2.2 Prototype Number 2

The second prototype battery was assembled in the same manner as the first with one exception. The 614T lockfoam was cured at room temperature with the cover removed. The cover was then welded to the container and the battery subjected to 135°C for 128 hours. The battery dimensions were measured before and after sterilization. It was found that the internal expansion problem experienced with battery number 1 had not been eliminated by the room temperature cure. The expansion obtained in this test included a 6.8% increase in the 7.1 inch dimension, an 8.3% increase in the 6.6 inch dimension and a 7.6% increase in the 6.1 inch dimension.

The battery was stabilized 16 hours at room temperature and activated with a 6 volt dc potential across a single ignitor of the gas generator. The battery terminal voltage was above 26 volts within 15 seconds after activation. The battery was then discharged as indicated by the discharge profile shown in Figure XX. Integration of the curve shows that the total capacity of the battery at an end voltage of 26 volts was 10 ampere hours. Using the end

FIGURE XIX

Discharge Characteristics
of
GAP 4374 Battery S/N 1
After Heat Sterilization

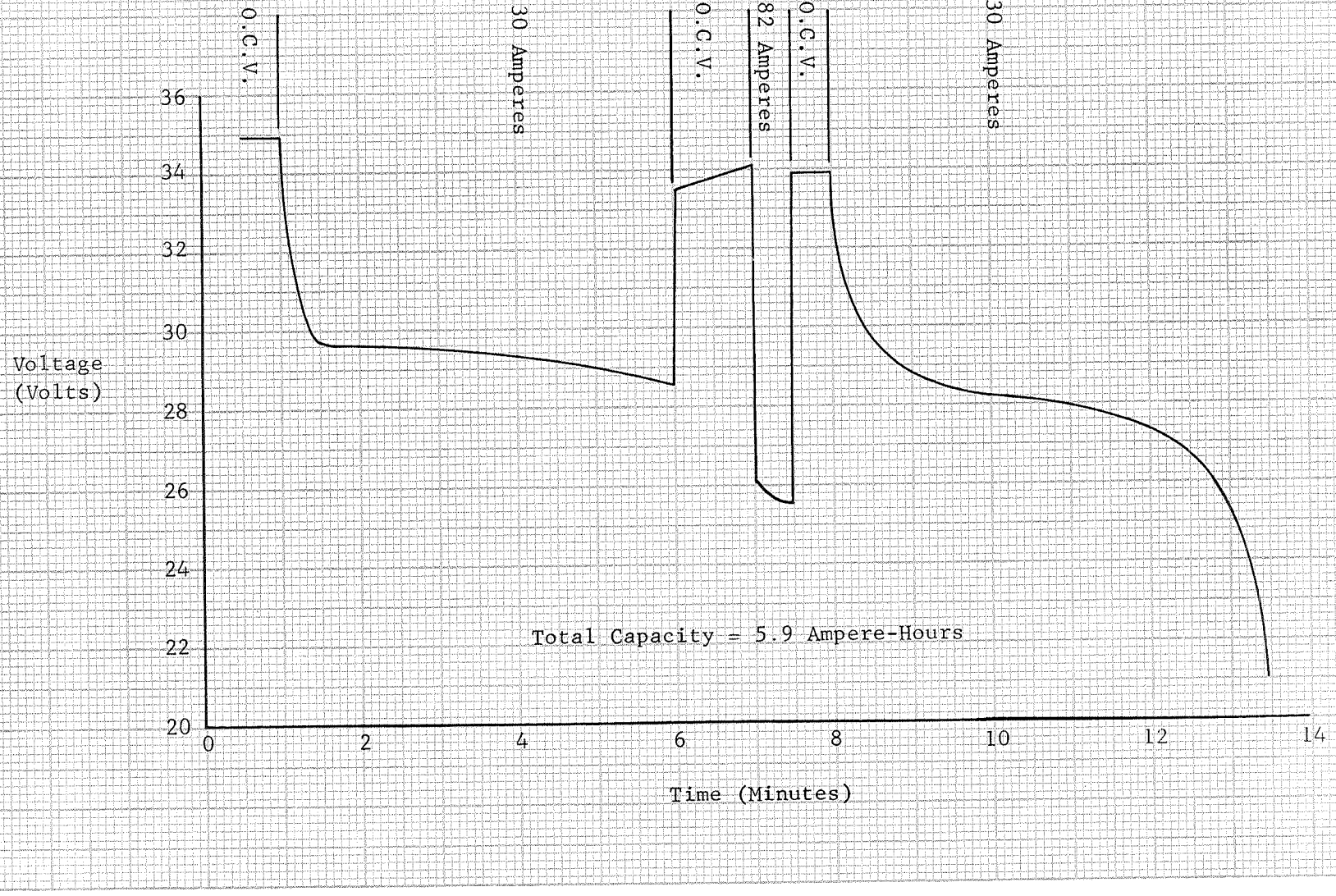

FIGURE XX

Discharge Characteristics
of
GAP 4374 Battery S/N 2
After Heat Sterilization

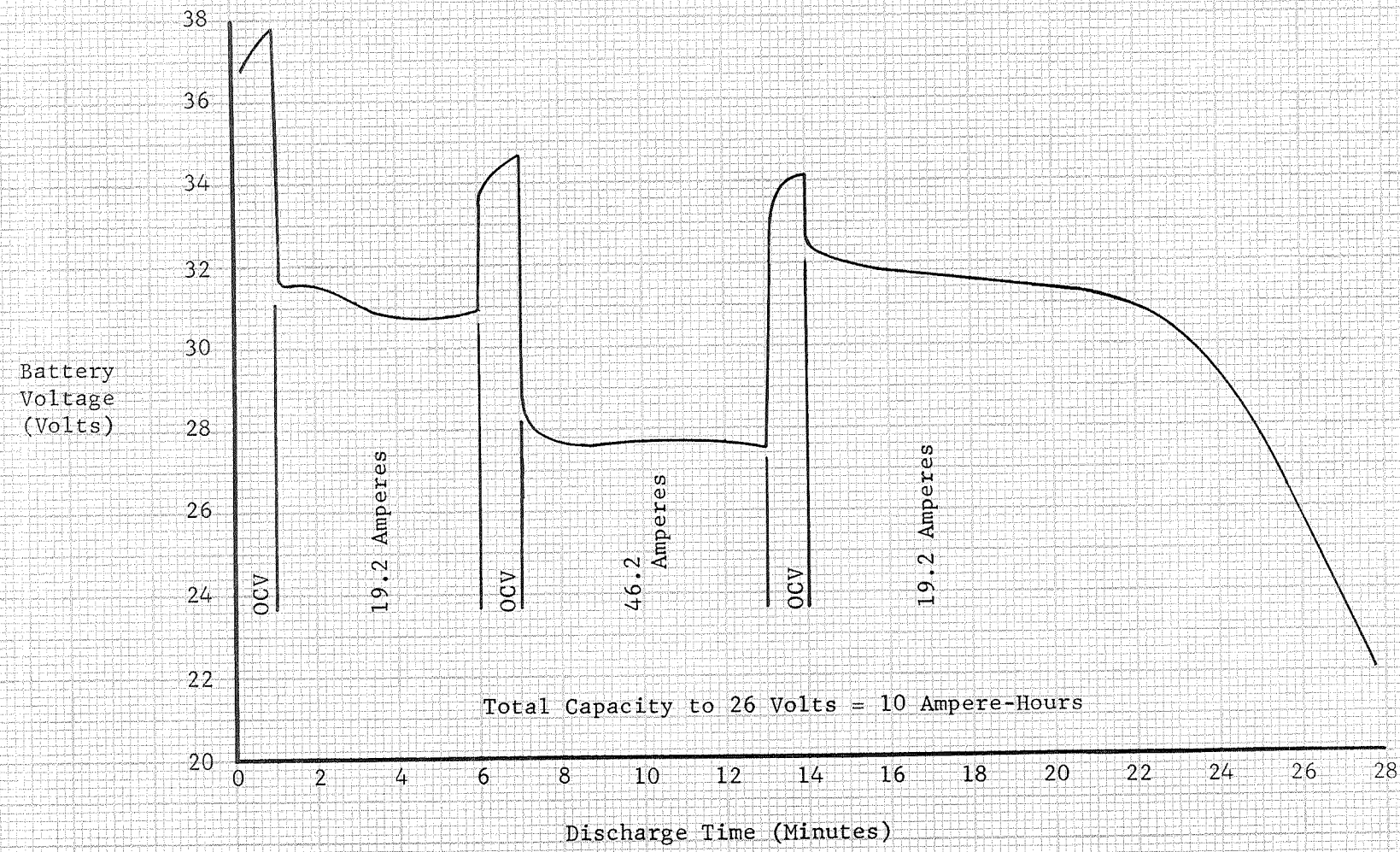

2.2.2.2 Prototype Number 2 (Continued)

voltage of 26 volts and a measured battery weight of 17 pounds the energy density was calculated to be 15.3 watt hours per pound. During activation and discharge pressure levels were monitored by a gage adapted to the last sump of the cell block. On activation a maximum value of 40 psig was recorded after which the internal pressure decreased to a level of 20 psig. The internal pressure remained at this level throughout the first 14 minutes of discharge. At this time the pressure increased steadily to a maximum of 100 psig recorded at 24 minutes into discharge. At the time the gage was loosened to prevent possible rupture of the case. The pressure build-up could have been a result of one or more of the following factors: the increase in battery temperature due to internal heat dissipation would cause some expansion in the gasses contained within the battery; the possibility of some electrolysis of the potassium hydroxide solution which would release oxygen and hydrogen gas could have contributed to the pressure build-up; the chemical reaction between the electrolyte and the zinc electrode would also free some hydrogen gas.

After discharge the battery was disassembled for analysis. It was noticed that the epoxy seal behind the electrolyte reservoir manifold adaptor had broken (see Figure XVI). By removing the epoxy it was found that the solder joint between the adaptor and the bolt through the adaptor had not been made leaving the seal dependent on the potting strength resulting in a leak to the outer battery case. The cells were removed and analyzed. Each was found to be sufficiently activated and in a completely discharged state. No evidence of internal cell shorting was found. The polysulfone seals were intact. In all appearances the battery had experienced a normal discharge

2.2.2.2 Prototype Number 2 (Continued)

with no malfunctions having occurred which would have contributed to the pressure levels recorded.

2.2.2.3 Prototype Number 3

The third battery assembled for testing had the same design characteristics as those previously described. However, during the potting operation the battery was stabilized at 135°C for 24 hours to properly cure the 614T lockfoam. This was done in order to eliminate expansion of the battery during sterilization. A gage was adapted to the battery in the same manner as before. Thermocouples were located against the cell case manifold, cell block and electrolyte reservoir. They were brought outside the container in a manner designed to insure the hermetic seal conditions of the battery. The battery was activated and discharged as shown in Figure XXI. A total capacity of 8.2 ampere hours was calculated for the battery. The internal pressure during the battery activation followed the same pattern as that of serial number 2 with the exception that lower levels were recorded. At the end of the 46.2 ampere discharge a leak was found at the pressure gage. At this time the battery case temperature was measured as being 135°F. The pressure leak was corrected after which the internal pressure increased to a level of 60 psig with an accompanying temperature of 149°F. At the end of discharge the battery manifold temperature was recorded as being 179°F. Due to the leak having occurred, an exact relationship between the battery temperature and pressure could not be made. However, it is believed that the battery temperature is directly related to internal heating of the battery during discharge.

FIGURE XXI:

Discharge Characteristics
of
GAP 4374 Battery S/N 3
after Heat Sterilization

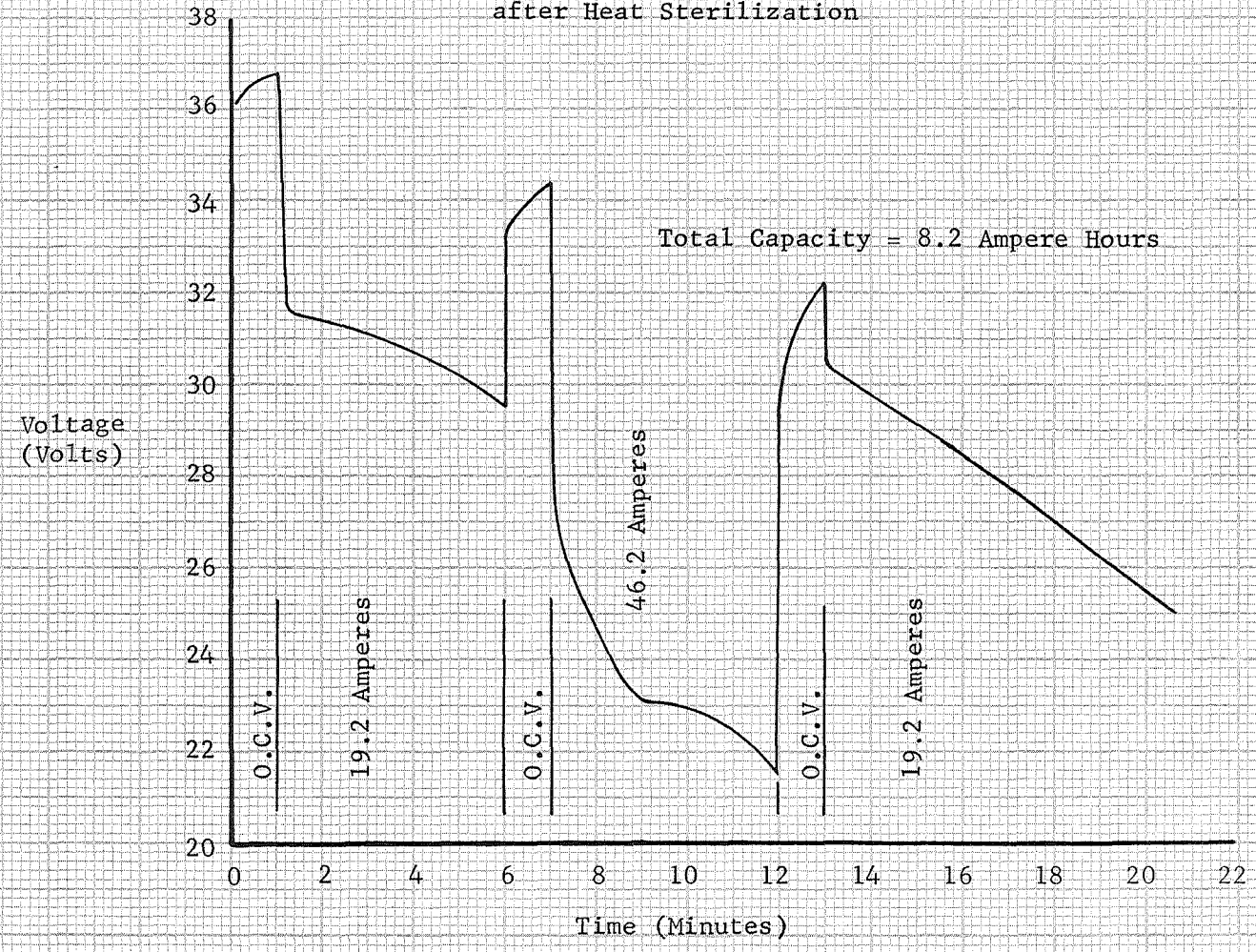

3.0 CONCLUSIONS

Based on this work the following conclusions can be made: The silver oxide plate experiences a loss in capacity of 40% during sterilization. The structure of the plate becomes more uniform and less dense as a result of the sterilization. The individual particles on unsterilized plates agglomerated into larger particles. This supports the data gathered showing an increase in physical size of the plates. Tests using multiple cycles of 128 hours at 135°C showed that the silver oxide plate tends to become stable as a function of time under the elevated temperature conditions. Gas collection data indicated that approximately 90% of the changes taking place within the electrodes occur within the first 24 hours of storage at 135°C.

The zinc electrode is relatively stable during the heat sterilization. B.E.T. measurements indicated very little change, if any, in the surface area of the zinc electrodes. Phase studies as well as microscope scanning shots revealed that no appreciable oxidation of the zinc electrode occurred during the 135°C storage.

Several separator materials were determined to be capable of satisfactory performance after heat sterilization. These included asbestos, nylon and cellulosic materials. The best separator for the requirements of the Statement of Work was determined to be 2409 cotton manufactured by Kendall Mills. This material offered the best wetting and absorption characteristics with no apparent degradation due to heat sterilization.

Investigation of various potassium hydroxide solutions revealed that heat sterilization had no apparent effect on the electrolyte when sealed within a copper reservoir.

3.0 CONCLUSIONS (Continued)

In working with various cell case materials polysulfone was found to be most suited to battery operation and heat sterilization. A reliable seal with ethylene dichloride requires a 72 hour vacuum cure at 85°C. This is necessary to prevent outgassing of solvent entrapped in the glue joints during the sealing operations. The material was found to be chemically resistant to a 31% solution of potassium hydroxide.

A tubular copper reservoir commonly used in Eagle-Picher remotely activated batteries, remained unaffected by heat sterilization. The design for a gas generator capable of heat sterilization consists of two NEI-3 ignitors in conjunction with a machined block of AN583AF propellant manufactured by Aerojet General. Tests using this design revealed a reasonable degree of reliability with consistent performance.

Batteries fabricated with the components selected from Phase I of the contract performed electrically as expected. Although equipment and fabrication problems were encountered during the testing, the overall performance of the battery was satisfactory. However, this battery would experience problems under high rate loading due to pressure increases with no means of relief. The batteries tested show that a unit capable of heat sterilization could be manufactured with an energy density of approximately 15 watt hours per pound. This value could be increased by using lighter components in the electrolyte reservoir.

4.0 RECOMMENDATIONS

Testing of the three prototype batteries indicates that without further study of the conditions existing, a pressure relief system should be incorporated into battery design. Further investigation should be made into the

4.0 RECOMMENDATIONS (Continued)

designing of a sealed remotely activated heat sterilizable battery.

5.0 NEW TECHNOLOGY

No new technology was formulated during the contractual effort.

APPENDIX I

MICROSCOPIC STUDY
OF
SILVER OXIDE ELECTRODES

300 Magnification

Silver Oxide Plate No. 35

As Received

Flat Surface

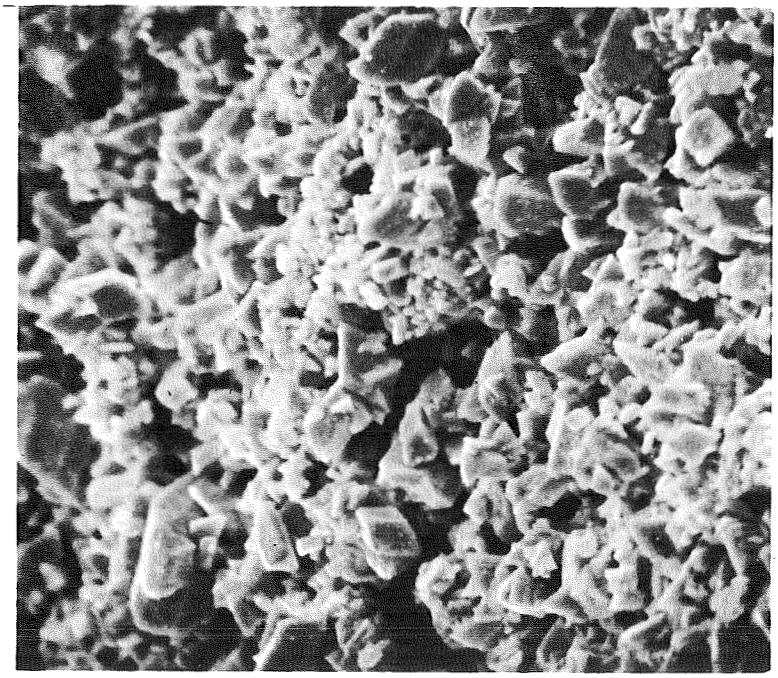

1000 Magnification

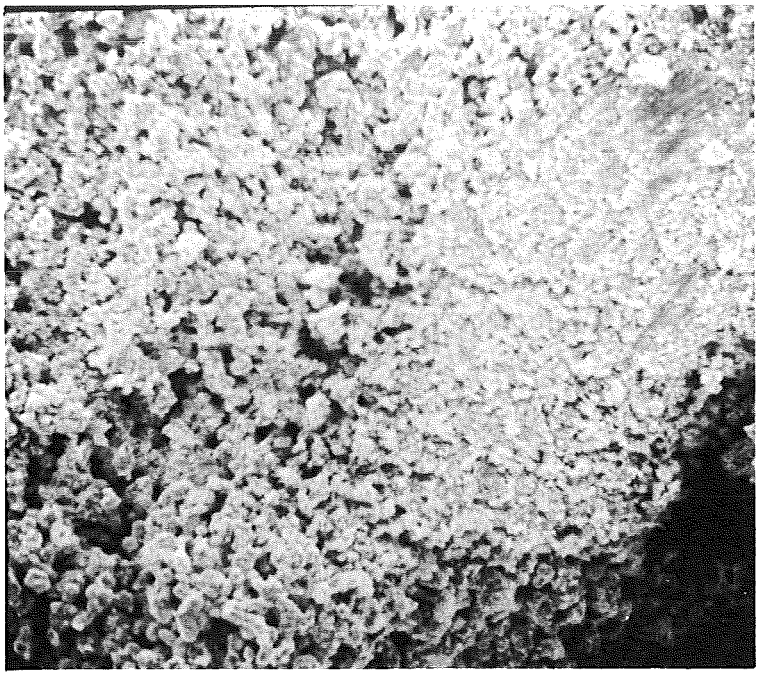

300 Magnification

Silver Oxide Plate No. 35

As Received

Transverse View

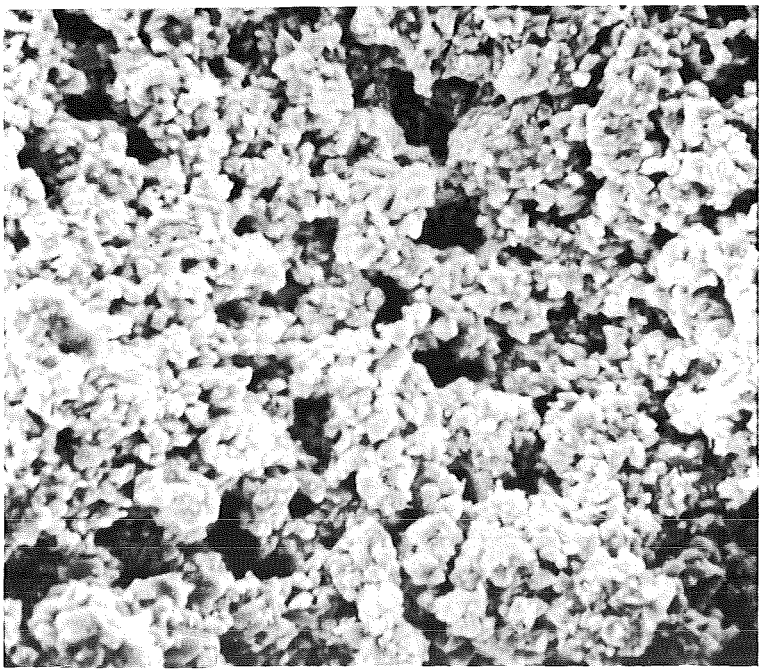

1000 Magnification

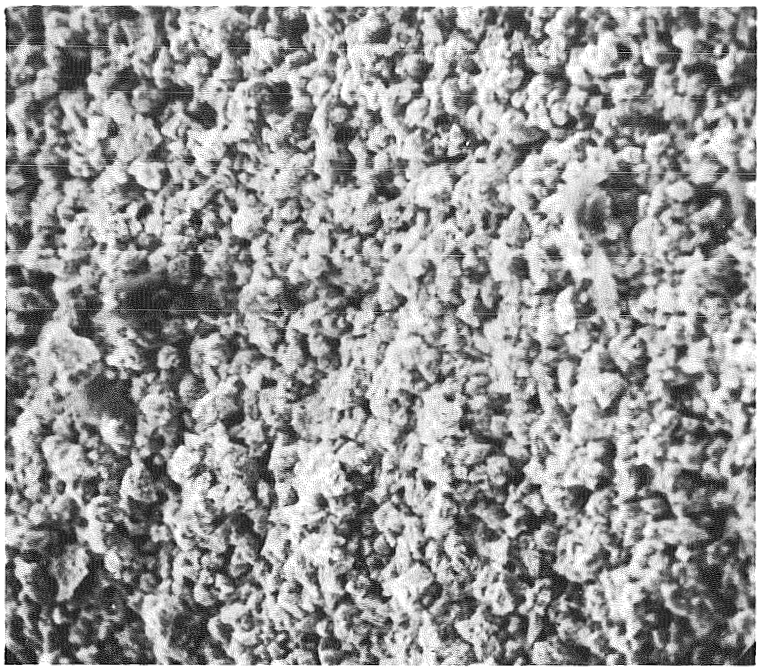

300 Magnification

Silver Oxide Plate No. 35

Sterilized

Flat Surface

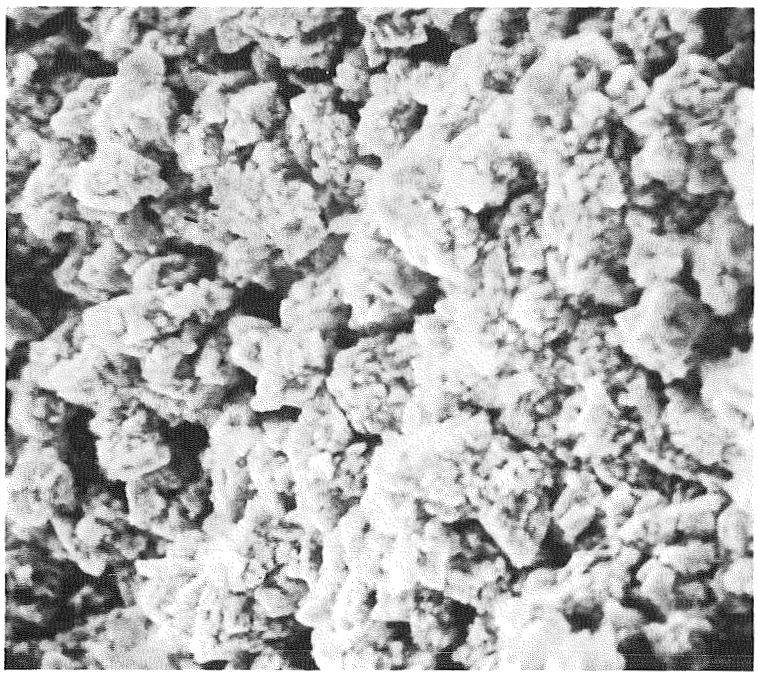

1000 Magnification

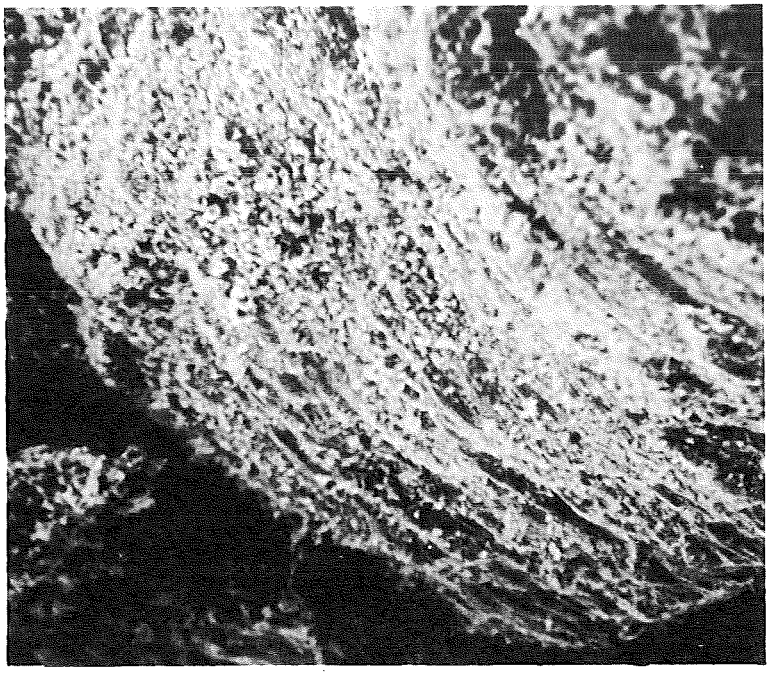

300 Magnification

Silver Oxide Plate No. 67

As Received

Transverse View

1000 Magnification

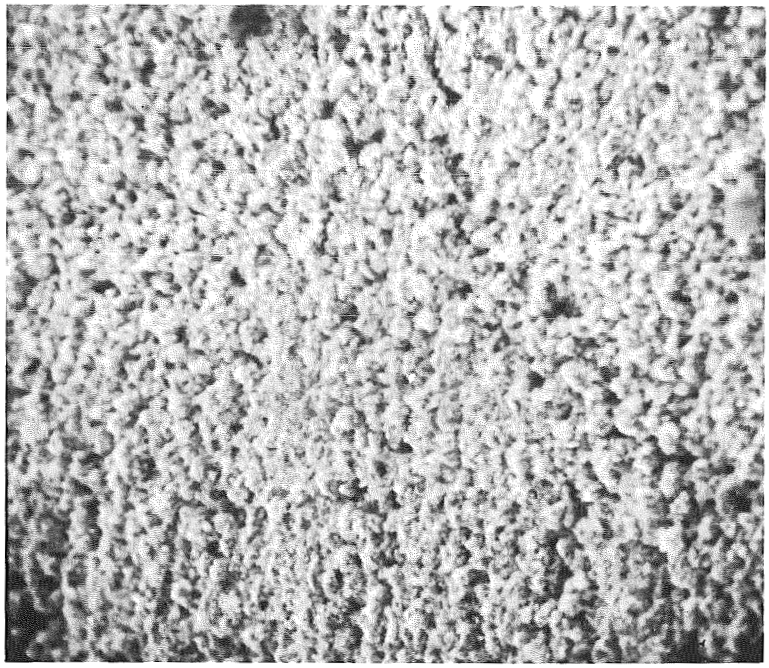

300 Magnification

Silver Oxide Plate No. 67

Sterilized

Flat Surface

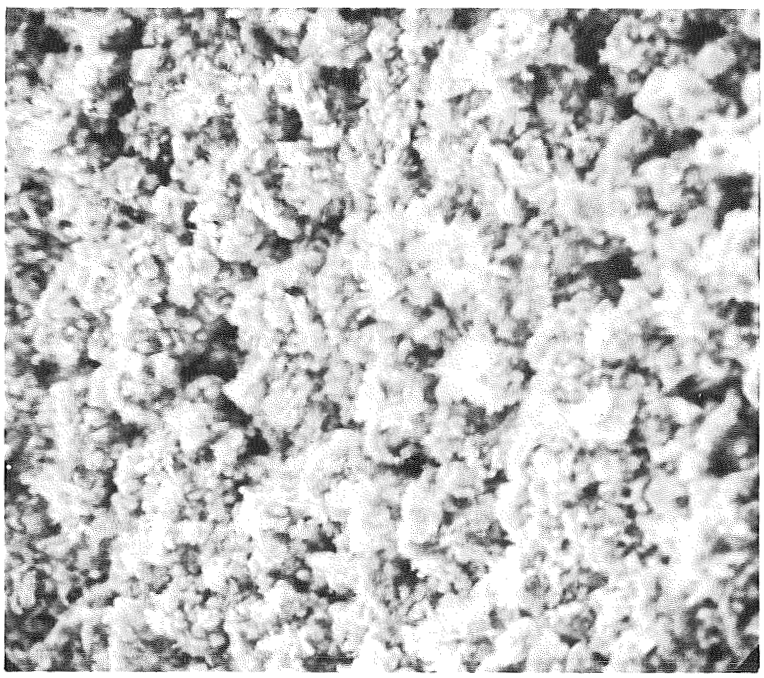

1000 Magnification

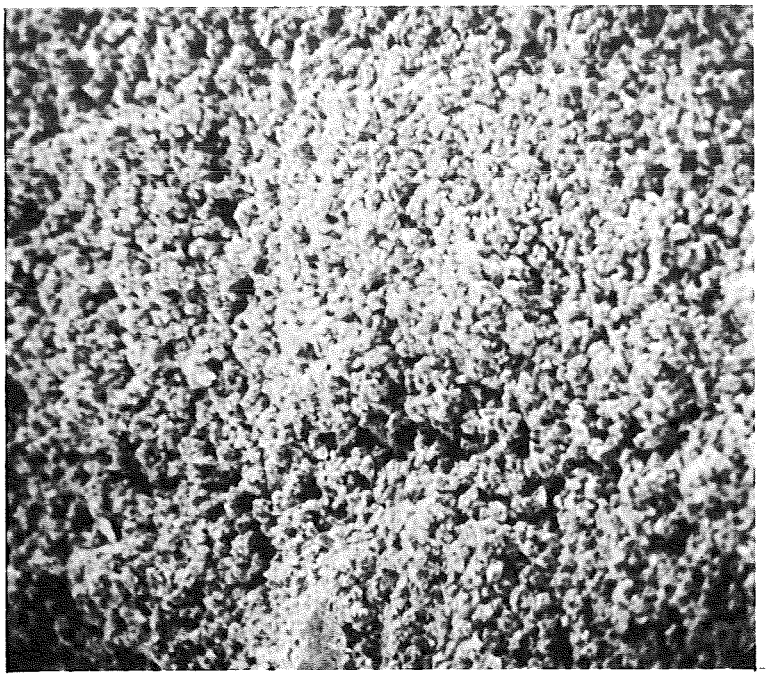

300 Magnification

Silver Oxide Plate No. 83

As Received

Flat Surface

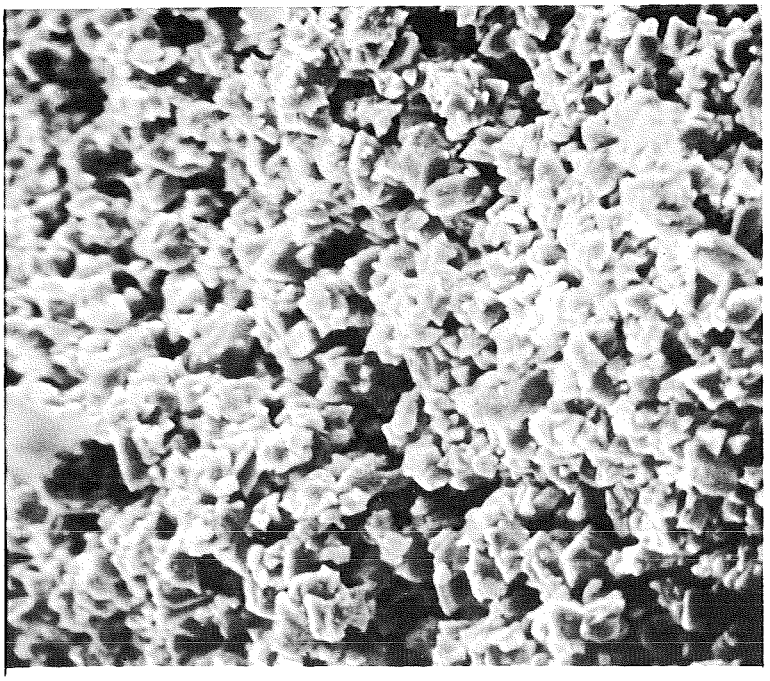

1000 Magnification

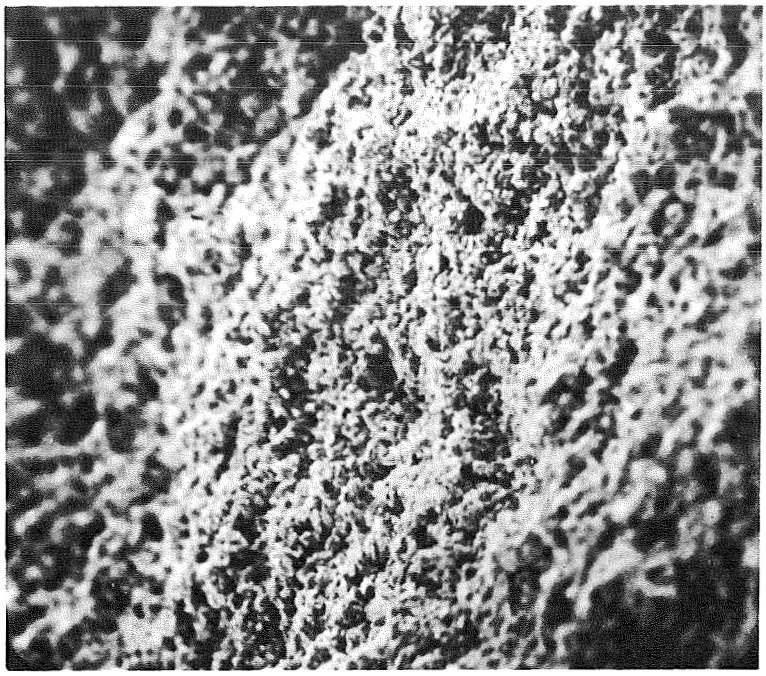

300 Magnification

Silver Oxide Plate No. 83

As Received

Transverse View

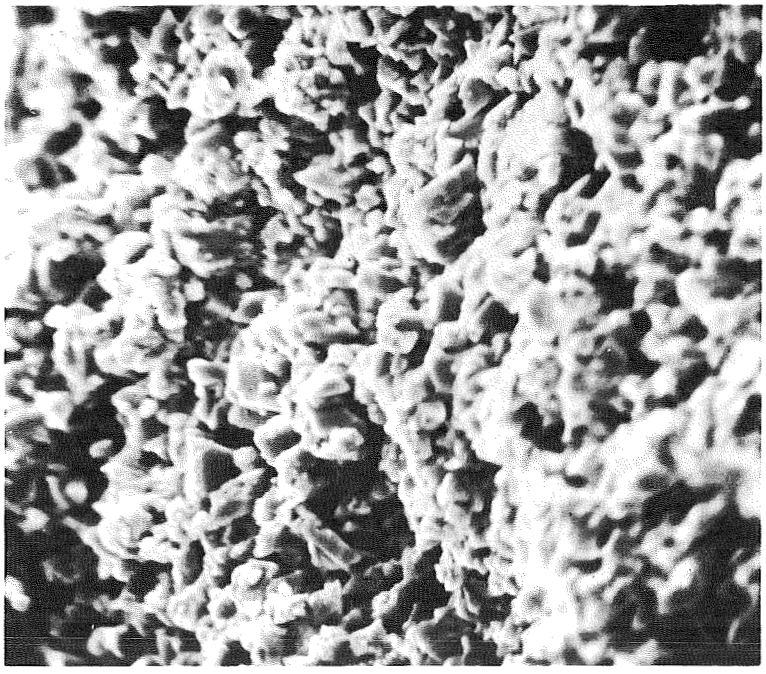

1000 Magnification

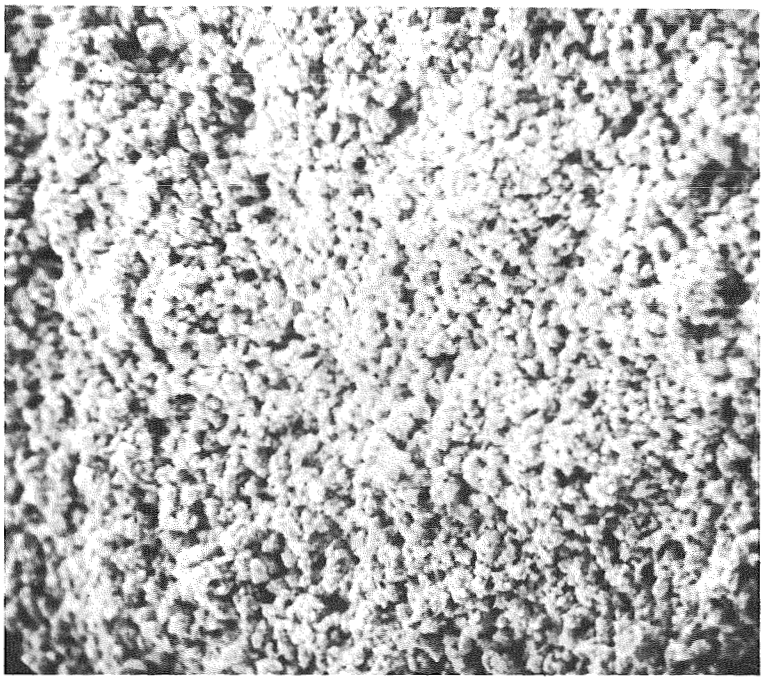

300 Magnification

Silver Oxide Plate No. 83

Sterilized

Flat Surface

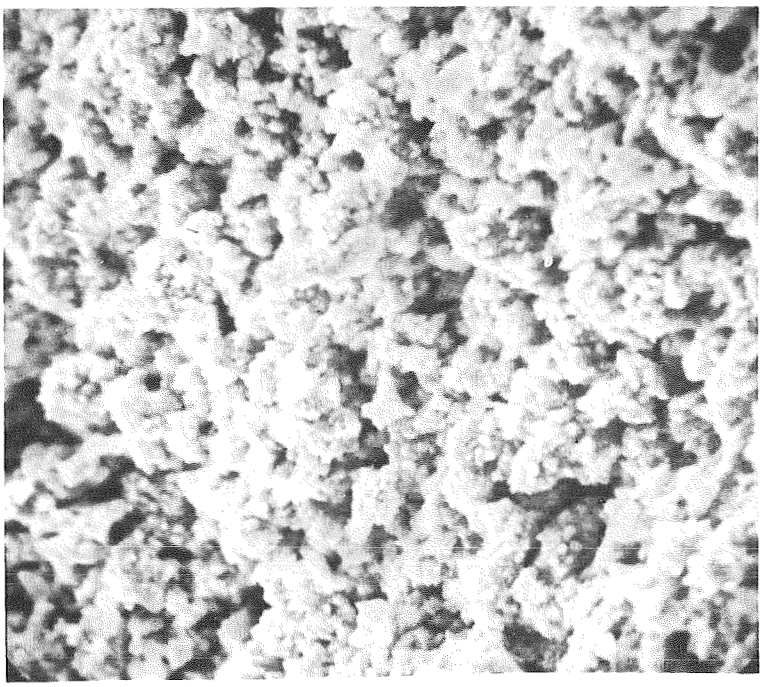

1000 Magnification

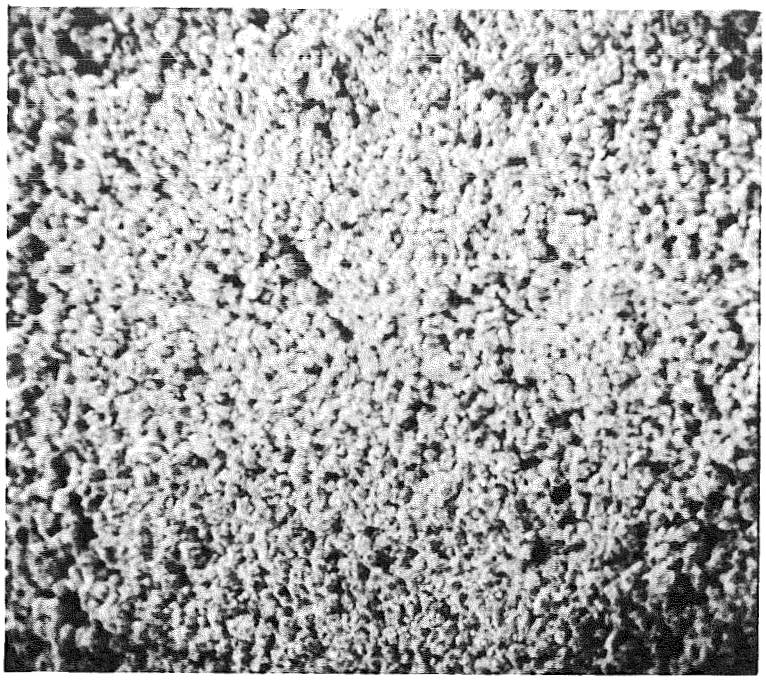

300 Magnification

Silver Oxide Plate No. 95

As Received

Flat Surface

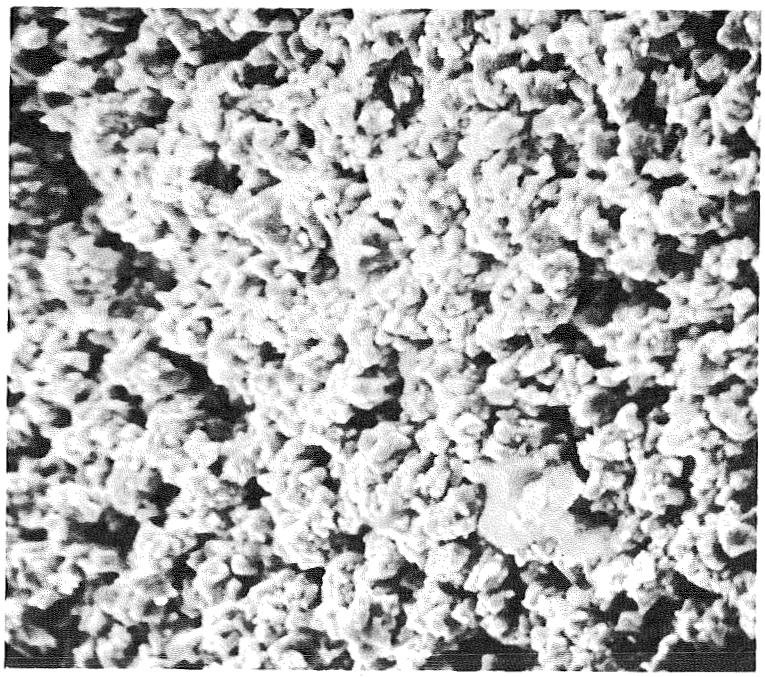

1000 Magnification

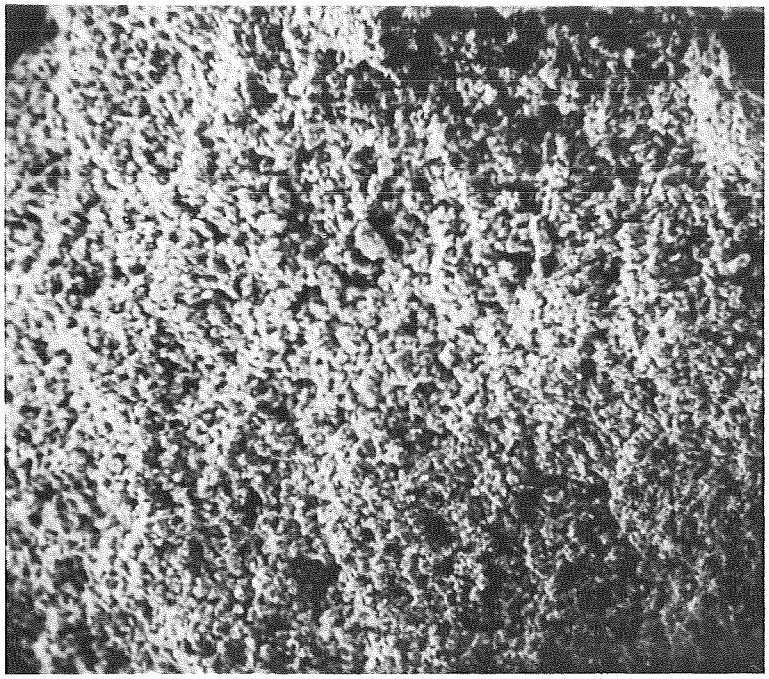

300 Magnification

Silver Oxide Plate No. 95

As Received

Transverse View

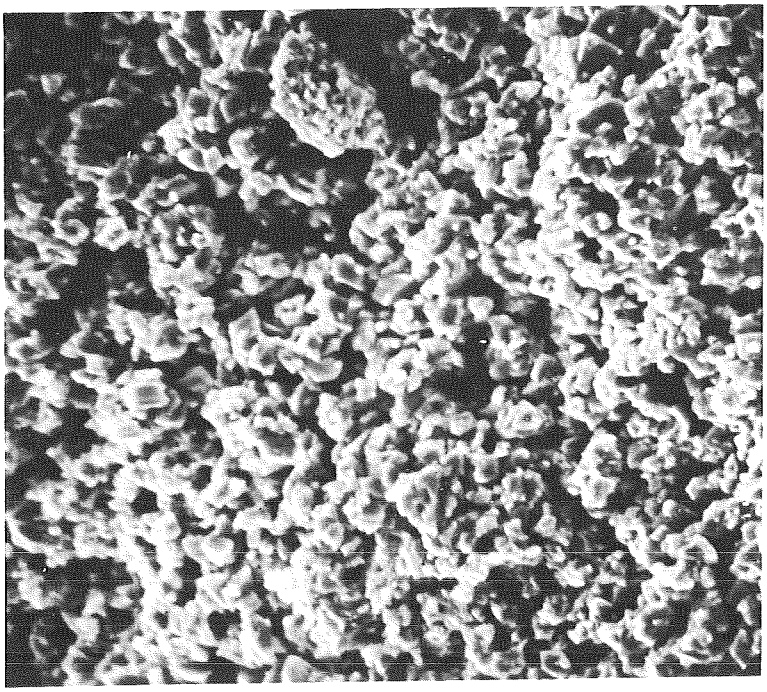

1000 Magnification

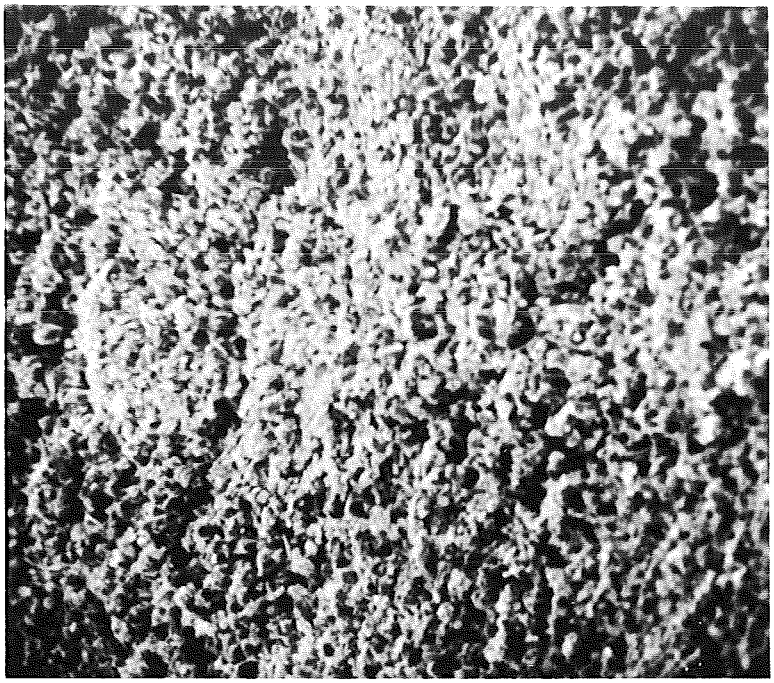

300 Magnification

Silver Oxide Plate No. 95

Sterilized

Flat Surface

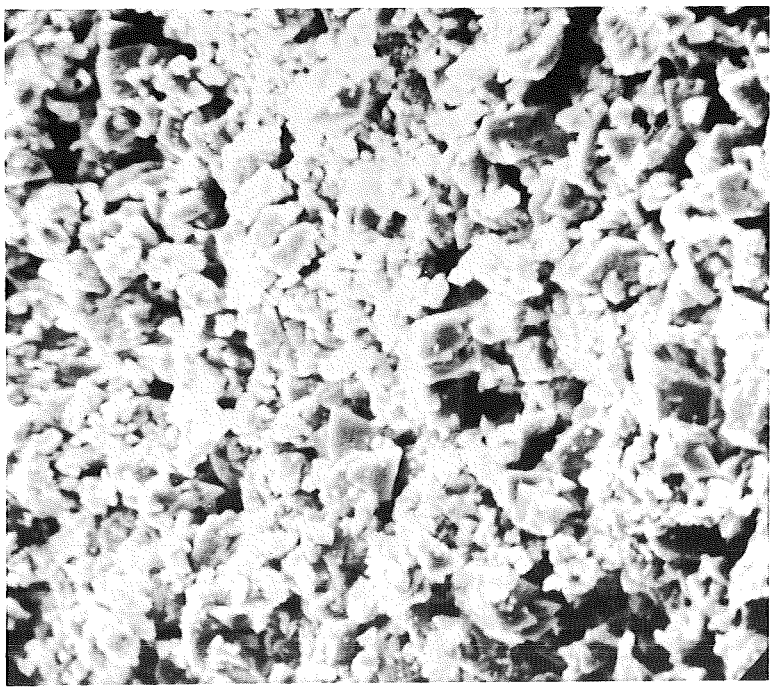

1000 Magnification

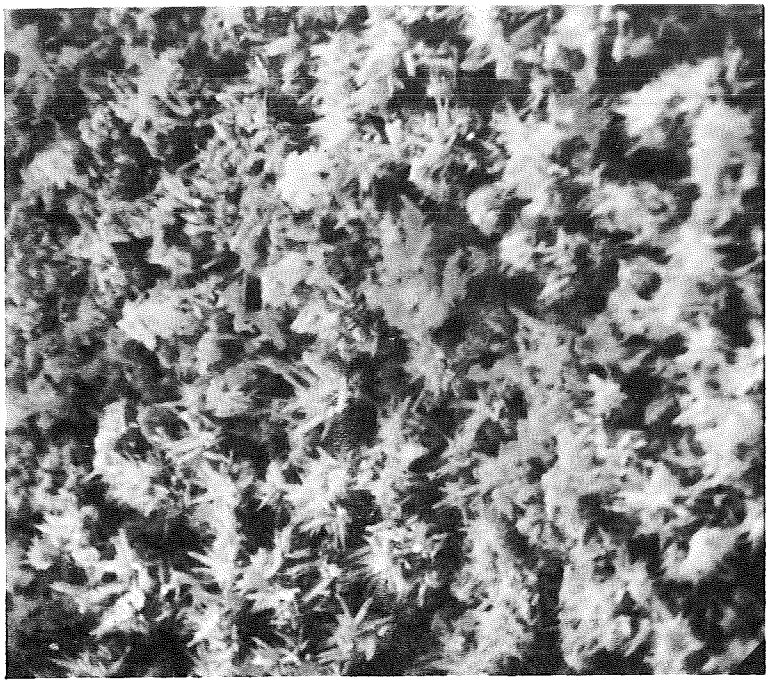

1000 Magnification

Silver Oxide Plate No. 95

Sterilized

Flat Surface

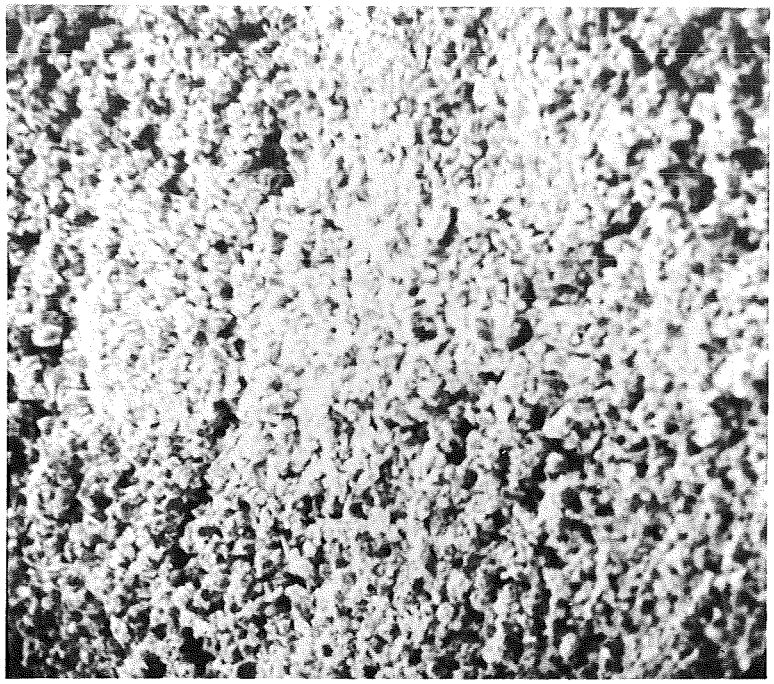

300 Magnification

Silver Oxide Plate No. 106
As Received

Flat Surface

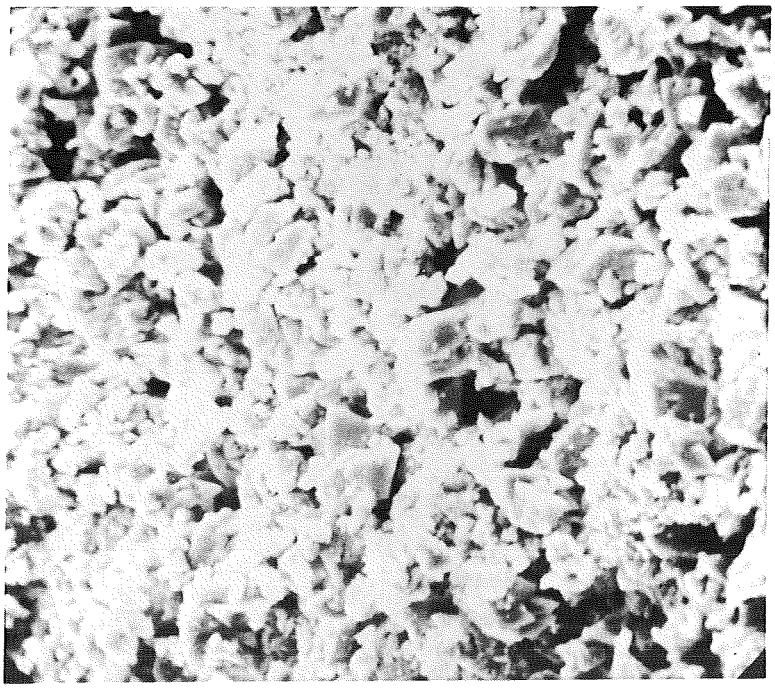

1000 Magnification

300 Magnification

Silver Oxide Plate No. 106

As Received

Transverse View

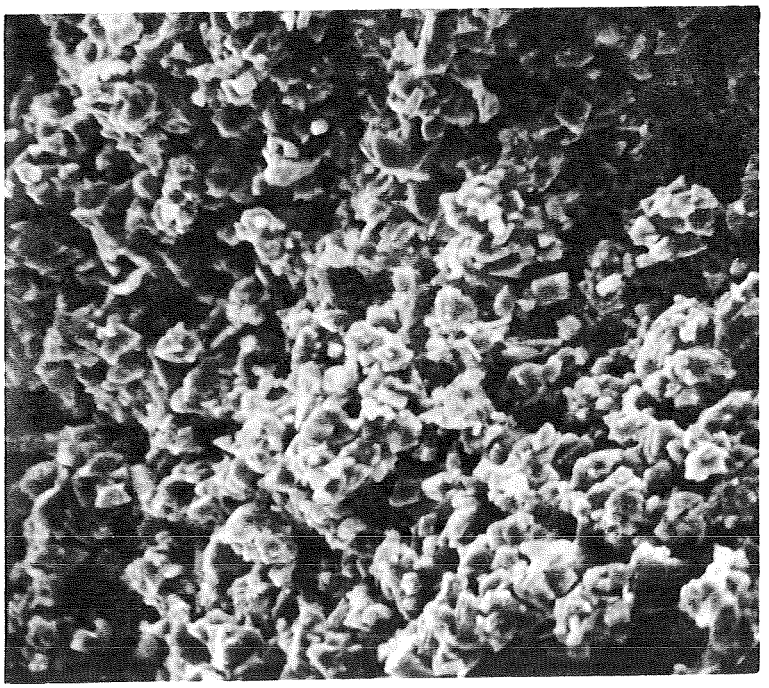

1000 Magnification

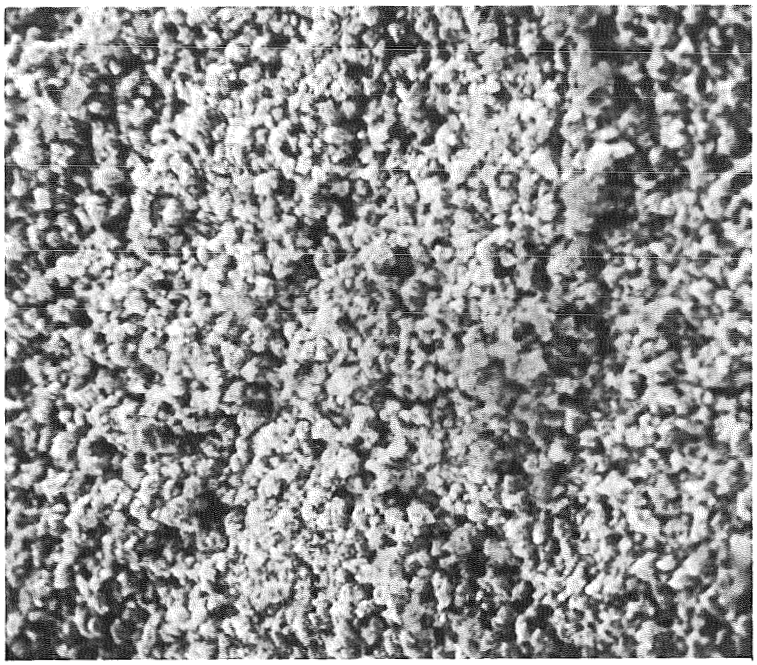

300 Magnification

Silver Oxide Plate No. 106

Sterilized

Flat Surface

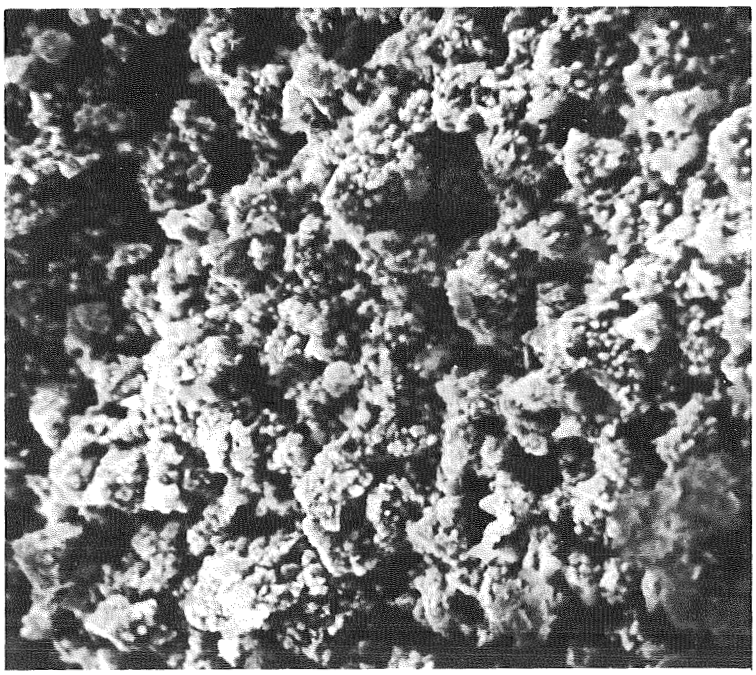

1000 Magnification

300 Magnification

Silver Oxide Plate No. 120

As Received

Flat Surface

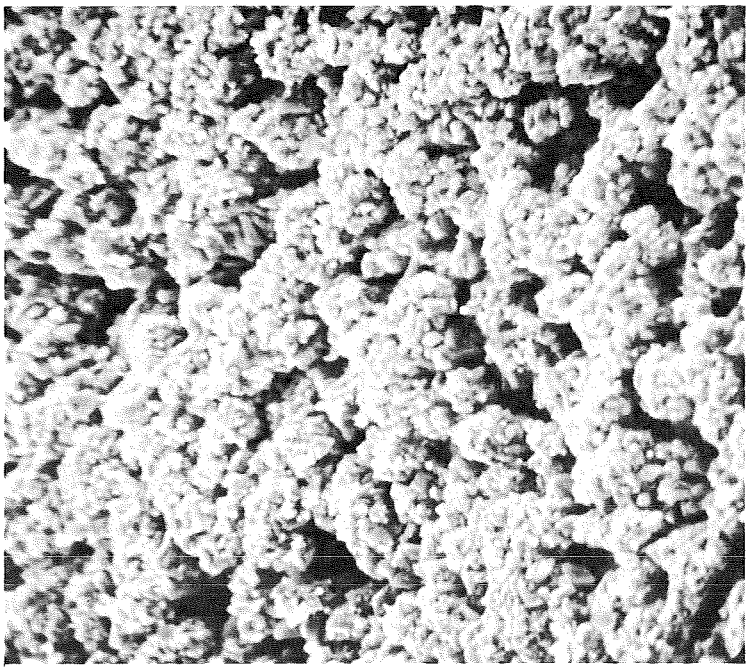

1000 Magnification

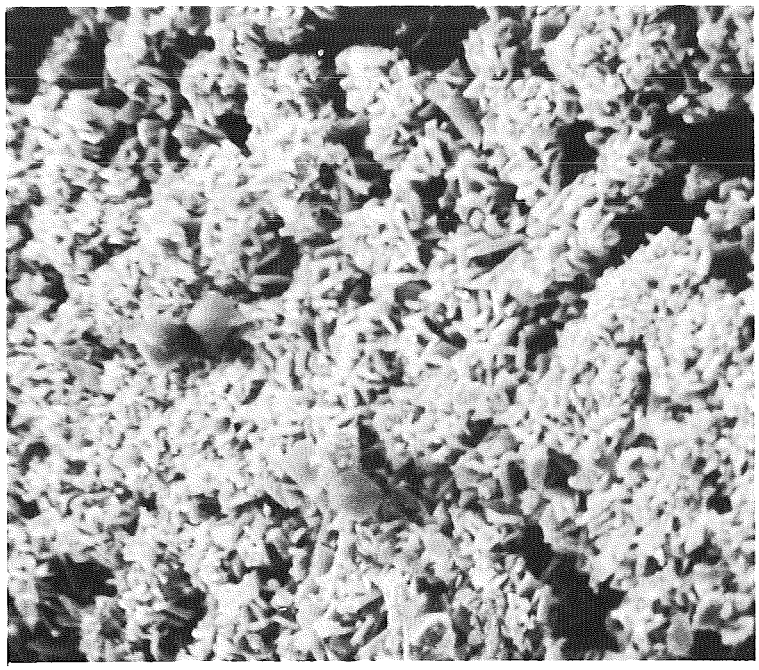

1000 Magnification

Silver Oxide Plate No. 120

As Received

Flat Surface

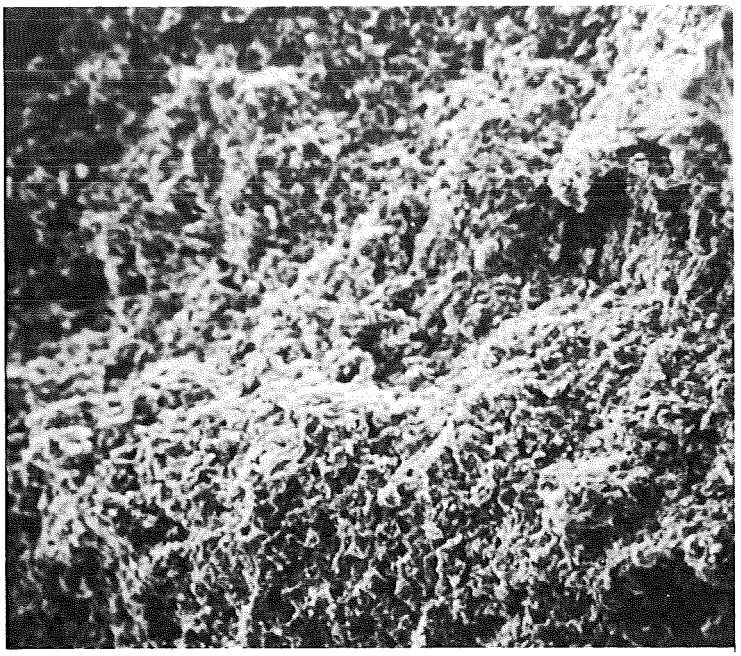

300 Magnification

Silver Oxide Plate No. 120

As Received

Transverse View

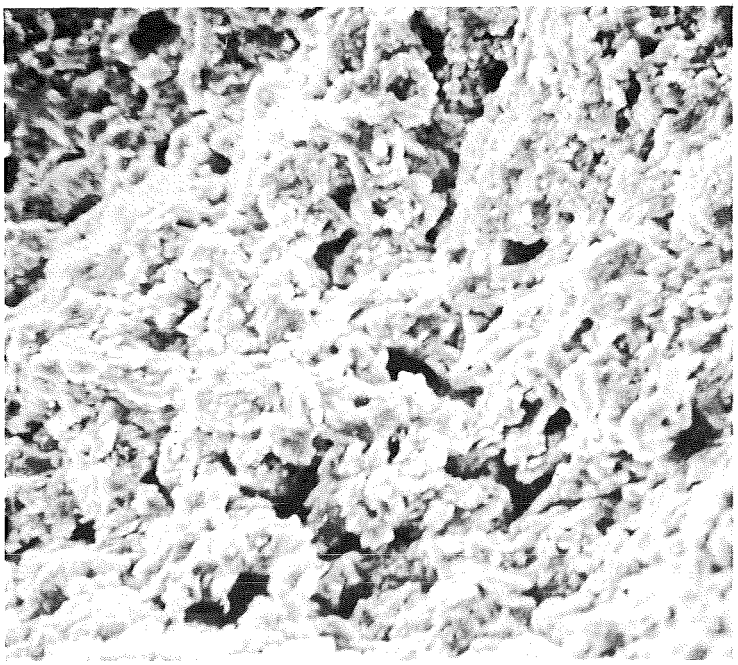

1000 Magnification

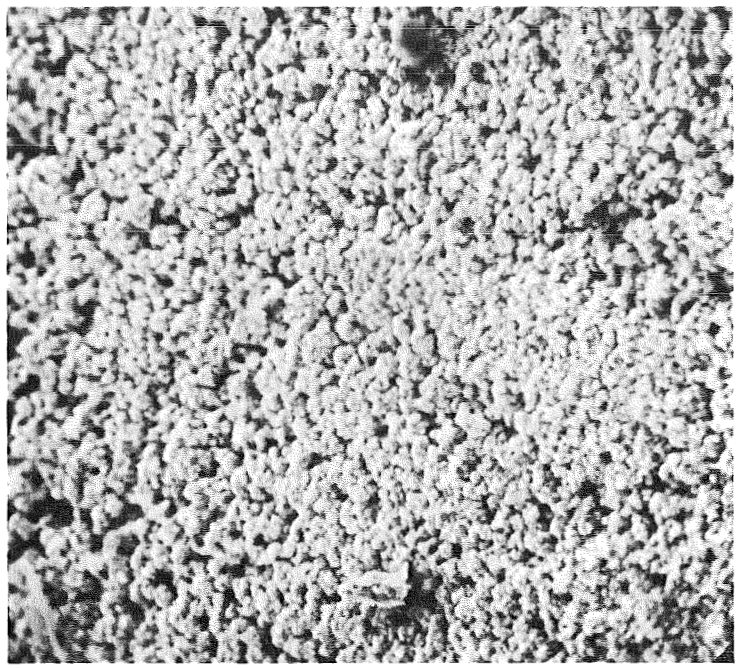

300 Magnification

Silver Oxide Plate No. 120

Sterilized

Flat Surface

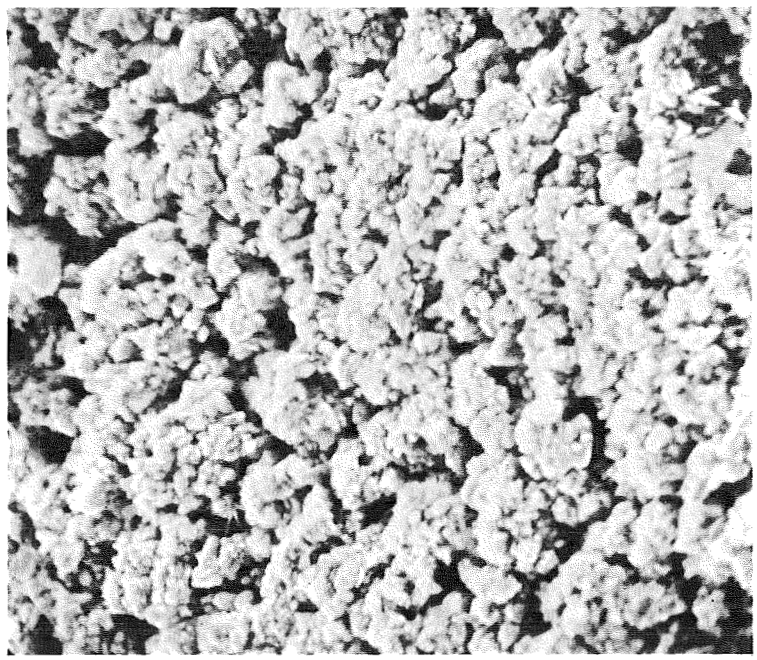

1000 Magnification

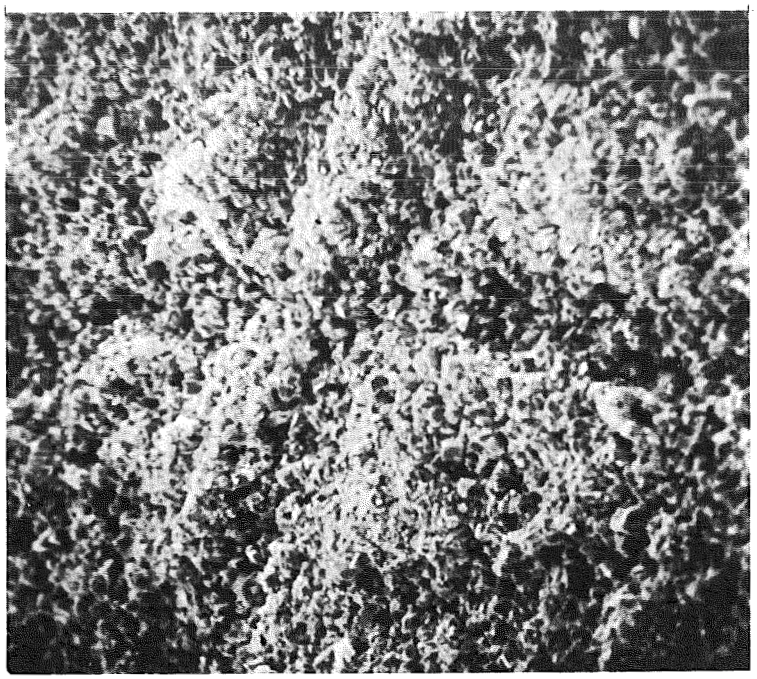

300 Magnification

Silver Oxide Plate No. 171

As Received

Flat Surface

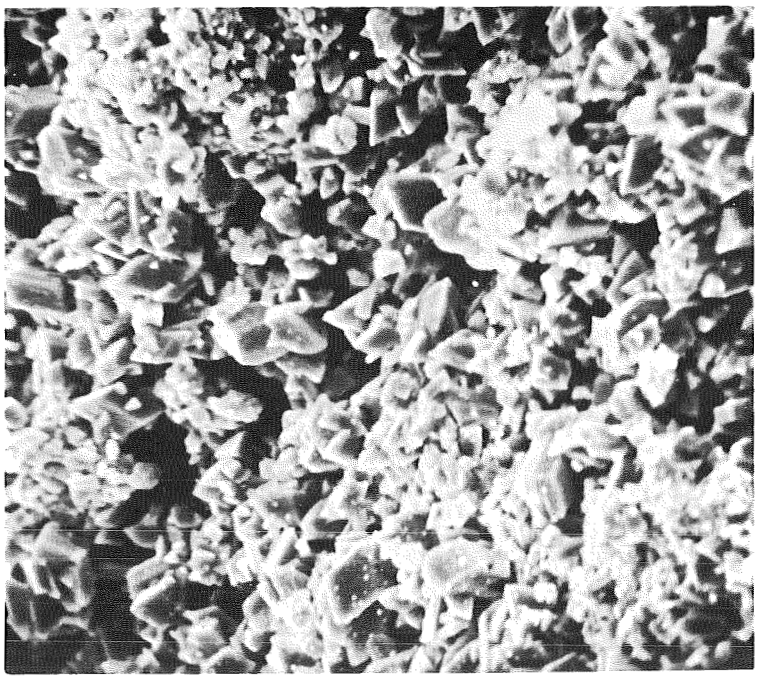

1000 Magnification

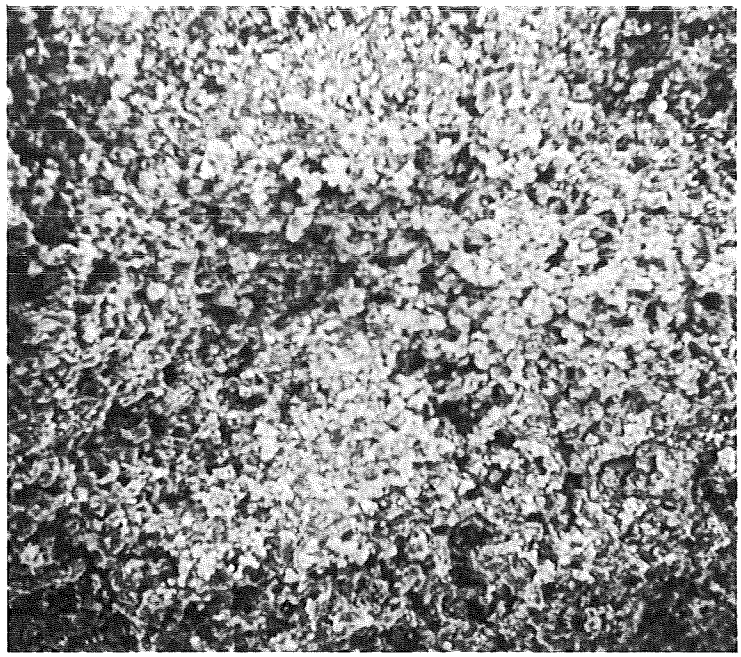

300 Magnification

Silver Oxide Plate No. 171

As Received

Transverse View

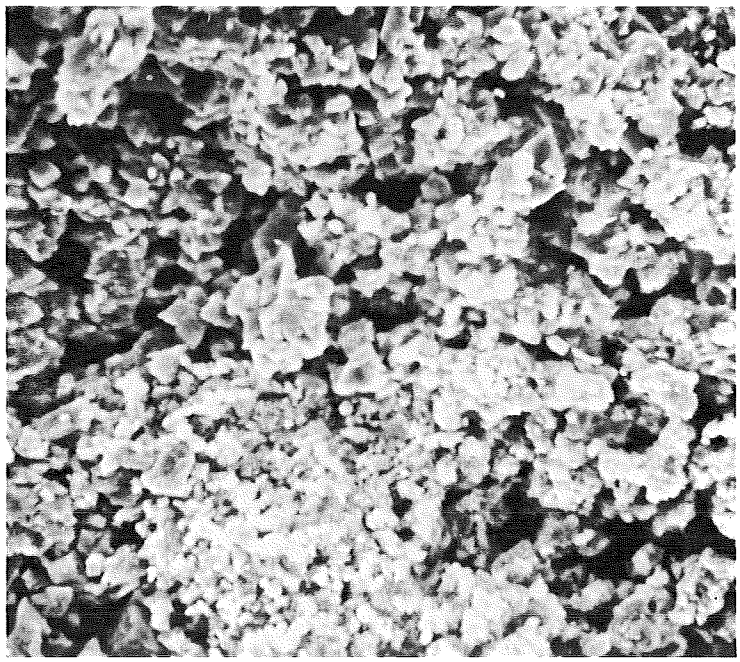

1000 Magnification

300 Magnification

Silver Oxide Plate No. 171

Sterilized

Flat Surface

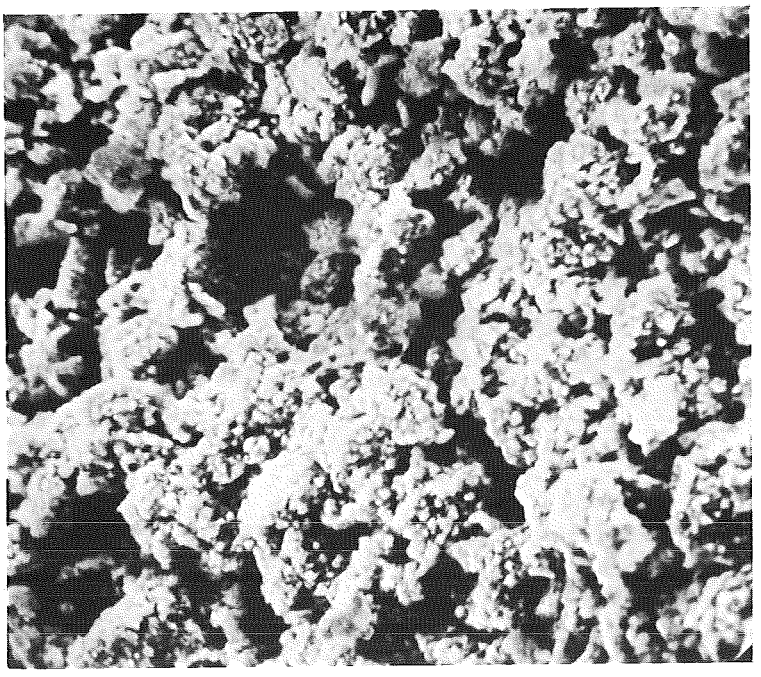

1000 Magnification

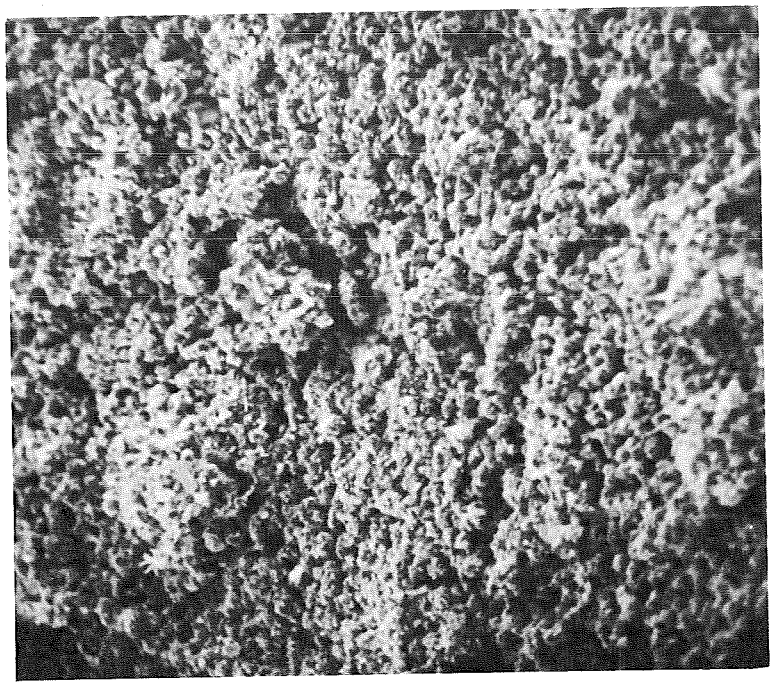

300 Magnification

Silver Oxide Plate No. 206

As Received

Flat Surface

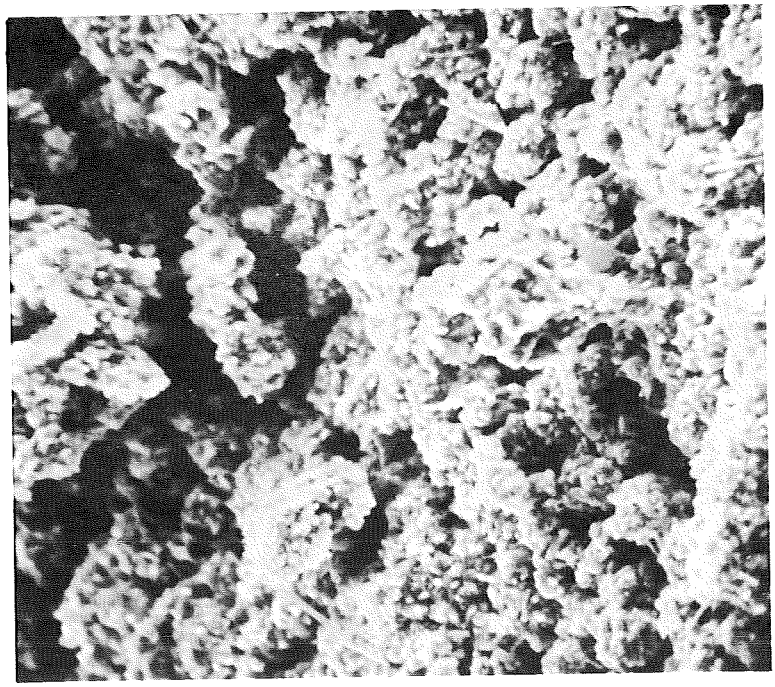

1000 Magnification

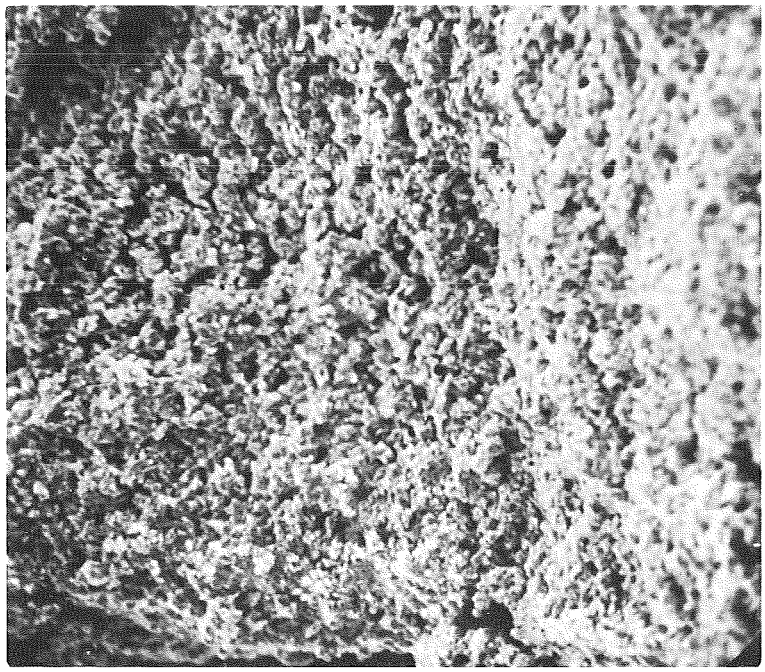

300 Magnification

Silver Oxide Plate No. 206

As Received

Transverse View

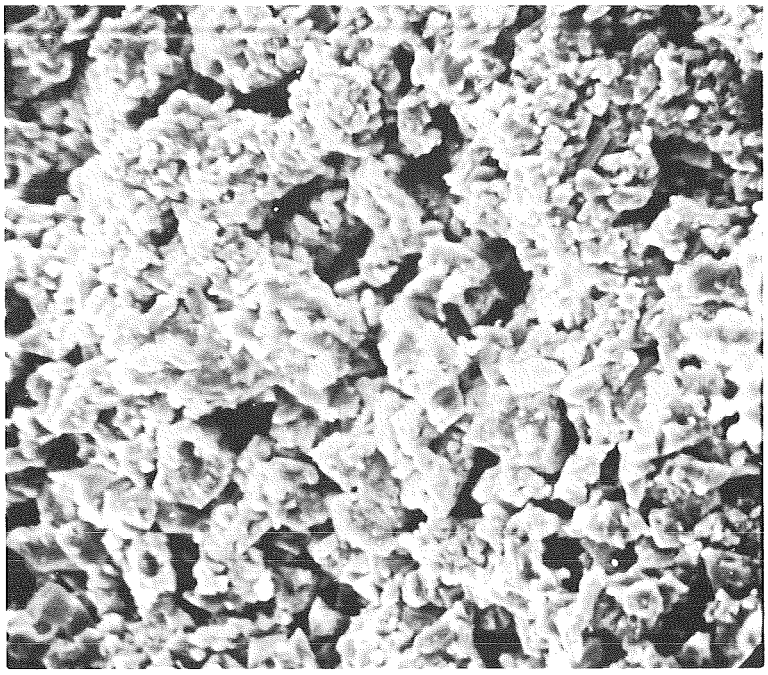

1000 Magnification

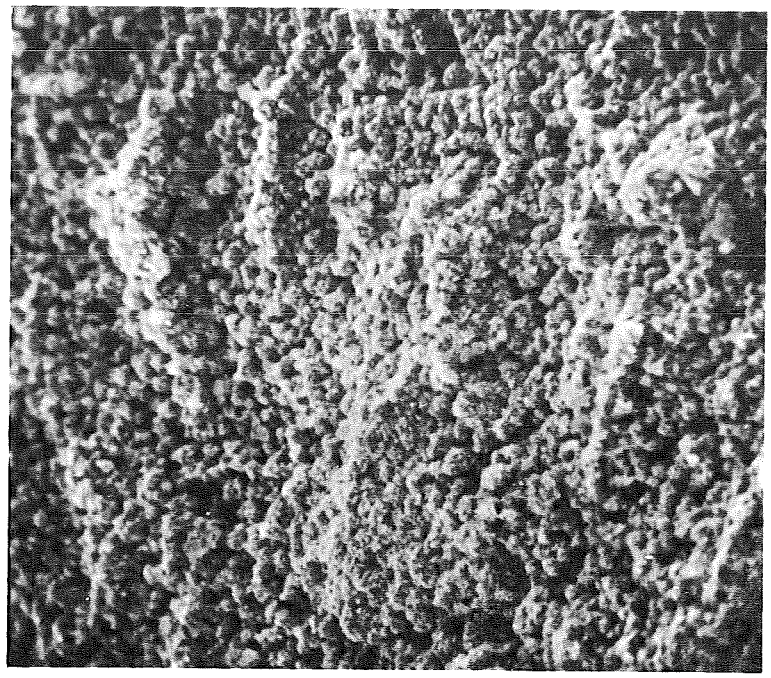

300 Magnification

Silver Oxide Plate No. 206

Sterilized

Flat Surface

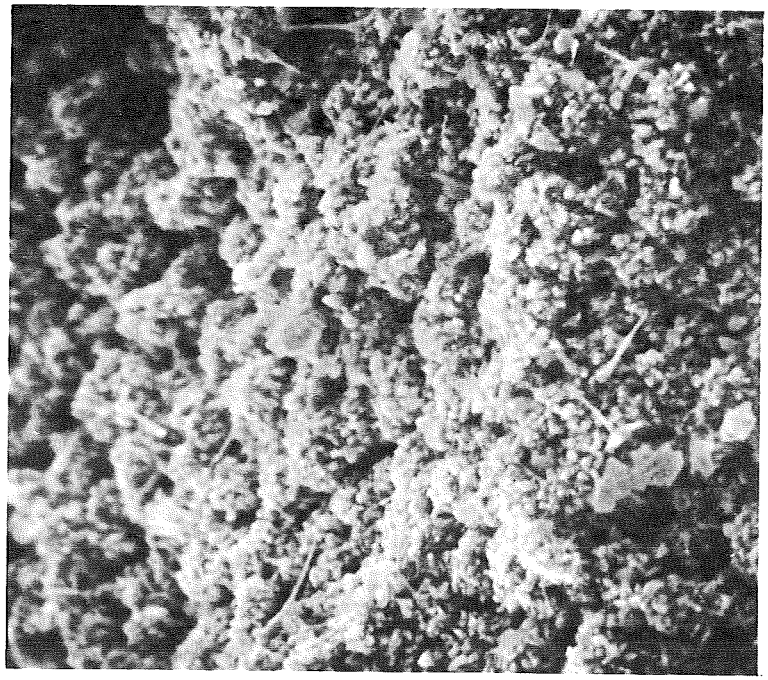

1000 Magnification

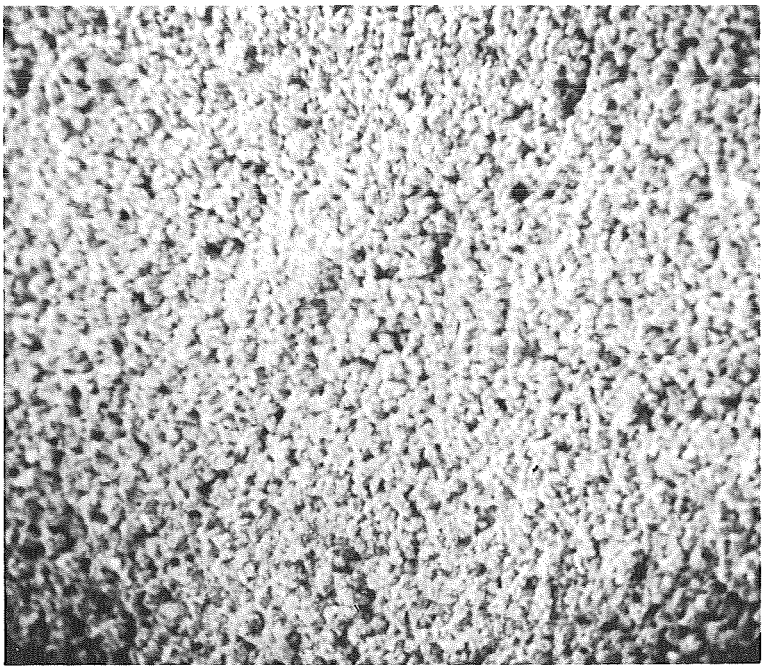

300 Magnification

Silver Oxide Plate No. 252

As Received

Flat Surface

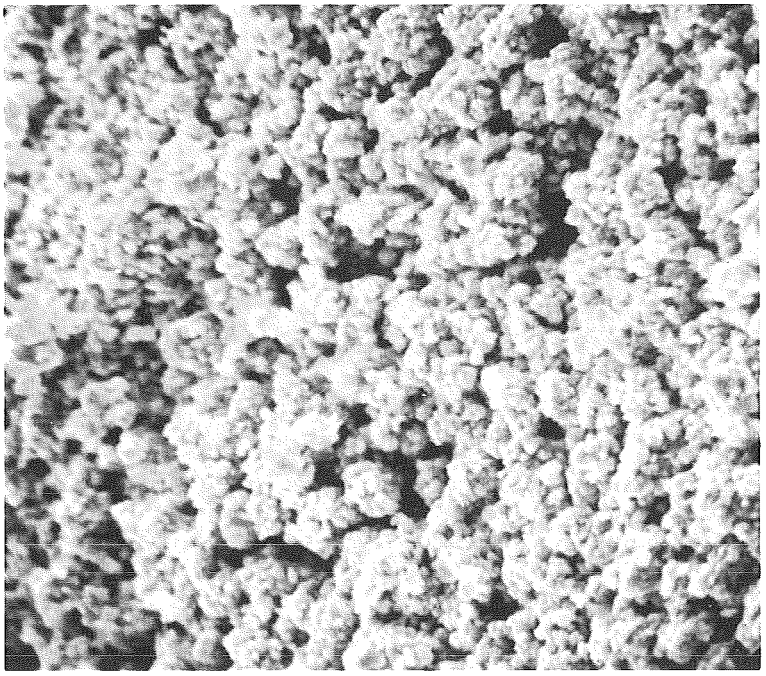

1000 Magnification

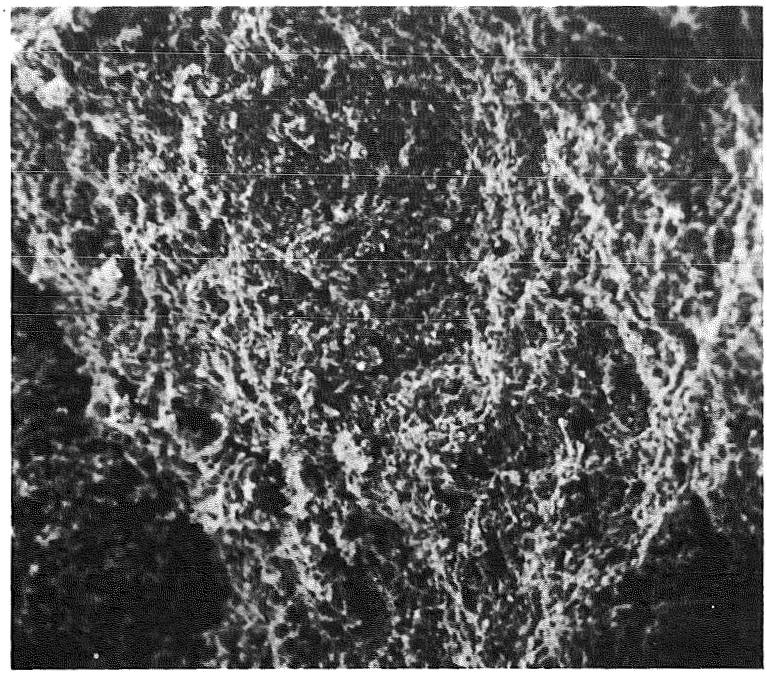

300 Magnification

Silver Oxide Plate No. 252

As Received

Transverse View

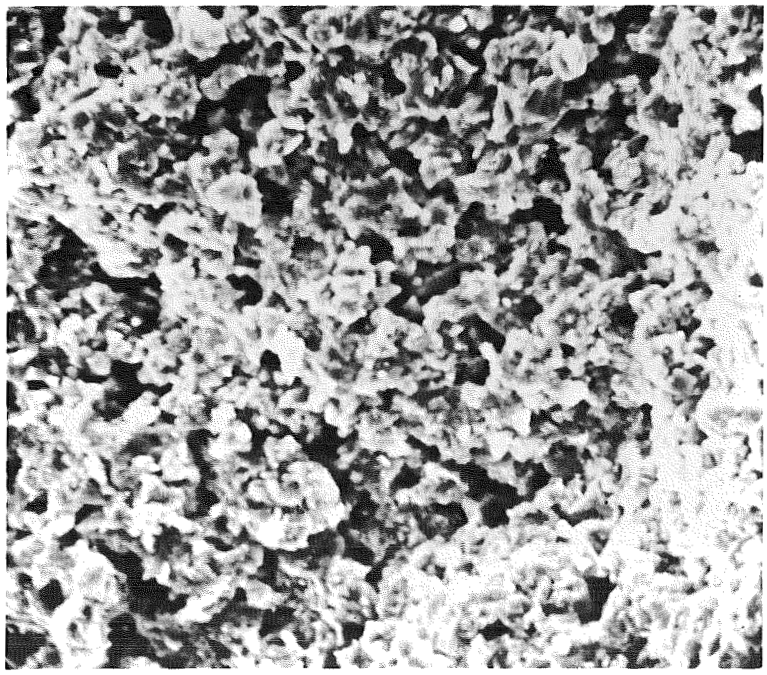

1000 Magnification

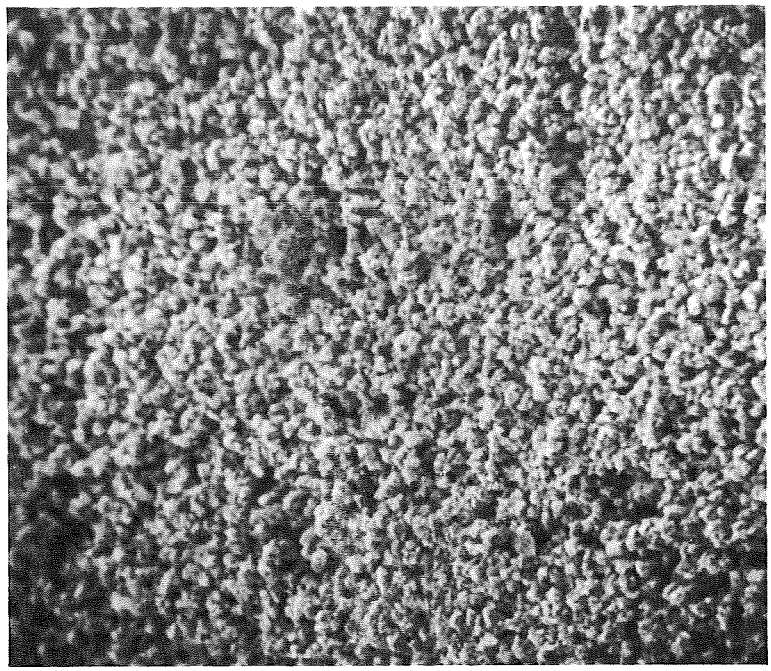

300 Magnification

Silver Oxide Plate No. 252

Sterilized

Flat Surface

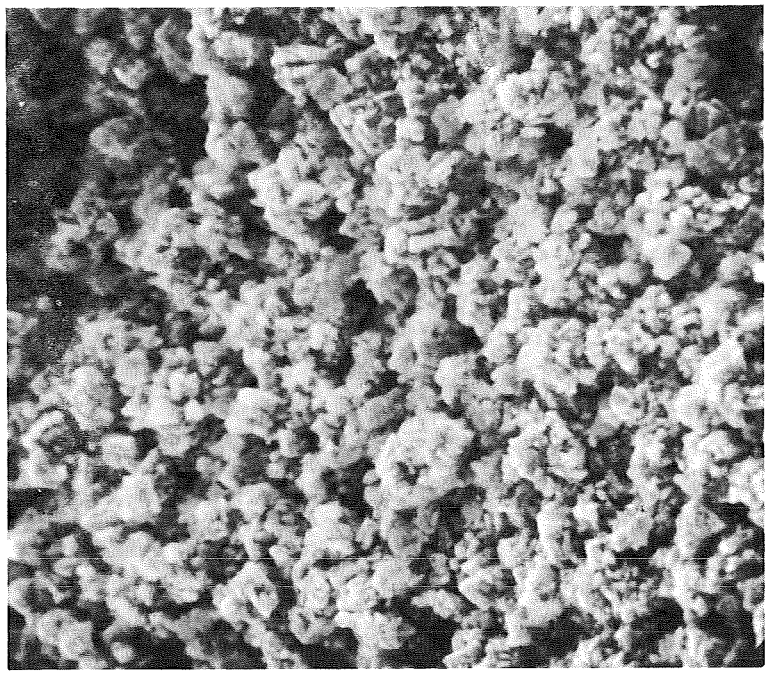

1000 Magnification

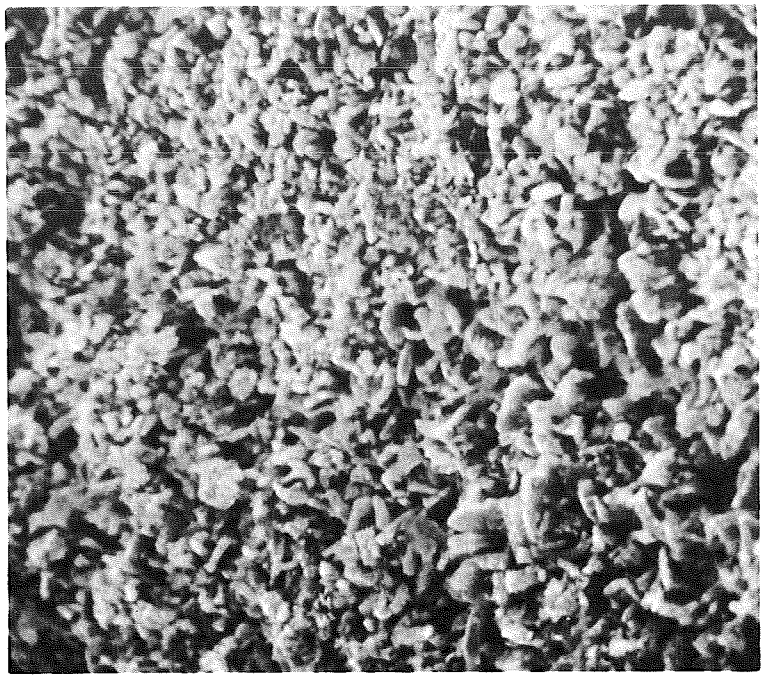

1000 Magnification
Silver Oxide Plate No. 252
Sterilized
Flat Surface

APPENDIX II

MICROSCOPIC STUDY OF ZINC ELECTRODES

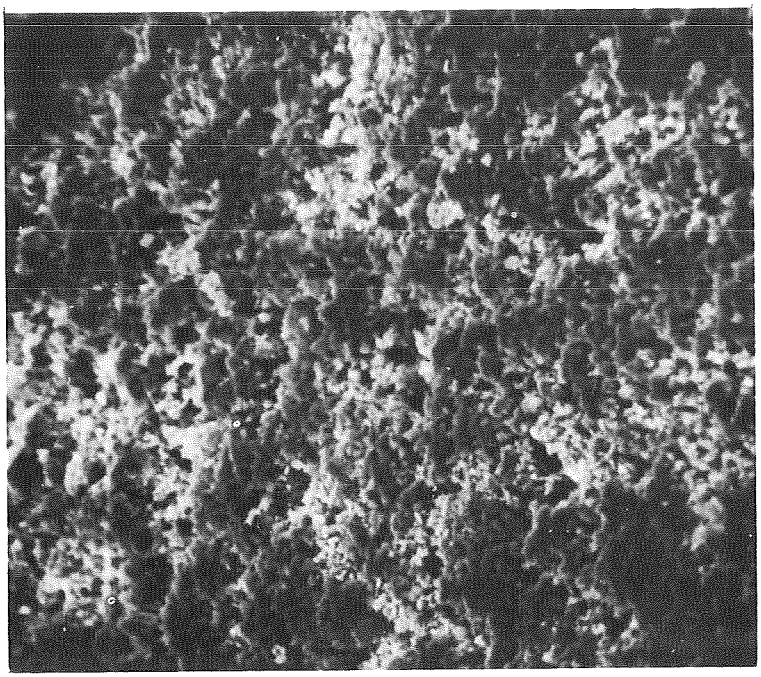

300 Magnification
Zinc Plate No. 51
Sterilized
Flat Surface

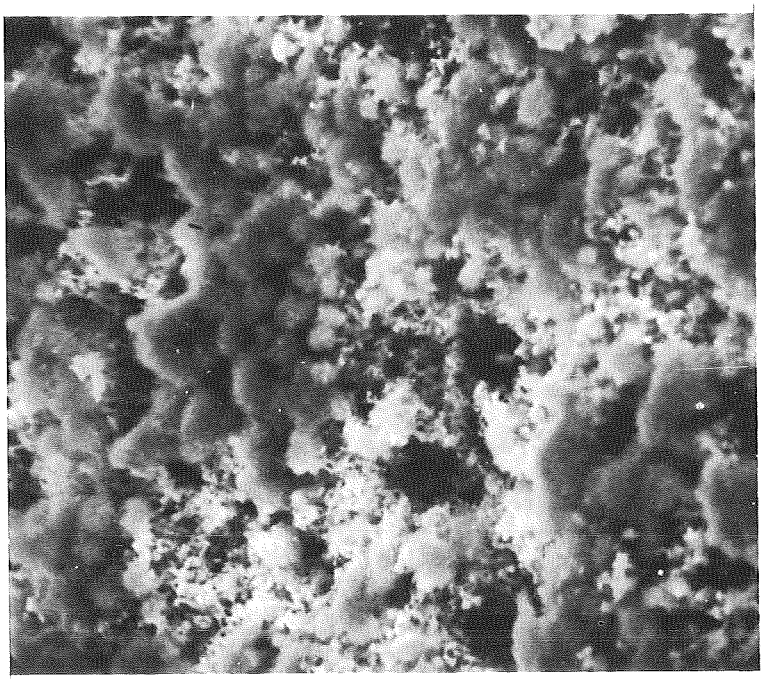

1000 Magnification

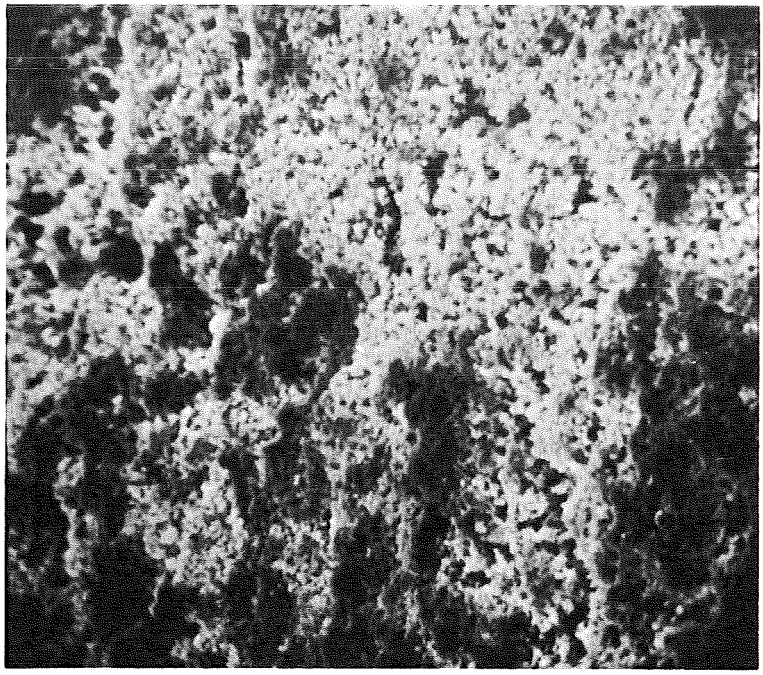

300 Magnification

Zinc Plate No. 78

As Received

Flat Surface

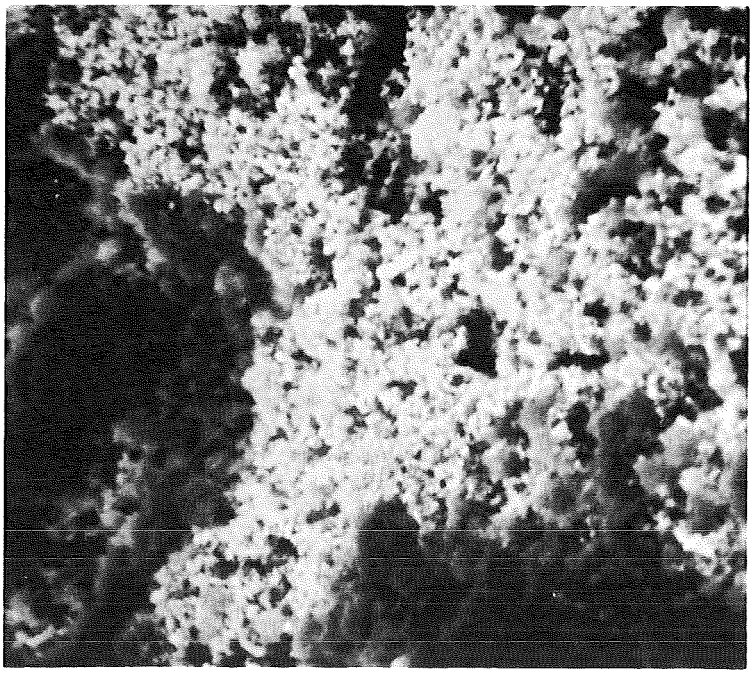

1000 Magnification

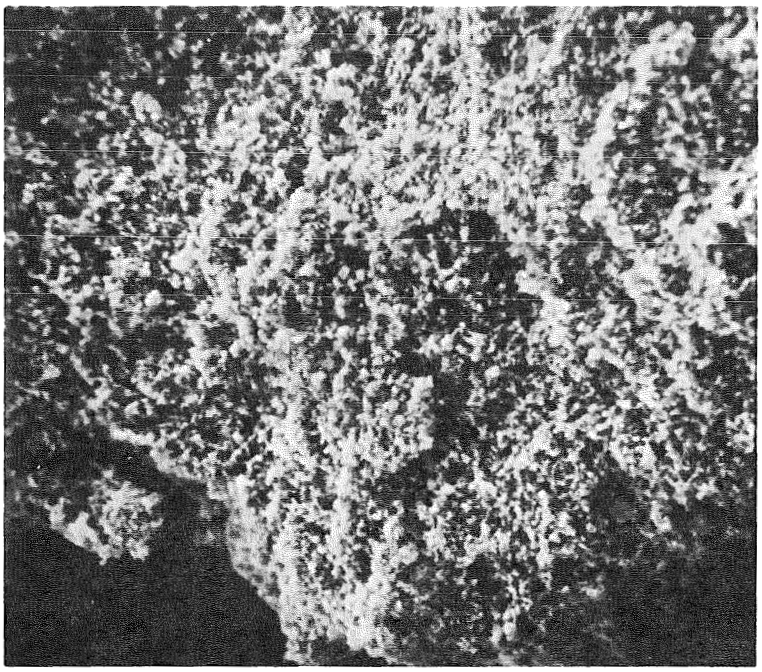

300 Magnification

Zinc Plate No. 78

As Received

Transverse View

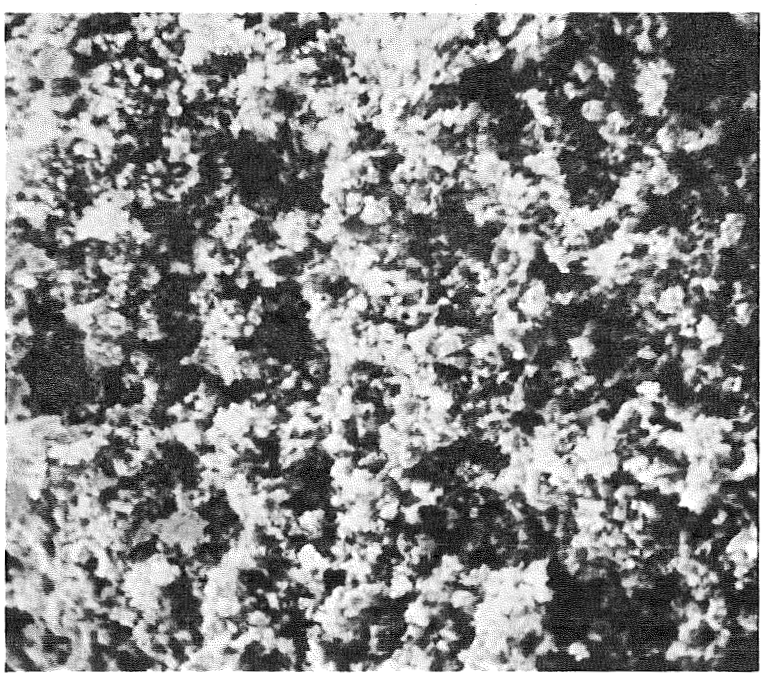

1000 Magnification

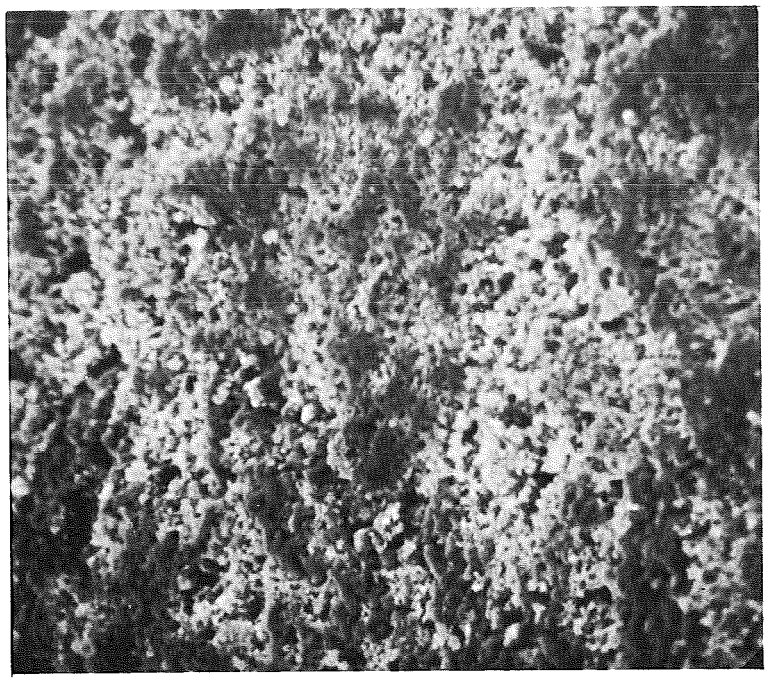

300 Magnification

Zinc Plate No. 78

Sterilized

Flat Surface

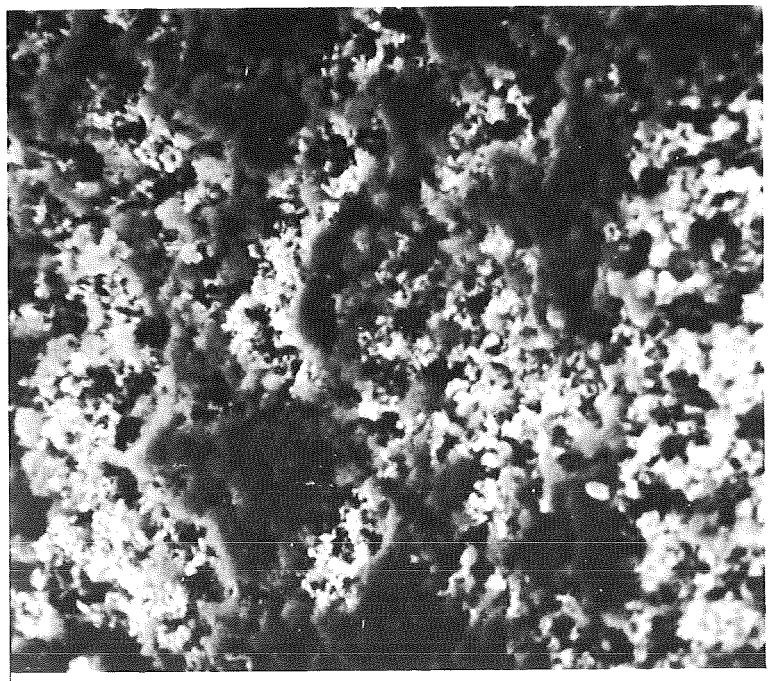

1000 Magnification

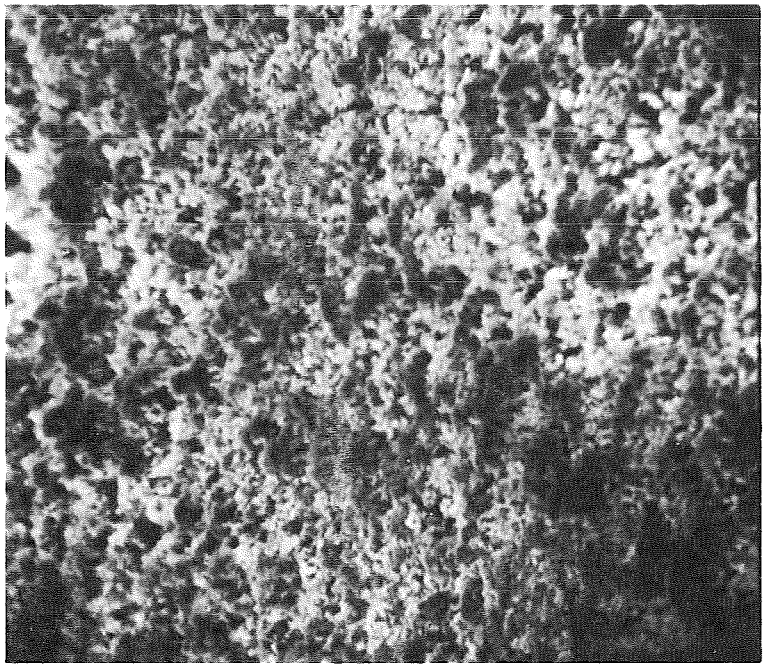

300 Magnification
Zinc Plate No. 162
As Received
Flat Surface

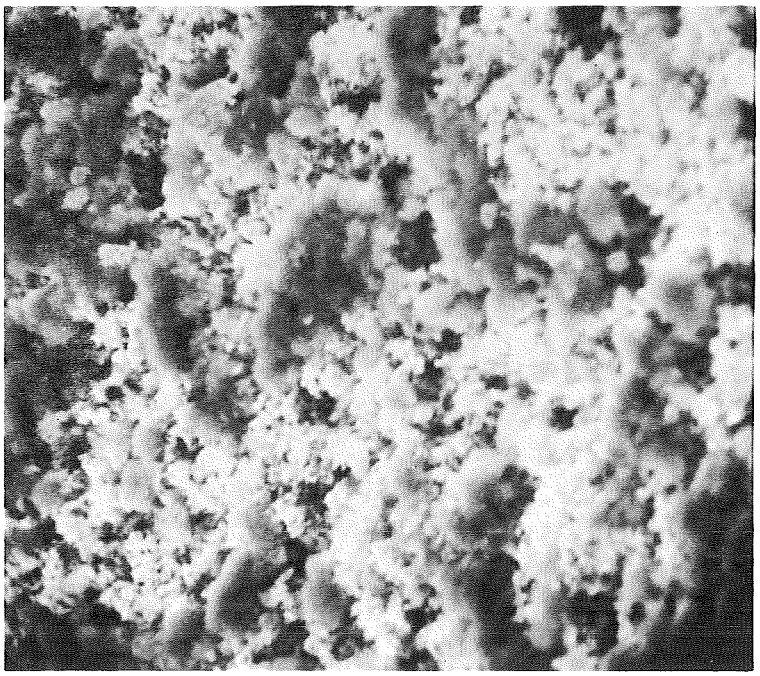

1000 Magnification

300 Magnification

Zinc Plate No. 162

As Received

Transverse View

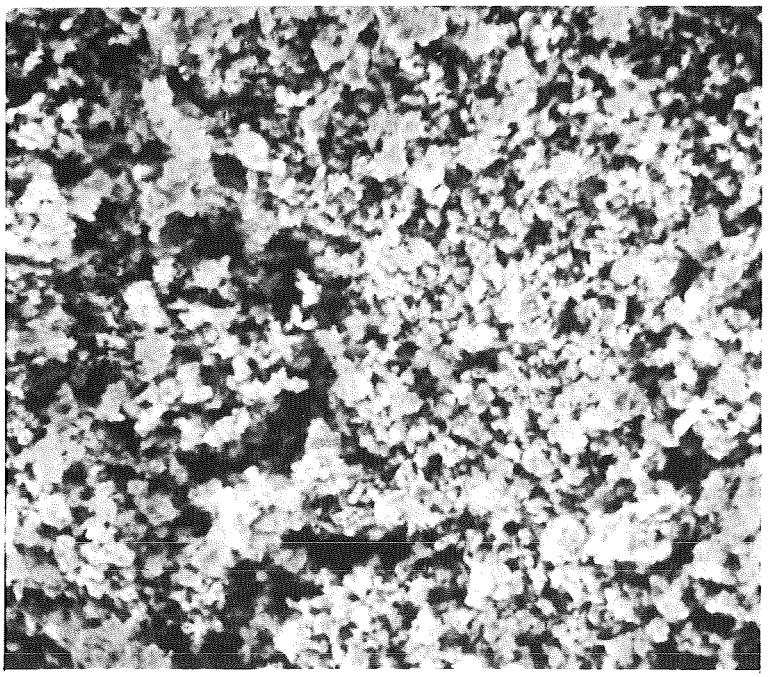

1000 Magnification

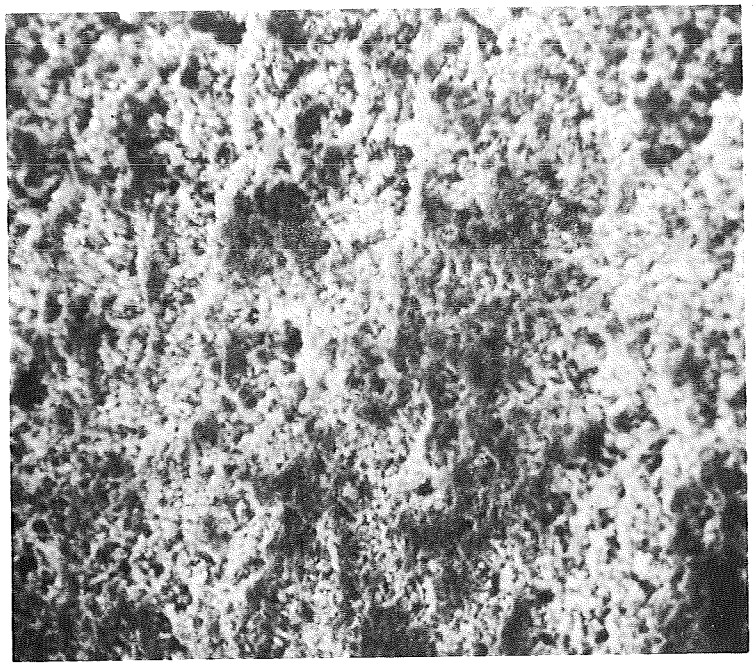

300 Magnification
Zinc Plate No. 162
Sterilized
Flat Surface

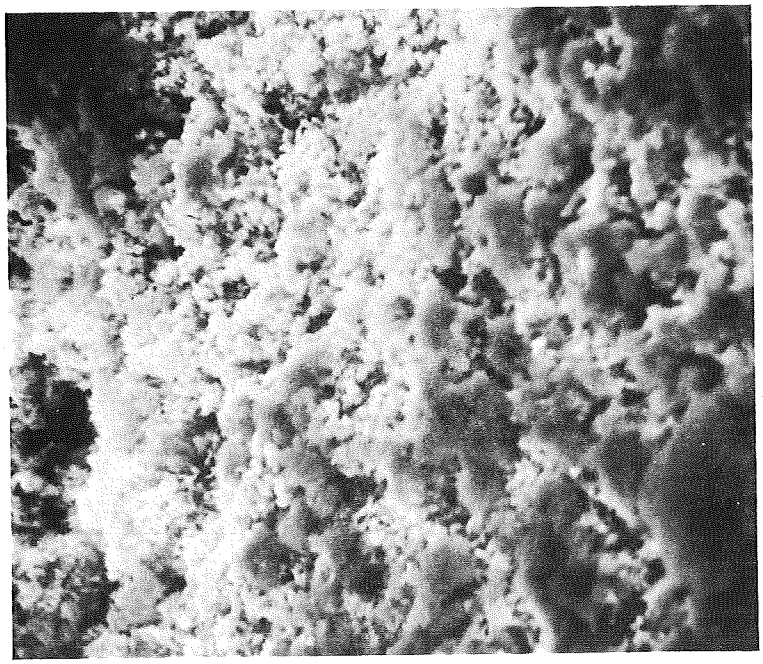

1000 Magnification